
UV NEWS

The official newsletter of the Thematic Network for Ultraviolet Measurements



Issue 8 / August 2006



HELSINKI UNIVERSITY OF TECHNOLOGY



Contents

The Sixth Workshop in Davos, Switzerland October 20 - 21, 2005	3
Solar UV-research on great grandpa's time	4
Extended Abstracts	6
Polysulphone and spore-film UV-dosimeters compared to a UVI-monitoring instrument and two radiation transfer model systems - Evaluations for a UV-dosimetry study 2004 of preschool children	6
UVEMA: A new project exploring degrading effects of UV radiation on materials	9
Standard MEAN Ultraviolet Radiation for non-Extreme Exposure Conditions: definition and indoor reproduction	11
Calibration of UV radiometers is needed to guarantee the relevance of measurements	14
Solar simulators as a tool for assessing the impact of UV radiation on organisms and ecosystems	17
Long-term measurements of UV-solar radiation in Dortmund (Germany)	20
Analysis of UV-B solar radiation in C.I.B.A. laboratory, Spain	22
UV-B and UVI measured and calculated in Valladolid, Spain.	25
Realising a primary spectral irradiance scale on deuterium lamps in the ultraviolet	29
Comparison of measurement devices for the measurement of erythral solar ultraviolet radiation during an outdoor-worker study in Austria	31
Realization of a new commercial radiometer for measurement of the total UV effective irradiance of sunbeds	33
Investigation of comparison methods for UVA irradiance responsivity calibration facilities	35
The use of a single-monochromator diode array spectroradiometer for UV-radiation measurements	37
GaAsP trap detector for UV measurement	39
Characterization of integrating spheres for ultraviolet radiometry	41
Surveillance of UV-sensors in UV-disinfection plants in water works	42
Calibration and characterization of UV sensors for water disinfection	44
Monitoring of low- and medium pressure mercury lamps in UV-disinfection plants for drinking water	46
Improved entrance optic for global irradiance measurements with a Brewer spectrophotometer	48
Time resolved measurements of spectral radiant flux from VUV to NIR ($160 \text{ nm} < \lambda < \approx 1000 \text{ nm}$) on Xe excimer lamps	49
Improvements of a fast scanning double monochromator for UV-B monitoring	51
Long-term experience in using deuterium lamp systems as secondary standards of UV spectral irradiance	52
Expanded Measurement Uncertainty of Spectral Measurements Outside of the Laboratory	54
UV-Monitoring at Outdoor Workplaces - A Base for Well-Balanced Health Prevention Regulations	56
Extreme Ultra-Violet Phototherapy	59
Photobiological quality control in UV phototherapy	61
Personal UV-monitoring in health prevention and risk analysis	62
Service Card	64

ISSN 1456-2537

Picaset OY, Helsinki 2006

UVNEWS is the official newsletter of the Thematic Network for Ultraviolet Measurements. The Network was earlier funded by the Standards, Measurements and Testing programme of the Commission of the European Communities, as project number SMT4-CT97-7510. *UVNEWS* is published at irregular intervals. It is aimed to exchange knowledge between the participants of the Network and to disseminate information on the forthcoming and past activities of the Network. The newsletter also contains scientific and technical articles on UV measurements and a news-section about activities in the field of UV measurements. The newsletter welcomes all announcements and articles that might be of importance for the readers. Material to be published in *UVNEWS* should be sent to:

Helsinki University of Technology
Metrology Research Institute
Petri Kärhä
P. O. Box 3000
FIN-02015 TKK, Finland
Telefax: +358 - 9 - 451 2222
E-mail: petri.karha@tkk.fi

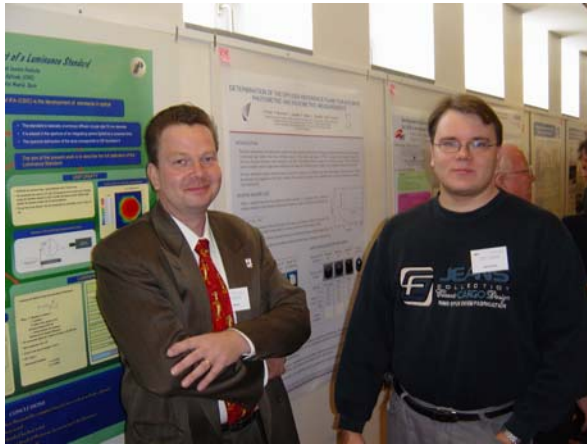
In case of longer articles or announcements, use of E-mail is preferred. The date of the next possible issue is not known. It will most likely be published with the 7th workshop around 2007 – 2008.

Photographs: Cover: Participants of the 6th Workshop, Page 3: Poster session (Picture taken by L. Ylianttila, STUK), Scenery of Davos, (Picture taken by François Christiaens, L'Oréal).

The Sixth Workshop in Davos, Switzerland October 20 - 21, 2005

*Petri Kärhä
Helsinki University of Technology, Finland*

The sixth workshop of the Thematic Network for Ultraviolet Measurements was arranged in Davos, Switzerland, on October 20 - 21, 2006. The meeting was hosted by the Physicalisch-Meteorologisches Observatorium Davos (PMOD/WRC). The number of participants in the workshop was approximately 110, which is an all-time record. This was mainly because the workshop was arranged in combination with a bigger event, NEWRAD 2005. Due to the high attendance, it should be considered that the workshop could also in future be arranged in connection with some other event.



The workshop contained 5 oral sessions:

- Uncertainty and intercomparison issues (3 talks)
- UV measurements techniques: Spectroradiometers (2 talks)
- UV measurements techniques: Detectors and sources (4 talks)
- UV measurements related with Healthcare and Health & safety (4 talks)
- UV material effects, testing and sterilisation (4 talks)

In addition, 18 posters were presented. The authors were given a chance to submit extended abstracts on their presentations, which can be found in the following section. Davos is one of the first places where solar UV was measured. During the excursion we had a chance to see some of the earliest equipment used. These early measurements are reviewed in an extra article kindly provided by Ulf Wester starting on page 4.

Between the scientific presentations, also the continuation of the Network was discussed. Continuation of the meetings was considered important, so the next workshop, already seventh in series, should be organised around 2008. The place is still unclear, but should be in Europe. Places suggested and favoured by participants included e.g. Norway, Scotland, Poland and Czech. Nevertheless, arrangement needs a volunteer local organiser. We should also bear in mind, that arrangement in combination with some other event, might bring broader attendance. This event might be on solar UV measurements, radiometry in general, photonics, medicine, health care, pharmacology, biotechnology, weathering and climate, because the spread of interests and research areas of participants is rather wide. The steering group of the network welcomes all useful ideas and volunteers.



Davos was a wonderful venue for the workshop, not only because of the nice scenery and climate, but mainly because of the efficient arrangements. Everything worked as a Swiss clock. On behalf of us participants, I would like to take this opportunity and thank again all organisers, especially Julian Gröbner and Werner Schmutz of PMOD/WRC. Those willing to visit Davos again might note that PMOD/WRC is celebrating its 100 years of solar observations by arranging a conference dedicated to solar UV measurements on September 18 - 20, 2007.

Solar UV-research on great grandpa's time

U. Wester

Swedish Radiation Protection Authority (SSI)

“Ultraviolet radiation has of late attracted a great deal of attention not only by reason of the photochemical processes, so important from a physiological point of view, which these rays are able to produce, but also on account of the prospects of closer investigations into the amount of the ozone of the atmosphere, which the study of ultra-violet radiation opens out.”

The quoted statement above stems from a report of UV-measurements 1926-27 (Aurén 1929), but is still valid in 2005. Observations of ultraviolet irradiance in the sunlight and with the object of investigating the amount of ozone in the atmosphere, had been made at a number of sites particularly at high altitude health resorts in Switzerland. It was known how the intensity of radiation

increased with altitude, that it varied at places of equal altitude due to differences in atmospheric transmission, that diffuse radiation from the sky at lower solar altitudes ($< 45^\circ$) is stronger than the direct UV-radiation which increases with solar altitude. It was also known that an overclouded sky may be of great intensity (Dorno, Götz, and others).

Appropriate instruments were available commercially. Photoelectric cells with a cadmium or a potassium cathode were charged to a reference voltage. The discharge current and time was measured with an electrometer as the cell was exposed to solar UV-radiation through, a for the cell and spectral range chosen, optical filter.

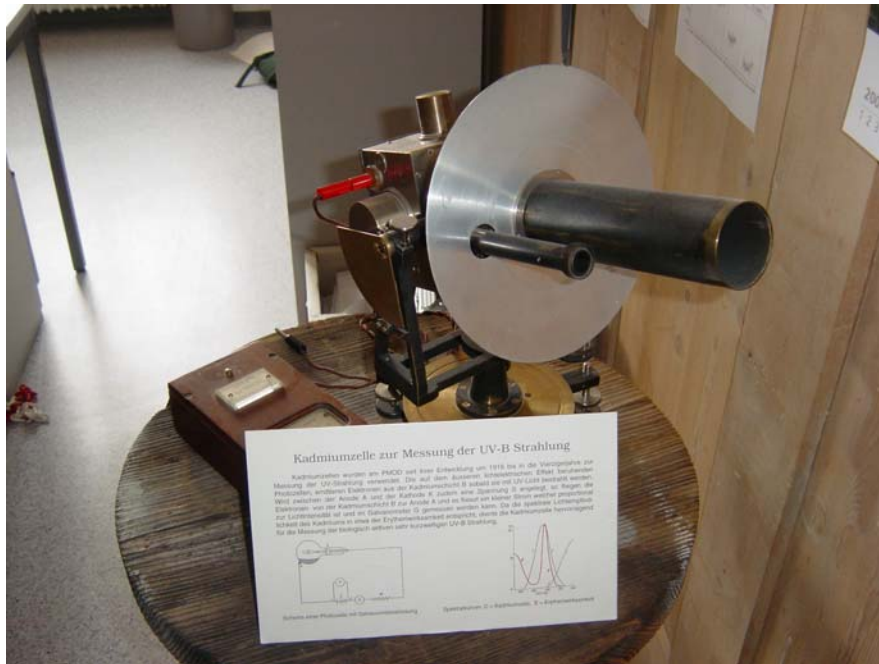


Figure 1. This UVB-measuring sun photometer, presently a museum object in PMOD/WRC at Davos, may be the normal cell used in the 1920's at the solar research center of Davos for intercomparisons with other similar UV-measuring instruments and for normalising their results into units of the "Davos-scale." (Photo: Lasse Yliantilla, STUK).

Solar UV-measurements were made at a number of places also outside Switzerland, even at Aswan in Egypt and at Bandung in Indonesia. In Sweden T.E. Aurén, a scientist funded by the Swedish Anthropological and Geographical Society, made measurements of both direct and diffuse solar UV-radiation with Cd-cells at five places, Abisko being the northernmost, during the summers of 1926 and 1927 "to ascertain in how far radiation depends on the geographical position of the place under observation". In Finland extensive measurements were made which also were well documented (Lunelund 1944; Lunelund et al

1929). On one occasion the UV-variation was studied during a solar eclipse.

Aurén's solar UV-measurements in the 1920's were made with electrometers and two filtered cadmium cell photometers (Manuf. Gunther & Tegetmeyer) with a spectral sensitivity ranging from approximately 244 to 366 nm, and a maximum around 313 nm. Aurén noted that in sunlight there is "hardly any radiation of a shorter wavelength than 291 nm" and that due to the comparatively small longwave UV-sensitivity of Cd-cells "the radiation observed with the cell generally

corresponds to the province that is interesting from a biological point of view, which extends from 320 nm to the (short-) end of the spectrum”.

During the 1920’s cadmium cells employed in research into ultraviolet radiation were compared with a so called

normal cell kept at the solar research centre at Davos in Switzerland. A Cd-cell photometer still exists as a museum object in the building of the World Radiation Center (PMOD/WRC) at Davos (Figure 1).

Table 1. Solar UV-irradiance mean values July-August in Davos-units (from Aurén).

Site	Latitude °N	Altitude (m. a.s.l)	Year	Solar elevation		
				25°	35°	45°
Muottas-Muraigl	46.5	2456	1923	102	216	341
Davos	46.8	1560	1916-18	66	136	223
Agra	46	565	1923	45	96	151
Stockholm	59.4	55	1926-27	30	85	141
Abisko	68.4	375	1926-27	39	93	169

After an intercomparison in 1927, repeated in 1929 to confirm an unchanged sensitivity of his cells, Aurén was able to compare his solar UV-measurement results with others expressed in units of the “Davos-scale” (Table 1).

During the 1990’s an increasing skin cancer incidence has been in the focus for preventive measures and of considerable media- and some public attention and has been attributed to depletion of the ozone layer, charter holidays at southern latitudes, longer vacations, more time spent outdoor, misguided beauty concepts promoting extensive habits of tanning and widespread use of sunbeds. This has resulted in UV-measurements with modern instruments. An internationally agreed UV-index has worldwide become a means to estimate erythemally harmful solar UV effects on the skin. Unfortunately it is presently not possible to compare data from old UV-measurements in the Davos-scale made early in the 20th century with modern measurements of the UV-index made in the beginning of the 21st century.

Literature and references:

1. Dorno: Grundzüge des Klimas von MuottasMuraigl (Braunschweig 1927).
2. Götz: Das Strahlungsklima von Arosa (Berlin 1926).
3. Süring: Meteorol Zeitschr., 41 (1924).
4. Aurén T.E.: Observations concerning ultraviolet solar radiation in some places in Sweden. Geogr. Annaler, 11, 257-267, (Stockholm 1929).
5. Lunelund H & Holmberg K.T.: Über die ultraviolette Sonnenstrahlung in Finnland. Soc. Scient. Fenn., Comm. Phys.-Math.,2, 1-41 (1929).
6. Lunelund H. Stärke der ultravioletten Sonnenstrahlung in Finnland. Soc. Scient. Fenn., Comm. Phys.-Math., XII(13), 1-21 (1944).
7. Wester U.: UV-monitoring in Sweden: Past, present and future. In: Diffey B. ed. Measurement and Trends of Terrestrial UVB Radiation in Europe. Sid 103-110, Milano; OEMF s.p.a. (1996).

Extended Abstracts

Polysulphone and spore-film UV-dosimeters compared to a UVI-monitoring instrument and two radiation transfer model systems - Evaluations for a UV-dosimetry study 2004 of preschool children

U. Wester

Swedish Radiation Protection Authority (SSI)

Summary

In this evaluation, measurements of global solar ultraviolet radiation (UV) with two types of dosimeters are compared: polysulphone badges with plastic film that changes its transmission after UV-exposure, and dosimeters which function by UV-induced DNA-damage to dried bacteria spores. The dosimeters agree well and are sufficiently precise. They agree also with data of daily global solar UV by two services (JRC, SMHI) which provide maps with radiation transfer (RT) model calculations of UV-exposures on a horizontal surface based on actual weather and ozone parameters from satellites. The two model calculations agree with each other too, for full day exposures, and with results from a UV-monitoring instrument.

Background

An evaluation of the accuracy of available polysulphone film UV-dosimeters and how they compare to bacteria spore dosimeters was desired when SSI cooperated with the Stockholm County Council, Center of Public Health, May 24 - June 9 2004 in a study of preschool children's UV-exposure. The study measured UV-exposures of 199 children at eleven daycare centers and how the exposures depend on different physical surroundings and shade structures of playgrounds. The children wore the same polysulphone film badges each day of their stay at the preschools to measure accumulated erythemal UV-exposure (Fig. 1).



Figure 1. PS-dosimeter on a child's shoulder.

The study of the children's UV-exposure was part of a larger project at the Stockholm County with the main objective to assess the influence of environmental playground factors on childrens physical activity and

health [1]. The study was a follow-up of a previous smaller pilot project 2002 where bacteria spore dosimeters (viospore, BioSense) had been used for personal UV-dosimetry of preschool children [2, 3].

Material and methods

It has become an established method to use polysulphone film as a dosimetric tool to measure exposure of ultraviolet radiation [4, 5]. The UV-exposure can be determined from changes in optical transmission of a thin plastic film, usually measured as a difference in absorbance at 330 nm [5, 6]. Polysulphone film dosimeter badges for the study of the children and for this evaluation were purchased from Newcastle General Hospital in UK and its Medical Physics dept headed by Prof B. Diffey. The badges came in card-board frames 4x4 cm with the polysulphone film mounted in it (Fig. 1, Fig. 2 left).



Figure 2. Polysulphone film badge under quartz glass (left), and spore dosimeter under quartz dome (right) on SSI's roof.

Bacteria spore dosimeters function by UV-induced DNA-damage to a film of dried bacteria spores (*Bacillus subtilis*) that with a filter and an angular response diffuser mimic the erythemal sensitivity of human skin [7, 8]. They can be used for solar UV-measurements too [9, 2]. Commercially available bacteria spore dosimeters (Viospore Blue line, type II, 0.4-22 MED) were purchased from BioSense, Germany (Fig. 2 right). Both kinds of dosimeters were returned to respective manufacturer after exposure for their data read-out.

During the study of the children both kinds of dosimeters were used daily in parallell at five sites on roofs or at positions with a free horizon for recording total global UV-exposure from dawn to dusk on a horizontal surface. Each of the sites was central or close to some preschools participating in the study. The roof platform of SSI at Solna Stockholm (59.35°N) was chosen as one of the sites because dosimeter data could be compared to instrument measurements of solar UV (Fig. 3).



Figure 3. SSI's UV-monitoring instrument is a multichannel UV-radiometer (Biospherical Instr. GUV541) at Solna, Stockholm (59.35°N). It reports the global solar UV-index in six-minute intervals on the SSI-website <http://uvindex.ssi.se>

The accuracy of the dosimeters was evaluated by comparing the daily exposure results at the SSI-site (59.35°N) to the solar UV-index monitoring instrument there and to data from two radiation transfer (RT) models by JRC and SMHI, which utilize satellite collected actual weather- and ozone-parameters. Dosimeter results from the northernmost (59.5°N) and the southernmost (59.2°N) sites were compared too to the RT-models for those coordinates.



Figure 4. Ten polysulphone film badges (front) and ten bacteria spore dosimeters (behind) exposed to a full day of summer sunshine 4.6.2004 on SSI's roof platform.

SMHI's and JRC's calculations produce fields of CIE-weighted UV radiation with different spatial and temporal resolutions based on clear sky RT-models, satellite total ozone measurements and recorded data of clouds, precipitation, etc. The SMHI model covers Scandinavia and the Baltic sea area with a 22x22 km grid and one hour temporal resolution (www.smhi.se/strang). The JRC-model covers most of Europe with higher spatial and temporal (1/4–1/2 h) resolution than SMHI's model. JRC's RT-model results are not directly accessible on the web, but data for the exposure study of the children at the coordinates of three sites in Stockholm county were kindly communicated (by Dr J. Verdebout, JRC).

Variability of both kinds of dosimeters to the same exposure was measured on a sunny June 4, with ten dosimeters of each kind at the roof platform of SSI in Solna, Stockholm (Fig. 4).

The weather during the measurement period varied from unbroken cloudcover with heavy rain, broken cloudcover with occasional showers and some sun to varying

cloudiness with intermittent direct sunshine to cloudfree sky with uninterrupted sunshine.

Results of the comparisons

Comparison of the dosimeters at the reference sites during the measurement period show polysulphone measured exposures slightly below viospore measured exposures. Model calculations by SMHI and JRC respectively either are in between the dosimeters results, closer to the viospore results or higher (Fig. 5).

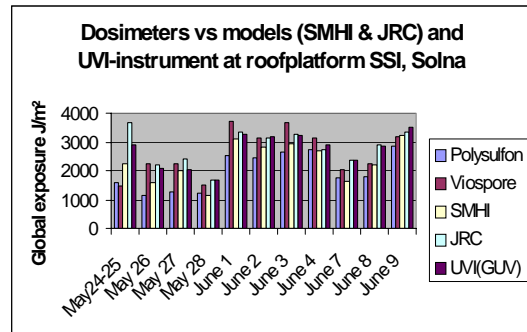


Figure 5. Polysulphone- and spore dosimeters vs SSI's UV-index monitor and the RT-model results of SMHI and of JRC for 59.35° N during weekdays May 24 – June 9 2004.

The dosimeters at the northernmost (59.5°N) and southernmost (59.2°N) sites compare in a similar way to the RT-models (not shown).

Results of the exposure of ten dosimeters of each kind June 4 show good agreement with the RT-models and SSI's solar UV-instrument that continuously measures and reports the UV-index for Stockholm. The two RT-models agree well with each other and with the UV-index instrument (Fig. 6).

Viospor- and polysulfonfilm dosimeters compared to models (SMHI & JRC) and SSI's UV-index instrument at the SSI roofplatform 4.6.2004

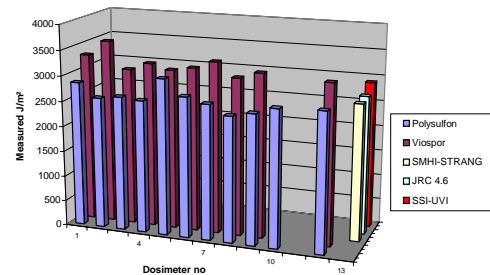


Figure 6. Results of the exposure of 10 dosimeters of each kind (plus one of each kind under quartz glass, fig. 2) compared to the two RT-models and to SSI's UV-monitoring instrument 4.6.2004 59.35° N. 1st row polysulphone results, 2nd row viospore results (1 read-out failed). 3rd–4th rows: results of the RT-models (SMHI, JRC). 5th row: result of the SSI-instrument.

An analysis shows that Viospore measured exposures June 4 on the average were a little higher than polysulphone measured exposures. Polysulphone measured exposures agreed very well with the two RT-models and possibly varied slightly less than the exposures measured with spore dosimeters (Table 1).

Thematic Network for Ultraviolet Measurements

Table 1. Average results of 10 polysulphone- and 10 bacteria spore dosimeters 4.6.2004 (and relative standard deviations) as compared to a "reference", here formed by the average of the results from JRC, SMHI and SSI.

Global erythemat exposure	Exposure ($J_{CIE} m^{-2}$)	Ratio to reference	Variability (%)
Stockholm 59.35°N, 4.6.2004			
SMHI	2691	0.97	
JRC	2732	0.98	
SSI	2899	1.05	
<i>Average</i>	<i>2774</i>	<i>1.00</i>	<i>(Reference)</i>
Viospore dosimeters	3264	1.18	6
Polysulphone badges	2699	0.97	5

The two services JRC's and SMHI's calculated global UV-exposures on a horizontal surface with free horizon agree well for full days - and for days without clouds also diurnally during the hours of the day. However for varying cloudiness and at a specific site and time of the day they may vary - because of different spatial and temporal resolutions (e.g. 1/2h of JRC's model vs 1h of SMHI's).

In the study of the children as accurate as possible temporal information of irradiance changes was needed to estimate the total available global exposure during the time periods the children spent outdoor. Therefore diurnal temporal accuracy of the RT-models of the two services JRC and SMHI was evaluated using SSI's UV-monitoring instrument for days with varying cloudcover. JRC's RT-model agreed better than SMHI's with measured changes in the UV-irradiance during days with varying cloud cover (Fig. 7).

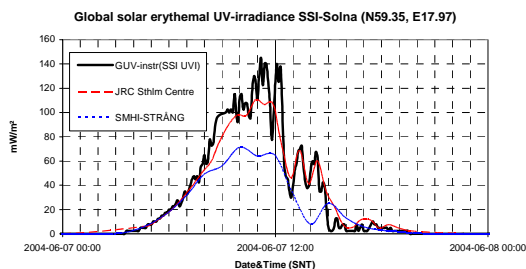


Figure 7. Temporal accuracy of RT-calculations by JRC and SMHI vs continuously measured irradiance during a changing cloud cover. Upper line (thick detailed curve): SSI's UVI-instrument (6-minute data). Middle line: 30-minute data of the JRC-model (smoothed). Lower line: 1h-data of the SMHI-model (smoothed).

Conclusions

1. Results of measurements with polysulphone badges in the study of the children's exposures did not need to be corrected.
2. The JRC-model offers higher spatial and temporal resolution than the SMHI-model, resulting in better agreement with a groundbased continuously measuring

instrument during the time course of the day, and is better suited for estimates of fragmented part-day global exposure.

Summary of the results of the study of the children

Depending on preschool, its type of surroundings and the available shade of playground installations, the children received:

- 4 – 10 % of total global full day UV
- 10 – 40 % of global UV during outdoor stay, and in terms of absolute exposure
- 100 – 270 J/m^2 erythemat UV/day

A conclusion of the study of the children was that they, if not protected, may receive considerable exposures [1]. Playground surroundings at preschools influence heavily childrens UV-exposure – and careless playground planning might double it.

Acknowledgements. The author would like to thank Dr Jean Verdebout, European Commission Joint Research Centre (JRC), Weine Josefsson and Tomas Landelius, Swedish Meteorological and Hydrological Institute (SMHI), and Dr L.-E. Paulsson, Swedish Radiation Protection Authority (SSI) for providing reference data for the research.

References

1. Boldemann C., Blennow M., Dal H., Mårtensson F., Raustorp A., Yuen K., Wester U: "Impact of pre-school environment upon children's physical activity and sun exposure", Preventive Medicine (in press 2006).
2. Wester U., Boldemann C., Dal H., Josefsson W., Landelius T., Paulsson L-E., Yuen K.: "Dosimeter study of pre-school children's UV-exposure – A measurement evaluation", UV-News #7, 35-38, 2002.
3. Boldemann C., Dal H., Wester U.: "Swedish pre-school children's UVR exposure – a comparison between two outdoor environments", Photoimmunol Photomed 2004, 20:2-8.
4. Davis A., Deane G., Diffey B.: "Possible dosimeter for ultraviolet radiation", Nature 1976, 261, 169-170.
5. CIE: "Personal Dosimetry of UV Radiation", Technical Report No CIE98, International Commission on Illumination (CIE), 1992.
6. Diffey B.: "Ultraviolet radiation dosimetry with polysulphone film", in: Radiation measurement in photobiology, Academic Press Ltd, New York, London, 1989; 136-159.
7. Quintern L., Horneck G., Eschweiler U., Bucker H.: "A biofilm used as ultraviolet dosimeter", Photochem. Photobiol.; 55, 389-395 (1992).
8. Quintern L., Furusawa Y., Fukutsu K., Holtschmidt H.: "Characterization and application of UV detector spore-films: the responsivity curve of a new detector system provides good similarity to the action spectrum for UV-induced erythema in human skin", J. Photochem. Photobiol. B: Biol. 37, 158-166 (1997).
9. Kazadzis S., Bais A., Quintern L., Holtschmidt H.: "International instrument intercomparison of the biological UV-detection film system Viospore versus high sophisticated spectroradiometers in a blind study – Weighting according to MED-CIE or DNA (Setlow)", UV-News 5, 12-14 (2000).

UVEMA: A new project exploring degrading effects of UV radiation on materials

A. Heikkilä¹, K. Hanhi², J. Kaurola¹, T. Koskela¹, J. Koskinen¹, P. Kärhä³, A. Tanskanen¹, and T. Ture⁴

1. Finnish Meteorological Institute, Helsinki, FINLAND
2. Tampere University of Technology, FINLAND
3. Helsinki University of Technology, FINLAND
4. Elastopoli Oy, Vammala, FINLAND

Introduction

UV radiation belongs to the most important environmental factors that deteriorate a variety of materials, resulting in considerable limitations in the service lifetime of many articles and structures [1-3]. Albeit the phenomenon of degradation itself is well known and recognisable, the underlying chemical and physical processes are not fully understood. Ageing experiments in laboratory do yield valuable information on these intricate phenomena. In natural conditions, however, co-operative action of UV radiation and other environmental parameters, including temperature, humidity, precipitation, and air pollutants, makes the picture utterly complicated. Due to the synergistic action of these various factors, the contribution of UV radiation alone to an observed damage is not by any means easily distinguished. To investigate degrading effects of UV radiation on materials with an emphasis on the gaps clearly identified [4-6], a project called UVEMA (Effects of UV Radiation on MAterials) has been recently launched by the Finnish Meteorological Institute with partners.

Materials and methods

Within the UVEMA project, a programme of long-term outdoor material testing has been set up at seven European observatories, covering a wide range of latitudes (28°N-68°N) and various climatological environments. Prevailing UV radiation and weather conditions will be monitored alongside with the programme at each station. Testing platforms with a set of selected material samples has been installed next to a spectroradiometer measuring global horizontal UV irradiance. Each set consists of 77 specimens fixed onto 8 racks (Fig. 1.). The samples will exit the exposure rack by rack according to a pre-defined timetable. The materials to be studied include rubber compounds, natural fibre composites, and reinforced glass fibers. Part of the rubber specimens are exposed in stretch of 10 % of their nominal length.

In addition to naturally prevailing UV radiation, artificially produced UV radiation shall be deployed in the ageing experiments of the materials. A UV irradiating device will be designed and constructed for accelerated degrading of materials on narrow wavelength bands. This is expected to yield material-specific action spectra for the properties significant to the appearance or performance of the materials. In addition, radiative characteristics of a commercially available weatherometer, widely used in artificial and accelerated

weathering tests, will be measured. As a result, a reliable estimate for the comparability of these artificial ageing conditions to those prevailing outdoors will be obtained.

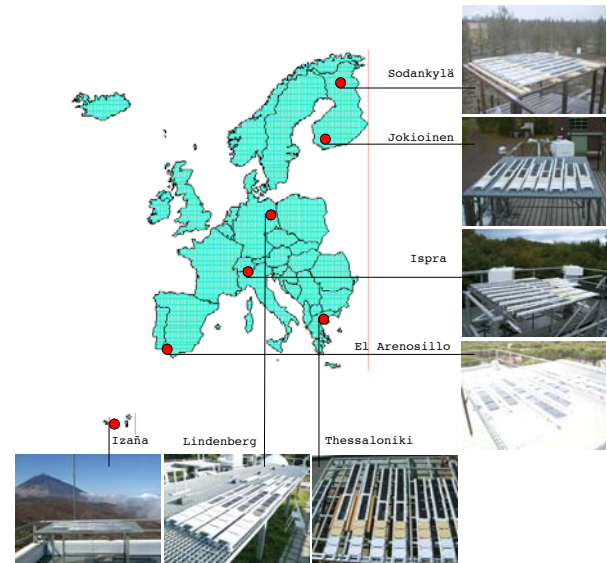


Figure 1. Material testing platforms at seven European sites within the framework of the UVEMA project.

Using appropriate tests, materials exposed to natural and artificial UV radiation will be investigated in respect of various properties. The most interesting properties are expected to include colour, quality/coarseness of the surface and compression/flexural/tensile strength. Post-exposure testing methods range from visual inspection and non-destructive testing to dynamical mechanical analysis. Optical and scanning electron microscopy as well as UV/VIS, FTIR and ED spectroscopy will be used.

The project is a joint effort of the Finnish Meteorological Institute, the Helsinki University of Technology and the Tampere University of Technology, Elastopoli Oy, and the following industrial partners: Oy All-Plast Ab, Exel Oyj, MacGregor (FIN) Oy, and Nokian Tyres plc. In addition, the following observatories cooperate in the project:

- Finnish Meteorological Institute, Arctic Research Center, Sodankylä, Finland
- Finnish Meteorological Institute, Jokioinen Observatory, Finland
- German Weather Service, Meteorological Observatory Lindenberg, Germany

Thematic Network for Ultraviolet Measurements

- Joint Research Center, Institute for Health and Consumer Protection, Ispra, Italy
- Aristotle University of Thessaloniki, Laboratory of Atmospheric Physics, Greece
- National Institute for Aerospace Technology, El Arenosillo Sounding Station, Mázagon, Spain
- Instituto Nacional de Meteorología, Observatorio Atmosférico de Izaña, Tenerife, Spain

The project is financed by the National Technology Agency (Tekes), the Finnish Meteorological Institute and the industrial partners. The project has been launched on the 1st of May 2005, with a time frame of four years. WWW-homepage for the project has been established at address <http://uvema.fmi.fi/>.

Results and discussion

Analysis of the specimens exposed to UV radiation at separate wavelengths in laboratory will give new spectrally resolved knowledge of how the materials respond to UV. Action spectra for the UV induced degradation of the most important properties shall be derived from the results of these studies. By careful characterization of a weather chamber, a relation between the artificial ageing conditions and natural outdoor environments can be established. In conjunction with the analysis of the long-term outdoor exposure tests, this will result in more reliable interpretation of the findings gained by using the current accelerated ageing methods. By incorporating all the environmental data gathered

along the outdoor exposure into the analysis, a realistic ageing model for the materials will be obtained. In the end, the results of the different workpackages of the project will be pulled together to develop a method for reliably predict the service lifetime of a material in the very environment it is used.

Acknowledgement. This work has been supported by the Finnish Funding Agency for Technology and Innovation (Tekes).

References

- [1] J.F. Rabek, *Polymer Photodegradation*, Chapman and Hall, London, 1995.
- [2] G. Wypych, *Weathering of Plastics, Testing to Mirror RealLife Performance*, Plastics Design Library, Canada, 1999.
- [3] R.L. Feller, *Accelerated Aging, Photochemical and Thermal Aspects*, The Getty Conservation Institute, Los Angeles, 1994.
- [4] The Civil Engineering Research Foundation (CERF), *Gap Analysis for Durability of Fiber Reinforced Polymer Composites in Civil Infrastructure*, Report No. 40578, 2001.
- [5] A.L. Andradý, S.H. Hamid, X. Hu, A. Torikai, "Effects of increased solar ultraviolet on materials," *J. Photochem. Photobiol.*, 1998, **46**, 96-103.
- [6] A.L. Andradý, S.H. Hamid, A. Torikai, "Effects of climate change and UV-B on materials," *Photochem. Photobiol. Sci.*, 2003, **2**, 68-72.

Standard MEAN Ultraviolet Radiation for non-Extreme Exposure Conditions: definition and indoor reproduction

*François J. Christiaens and Alain Chardon
L'Oréal Recherche, Clichy, France*

The skin is exposed to ultraviolet radiation (UVR) from natural or artificial sources on a daily basis. The solar UV irradiance is variable as it depends on geo-orbital and environmental parameters. Although ground level solar spectral irradiance is continuously varying, the research community has found it convenient to use reference spectra to assess the effects of solar UV radiation (1-5). Many of these reference spectra are representative of the “worst” case scenario, i.e. summer global sunlight (diffuse skylight + direct beam sunlight) with a clear sky, and the sun elevation being at least 80° (quasi-zenithal sun irradiance). Such extreme exposure conditions only occur at limited dates (e.g. around the 21st of June for the Cancer Tropic), near solar noon, and at specific locations ranging from 33.5° North to 33.5° South, i.e. 10° wider than the Tropical belt. Now, only a part of the world population is exposed to such radiation and many people never receive this extreme spectral power distribution. There has been much less interest in what is likely to happen under more usual conditions.

At high latitudes and shortly after sunrise or before sunset, the solar elevation angle (SEA) may be lower than 10° for time periods longer than one hour. Although the irradiance is low, individuals may be exposed for long times and biologically relevant UV doses may hit their skin; e.g. more than 7 Standard Erythema Doses (SED) may be received by a horizontal plane between 3 p.m. and 7 p.m. at latitude of 60 °N in mid-June. Because the skin of the face can be seen roughly as a vertical surface, the dose it receives can be significantly higher than 7 SED, when one enjoys staring at a sunset. The UVB proportions of the corresponding irradiance values are significantly lower than those found in zenithal sunlight. The effects of chronic cumulative low dose exposure merit investigation, even when these effects are neither conspicuous nor clinically assessable after only a limited number of exposures.

The first purpose of the present study was to define a relative spectral UV irradiance that is representative of frequent non-extreme sun exposure conditions. Solar spectral UV irradiance values were calculated for different dates and locations, using an updated version of the radiative transfer model originally described by Frederick and Lubin (6). The spectral irradiance values obtained when the solar elevation is lower than 45° were averaged. An important feature is the dUVA (320-400 nm) to dUVB (290-320 nm) irradiance values ratio [dUVB stands for “dermatological UV-B”, a convenient short-hand notation that designates the 290-320 nm wavelength range and which is already widely used in scientific communications, in comparison to the 280-315 nm UV-B waveband which was designated by the International Commission on Illumination (CIE). In turn, the 320-400 nm waveband is referred to as dUVA.]

As a result, this ratio was found to be 27.3 for the overall average (standard deviation estimated using the bootstrap method, i.e. re-sampling 50 paired dUVA and dUVB irradiance values: 0.18). When the months corresponding to extreme irradiance values (low or high) were excluded from the calculations, the dUVA to dUVB ratio ranged from 27.2 to 27.5. This work is described in an article recently published in *Photochem. Photobiol.* (7)

The usual aim of solar UV simulation is to provide relevant tools to study, under laboratory conditions, what would happen to people when exposed outdoors. Solar UV simulators are designed in such a way that their emission spectrum resembles the spectrum of summer sunlight at noontime. These exposure conditions maximize the content of dUVB radiation. Specific simulators are needed to study and assess the effects of exposure to the above mentioned standard UV daylight. Furthermore, criteria are required to check whether standard UV daylight simulators properly match the daylight spectral irradiance.

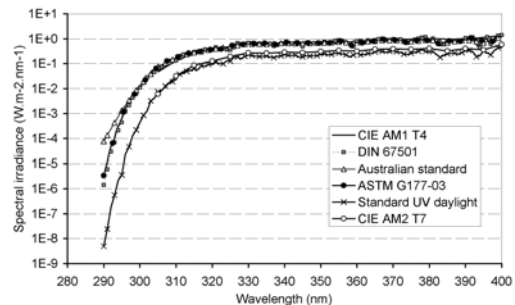


Figure 1. Solar spectral UV irradiance of several solar spectra and of the proposed standard UV daylight spectrum. “CIE AM1 T4” stands for the spectrum that can be found in the CIE report n° 85 (1989), Air Mass 1, Table 4, and “CIE AM2 T7” for the spectrum found in the same report, Air Mass 2, Table 7. “DIN 67501” stands for the spectral data published by Grothmann & Kaase. “Australian standard” refers to the Bernhard et al. publication (1997).

The second purpose of this study was to create standard UV daylight simulators and the third purpose was to define and use criteria to assess the simulators’ compliance with the above reference spectrum.

As a first criterion for UV daylight simulators, it is proposed that the ratio of dUVA / dUVB irradiance values ratio be close to 27.3, actually within the range 23-32.

Sources equipped with a xenon bulb are the most appropriate simulators of solar UV radiation. These sources can be equipped with short cut-off filters that

Thematic Network for Ultraviolet Measurements

reproduce the steep slope of the atmospheric ozone absorption. It is far much pragmatic to adapt a specific filter to existing sources than to create an entirely new source from scratch. Schott WG320 filters of appropriate thickness (around 2 mm) enable to achieve this result.

To guarantee the steepness of the short cut-off slope, a second criterion is proposed, as follows: the ratio of the spectral irradiance value at 320 nm over the spectral irradiance value at 295 nm should be more than 1,500.

We calculated the appropriate thickness of a Schott WG320 filter. The absorption of the WG-320 filter directly depends on glass thickness according to relationship as follows:

$$\log \left[\frac{T(\lambda, d_1)}{90\%} \right] = \frac{d_1}{d_2} \cdot \log \left[\frac{T(\lambda, d_2)}{90\%} \right], \quad (1)$$

where $T(\lambda, d_i)$ is the measured transmittance at a thickness d_i and 90% is the relative effect on total absorbance of the glass itself (remaining 10% due to loss by multiple reflections on filter faces). Adjusting the thickness of the glass filter enabled us to tune the absorption, so that, once the commercially available Oriel solar UV simulators were equipped with this filter, the irradiance values complied with the two first above criteria.

In accelerated tests, it may be needed that the irradiance be higher than the irradiance of the standard UV daylight. This assumes that the photo-effects depend only on the dose and not on the irradiance, in other words that they comply with the law of reciprocity. However, the irradiance integrated over the 250-2500 nm waveband should not exceed $1600 \text{ W}\cdot\text{m}^{-2}$, to avoid overheating of exposed volunteer's live skin or *in vitro* cells. This can be obtained by adjusting the radiation output of the solar simulator, which is achieving for example by tuning the current intensity delivered by the power supply or inserting a neutral density in the beam path.

Recently, Schauburger *et al.* demonstrated that the spectral match between a candidate source and a reference source had to be tested by an appropriate numerical method (8). The method involves a zenithal solar spectrum reference; however, this reference can be replaced with the standard UV daylight spectrum. In the published method, the spectral irradiance data are weighted with the CIE standard erythema action spectrum (9). The corresponding calculations have been made here: the Index of Spectral Fit exceeded 90% for all the sources and the absolute difference of the relative spectral irradiance and the relative reference UV daylight spectrum was less than 0.01. In addition, calculations using spectral irradiance data not weighted by any action spectrum have also been performed, to take into account that erythema may not always be the most relevant parameter when assessing the effects of exposure to non-extreme UV rays. The Index of Spectral Fit was higher than 80% and the absolute difference of the relative spectral irradiance and the relative reference UV daylight spectrum was less than 0.02.

Sayre *et al.* pointed out that the risks from UV exposures change throughout the day (10) and Diffey raised the issue of an appropriate protection throughout the whole

year (11): there is a necessity to use an appropriate tool to assess the required specific protection against UVR under non extreme exposure conditions. The proposed daylight spectral irradiance is representative of mean environmental UV exposure conditions that most of the population is exposed to.

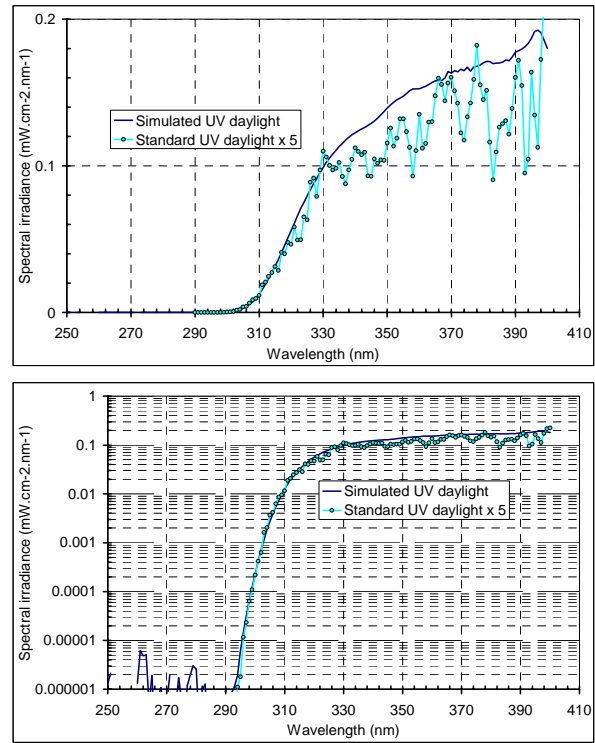


Figure 2. Standard and simulated UV daylight, plotted respectively on a linear and a semi-logarithmic scale.

In vivo studies (12) confirmed that the proposed standard UV daylight is a relevant new tool to assess the biological effects of exposure to nonextreme UVR. In addition, *in vitro* biological effects induced by the simulated standard UV daylight as defined in this paper have been studied and will be further published.

Therefore, this standard UV daylight spectrum is appropriately used both as a reference to investigate the biological effects of a non-extreme UVR and to assess the effectiveness of skin care products for daily protection.

REFERENCES

1. Commission Internationale de l'Éclairage (CIE) (1989) *Solar spectral irradiance*. Vienna, Austria. Publ. N°85. (<http://www.cie.co.at/cie/>, Central Bureau, Kegelstrasse 27, 1030 Vienna, Austria).
2. The European Cosmetic and Toiletry Association (Colipa) (1994) *Sun Protection Factor test method*. Brussels, Belgium.
3. Bernhard, G., B. Mayer, G. Seckmeyer, and A. F. Moise (1997) Measurements of spectral solar UV irradiance in tropical Australia. *J. Geophys. Res.* **102**, 8719-8730.
4. Deutsches Institut für Normung e.V.(DIN) (1999) *Experimentelle Bewertung des Erythemschutzes von externen Sonnenschutzmitteln für die menschliche Haut (Experimental evaluation of the protection from erythema*

- by external sunscreen products for the human skin). Berlin, Germany.
5. ASTM (2003) *Standard tables for reference solar ultraviolet spectral distributions: hemispherical on 37° tilted surface*. 100 Barr Harbor Drive, PO Box C700, PA 19428-2959.
 6. Frederick, J. E. and D. Lubin (1988) The budget of biologically active ultraviolet radiation in the Earth-atmosphere system. *J. Geophys. Res.* **93**, 3825-3832.
 7. Christiaens, F. J., A. M. Chardon, A. Fourtanier, and J. E. Frederick (2005) Standard Ultraviolet Daylight for non Extreme Exposure Conditions. *Photochem. Photobiol.* **81**, 874-878.
 8. Schauburger, G., H. Maier, A. Cabaj, and A. W. Schmalwieser (2004) Evaluation of the goodness of fit of solar simulated radiation to a reference solar spectrum for photobiological experiments. *Med. Phys.* **31**, 2509-2519.
 9. Commission Internationale de l'Éclairage (CIE). Erythema reference action spectrum and standard erythema dose. 1998. Vienna, Austria, CIE Central Bureau.
 10. Sayre, R. M., N. Kollias, R. D. Ley, and A. H. Baqer (1994) Changing the risk spectrum of injury and the performance of sunscreen products throughout the day. *Photodermatol. Photoimmunol. Photomed.* **10**, 148-153.
 11. Diffey, B. L. (1996) Population exposure to solar UVA radiation. *Eur. J. Dermatol.* **3**, 221-222.
 12. Seité, S., Medaisko, C., Christiaens, F., Bredoux, C., Compan, D., Zucchi, H., Lombard-Girard, D., and A. Fourtanier (2006) Biological effects of simulated ultraviolet daylight: a new approach to investigate daily photoprotection. *Photodermatol. Photoimmunol. Photomed.* **22**(2), 67-77.

Calibration of UV radiometers is needed to guarantee the relevance of measurements

François J. Christiaens and Alain Chardon
L'Oréal Recherche, Clichy, France

Introduction

Nowadays, the protocol of any biological study involving a source that emits ultraviolet (UV) radiation implies the measurement of the UV dose received by the irradiated sample or skin. Most of the time, the dose is calculated by multiplying the measured irradiance by the duration of exposure.

UV sources may differ from one laboratory to another or from one study to another. Several authors evidenced wide divergences between radiometric readings, especially in the dUVB range (dUVB: 290-320 waveband) (1-4). These errors can, and have to, be corrected, for example in phototherapy treatments (5).

Published results involve a limited set of radiometers. The objective of this study was to estimate the extent of variation of irradiances that are measured by different radiometers.

Materials and methods

The UV irradiance from a unique source has been measured with different commonly available UV meters and with a calibrated spectroradiometer. A 4'' x 4'' xenon UV source (LOT Oriel, Palaiseau, France) was equipped with a Schott UG-11 / 1 mm thick filter to fully remove visible and infrared radiation. For solar UV simulation, a Schott WG-320 / 1,5 mm filter was added. For selecting dUVA rays only, this filter was replaced by a Schott WG-335 / 3 mm thick filter (dUVA: waveband 320-400 nm). In the dUVB waveband, the shape of the measured solar UV simulated irradiance (upper curve, Fig. 1) corresponds to that of summer sun at noon. This spectrum complies both with the requirements for sunscreen Sun Protection Factor testing (6). The dUVA spectral irradiance (lower curve, Fig. 1) complies with the JCIA requirements for measuring the level of dUVA protection afforded by sunscreens using the Persistent Pigment Darkening test method (7).

Corresponding irradiances were measured with commonly available radiometers (Solar Light Co, Philadelphia, PA, type PMA2100, 3D600 & Dose Control System, Osram type Centra, International Light, Müller) in parallel with a double-monochromator spectroradiometer (9910, Macam Photometrics Ltd, Livingston, UK). The spectroradiometer had been previously calibrated against a standard Quartz Tungsten Halogen lamp, which is traceable to the National Physical Laboratory (Teddington, Middlesex, UK).

No correction has been made on the radiometers readings. The output of the UV source, which is equipped with a

photofeedback, was assumed to be constant for the whole duration of the measurement session. Some radiometers measured an erythema-weighted irradiance and displayed erythema-weighted units, e.g. MED·min⁻¹ (Minimum Erythemal Dose per minute). To calculate erythema-weighted dose rates from spectral measures, the spectral irradiances were weighted by the CIE MED action spectrum (8) and the threshold sensitivity to get an MED was set at 21 mJ·cm⁻²·ery, which corresponds to the sensitivity of a phototype 2 person (9).

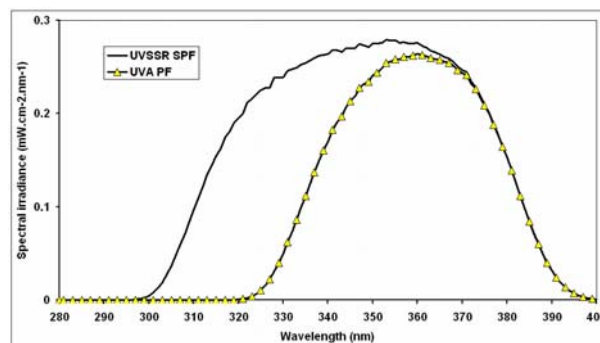


Figure 1. Spectral irradiances with the UV source. Such spectra are the only ones which are internationally used to assess the protection factors afforded by sunscreens.

In a second series of measures, irradiances were reduced by a tenfold factor, using a diaphragm inserted inside of the UV source. Measures were made in order to determine whether the correction factor calculated for high irradiance would be affected (test of the linearity of the radiometers).

Results

Tables 1 & 2 compare the integrated irradiances measured by the spectroradiometer and by the radiometers.

Wide differences in response were recorded, mainly between the various categories of instruments. The irradiance calculated from spectroradiometric measurements has been taken as the reference. For each radiometer and filtration of the source, a correction factor was calculated, with which the radiometer readings have to be multiplied to provide the same integrated fluence observed from spectroradiometric measurements. This correction factor ranges from 0.54 to 2.22 for erythemal irradiance, 0.86 to 5.51 for dUVA from the UVSSR source and from 0.77 to 4.32 for the dUVA source. This emphasizes the need for applying the correction factor.

Table 1.

UVSSR SPF high											UVA SPF high		
Meter	Brand	Model	Serial number	Probe(s)	Entrance optics	UVB irradiance (mW.cm ⁻²)	UVB correction factor	Erythral irradiance (MED.hr ⁻¹)	Erythral correction factor	UVA irradiance (mW.cm ⁻²)	UVA correction factor	UVA irradiance (mW.cm ⁻²)	UVA correction factor
Spectro	Macam	9910 V7	6065		Side-View diffuser	1.94	1.000	22.61	1.000	15.89	1.000	11.52	1.000
Radio	Solar Light	PMA 2100	-	Erythral UV: n° 2627 UVA: n° 2656	LLG			13.30	1.70	12.30	1.29	10.20	1.13
Radio	Solar Light	PMA 2100	-	Erythral UV: n° 2619 UVA: n° 2649	LLG			13.50	1.68	10.90	1.46	9.05	1.27
Radio	Solar Light	PMA 2100	-	Erythral UV: n° 4515 UVA: n° 4469	LLG			22.10	1.02	11.60	1.37	9.38	1.23
Radio	Solar Light	PMA 2100	-	Erythral UV: n° 4516 UVA: n° 4470	LLG			20.10	1.13	11.30	1.41	9.16	1.26
Radio	Solar Light	PMA 2100	-	Erythral UV: n° 2618 UVA: n° 2648	LLG			20.20	1.12	11.20	1.42	9.20	1.25
Radio	Solar Light	PMA 2100	-	Erythral UV: n° 4200 UVA: n° 2423	Flat, teflon diff.			19.20	1.18	16.90	0.94	13.45	0.86
Radio	Solar Light	PMA 2100	-	Erythral UV: n° 4201 UVA: n° 5273	Flat, teflon diff.			16.40	1.38	16.90	0.94	13.65	0.84
Radio	Solar Light	PMA 2100	-	Erythral UV: n° 2353 UVA: n° 5274	Flat, teflon diff.			21.68	1.04	17.30	0.92	13.70	0.84
Radio	Solar Light	PMA 2100	-	Erythral UV: n° 2306 UVA: n° 2399	External Use			21.80	1.04	18.50	0.86	14.95	0.77
Radio	Osram	Centra	1092	UVB: n° 1092 UVA: n° 1228	Teflon diffuser	0.977	1.99			12.25	1.30	9.14	1.26
Radio	Osram	Centra	1172	UVB: n° 1172 UVA: n° 1172	Teflon diffuser	0.098	19.81			8.22	1.93	6.57	1.75
Radio	Osram	Centra	2017	UVB: n° 2017 UVA: n° 2017	Teflon diffuser	1.73	1.12			3.40	4.67	9.12	1.26
Radio	Osram	Centra	2018	UVB: n° 2018 UVA: n° 2018	Teflon diffuser	0.93	2.09			9.98	1.59	8.70	1.32
Radio	Osram	Centra	2022	UVB: n° 2022 UVA: n° 2022	Teflon diffuser	1.02	1.90			11.21	1.42	9.82	1.17
Radio	Solar Light	Dose Control System	1212	Erythral UV: n° 1212 UVA: n° 1212	LLG			42.00	0.54	17.67	0.90	9.33	1.23
Radio	Solar Light	3D 600	310	Erythral UV: n° 310 UVA: n° 310	LLG			10.2	2.22	2.83	5.61	2.67	4.32
Radio	International Light	1700	1752	UVB: SED240 TW n° 3465 UVA: SED033 TW n° 3737	Teflon diffuser	1.07	1.31			11.60	1.37	9.16	1.26
Radio	International Light	1700	180	UVB: SED240 TW n° 1958 UVA: SED038 TW n° 1177	Teflon diffuser	0.318	6.11			8.46	1.38	6.77	1.70
Radio	Müller	Thermopile	-		LLG					7.60	1.67	4.80	2.40
	LLG: Coaxial for Liquid Light Guide				Mean	0.88	4.98	20.04	1.28	11.59	1.73	9.41	1.43
					Standard deviation	0.54	6.74	8.31	0.45	4.47	1.25	3.05	0.79
					Coefficient of variation	61%	136%	41%	35%	39%	72%	32%	56%

Table 2.

UVSSR SPF low											UVA SPF low		
Meter	Brand	Model	Serial number	Probe(s)	Entrance optics	UVB irradiance (mW.cm ⁻²)	UVB correction factor	Erythral irradiance (MED.hr ⁻¹)	Erythral correction factor	UVA irradiance (mW.cm ⁻²)	UVA correction factor	UVA irradiance (mW.cm ⁻²)	UVA correction factor
Spectro	Macam	9910 V7	6065		Side-View diffuser	0.20	1.000	2.34	1.000	1.66	1.000	1.22	1.000
Radio	Solar Light	PMA 2100	-	Erythral UV: n° 2627 UVA: n° 2656	LLG			1.40	1.67	1.33	1.25	1.14	1.07
Radio	Solar Light	PMA 2100	-	Erythral UV: n° 2619 UVA: n° 2649	LLG			1.40	1.67	1.21	1.37	0.99	1.23
Radio	Solar Light	PMA 2100	-	Erythral UV: n° 4515 UVA: n° 4469	LLG			2.27	1.03	1.24	1.34	1.05	1.16
Radio	Solar Light	PMA 2100	-	Erythral UV: n° 4516 UVA: n° 4469	LLG			2.10	1.12	1.23	1.35	1.03	1.19
Radio	Solar Light	PMA 2100	-	Erythral UV: n° 2618 UVA: n° 2648	LLG			2.19	1.07	1.21	1.37	1.04	1.17
Radio	Solar Light	PMA 2100	-	Erythral UV: n° 4200 UVA: n° 2423	Flat, teflon diff.			2.00	1.17	1.75	0.95	1.45	0.84
Radio	Solar Light	PMA 2100	-	Erythral UV: n° 4201 UVA: n° 5273	Flat, teflon diff.			1.64	1.43	1.77	0.94	1.52	0.80
Radio	Solar Light	PMA 2100	-	Erythral UV: n° 2353 UVA: n° 5274	Flat, teflon diff.			2.24	1.05	1.82	0.91	1.49	0.82
Radio	Solar Light	PMA 2100	-	Erythral UV: n° 2306 UVA: n° 2399	External Use			2.12	1.11	1.93	0.86	1.58	0.77
Radio	Osram	Centra	1092	UVB: n° 1092 UVA: n° 1228	Teflon diffuser	0.11	1.79			1.36	1.22	1.04	1.17
Radio	Osram	Centra	1172	UVB: n° 1172 UVA: n° 1172	Teflon diffuser	0.037	5.32			0.88	1.88	0.74	1.65
Radio	Osram	Centra	2017	UVB: n° 2017 UVA: n° 2017	Teflon diffuser	0.179	1.10			1.13	1.47	1.00	1.22
Radio	Osram	Centra	2018	UVB: n° 2018 UVA: n° 2018	Teflon diffuser	0.097	2.03			1.09	1.52	0.96	1.27
Radio	Osram	Centra	2022	UVB: n° 2022 UVA: n° 2022	Teflon diffuser	0.107	1.84			1.24	1.34	1.08	1.13
Radio	Solar Light	Dose Control System	1212	Erythral UV: n° 1212 UVA: n° 1212	LLG			18.00	0.13	0.80	2.07	0.70	1.74
Radio	Solar Light	3D 600	310	Erythral UV: n° 310 UVA: n° 310	LLG			1.2	1.95	0.20	8.28	-	-
Radio	International Light	1700	1752	UVB: SED240 TW n° 3465 UVA: SED033 TW n° 3737	Teflon diffuser	0.11	1.31			1.22	1.36	0.97	1.26
Radio	International Light	1700	180	UVB: SED240 TW n° 1958 UVA: SED038 TW n° 1177	Teflon diffuser	0.0325	6.06			0.87	1.80	0.73	1.68
Radio	Müller	Thermopile	-		LLG					0.70	1.85	1.50	0.81
					Mean	0.10	2.84	3.32	1.22	1.24	1.74	1.11	1.17
					Standard deviation	0.05	1.97	4.88	0.48	0.42	1.67	0.28	0.30
					Coefficient of variation	52%	69%	147%	39%	34%	96%	25%	26%

Thematic Network for Ultraviolet Measurements

For all the Solar Light PMA and Osram Centra radiometers, the same correction factor was applicable at high and low irradiances (ratio of correction factors did not differ by more than 6%). For some other (older) radiometers, the correction factor did depend on the irradiance level (e.g. correction factor for radiometer #1172 measuring low dUVB irradiance: 5.32; measuring high irradiance: 19.81); this encourages discarding their measurement.

Discussion

Such discrepancies between instruments are mainly due to the following causes:

- Manufacturers often calibrate their radiometers against standard sources with a spectrum different from the one measured;
- The spectral response of the meter; the response curves of the sensors given by the manufacturers suggest that they respond to wavelengths outside the waveband for which they were calibrated;
- In addition, the discrepancies might have even been greater if sources with more vastly different spectral and geometrical characteristics were involved, e. g. sources that would not emit a collimated beam like the one used here.

Conclusion

The proposed solution is to systematically measure every UV source both with a radiometer and a calibrated, double-monochromator spectroradiometer, calculate the irradiances, and then determine a specific correction factor and correct, or adjust when possible, the readings of the radiometer. The calibration of a UV meter against the spectral irradiance of a given source it measures is a prerequisite to guarantee the reliability of results.

References

1. Sayre, R. M. and L. H. Kligman (1992) Discrepancies in the measurement of spectral sources. *Photochem. Photobiol.* **55**, 141-143.
2. Wengraitis, S., D. Benedetta, and D. H. Sliney (1998) Intercomparison of effective erythematous irradiance measurements from two types of broad-band instruments during June '95. *Photochem. Photobiol.* **68**, 179-182.
3. Kolari, P. J., J. Lauharanta, and M. Hoikkala (1986) Midsummer solar UV-radiation in Finland compared with the UV-radiation from phototherapeutic devices measured by different techniques. *Photodermatology* **3**, 340-345.
4. Diffey, B. L. (1987) A comparison of dosimeters used for solar ultraviolet dosimetry. *Photochem. Photobiol.* **46**, 55-60.
5. Coleman, A. J., M. Collins, and J. E. Saunders (2000) Traceable calibration of ultraviolet meters used with broadband, extended sources. *Phys. Med. Biol.* **45**, 185-196.
6. Cosmetics, Toiletry and Fragrance Association of South Africa, The European Cosmetic, Toiletry and Perfumery Association (Colipa), Japan Cosmetic Industry Association and the Cosmetic, Toiletry, and Fragrance Association (2006) *International Sun Protection Factor test method*. Avenue Herrmann Debroux 15A, 1160 Auderghem, Brussels, Belgium, <http://www.colipa.com>.
7. Japan Cosmetic Industry Association (JCIA) (1995) *Measurement standards for UVA efficacy*. Tokyo, Japan.
8. Commission Internationale de l'Éclairage (1998) *Erythema reference action spectrum and standard erythema dose*. Publ. N° S 007. CIE Central Bureau, Keglestrasse 27, 1030 Vienna, Austria, <http://www.cie.co.at>.
9. The Working Group 4 of the COST-713 Action 'UVB Forecasting' (2000) *UV-Index for the Public -- A guide for publication and interpretation of solar UV Index forecasts for the public*. The European Communities Eds, ISBN 92 828 81542 3, <http://www.lamma.rete.toscana.it/uvweb/uvbooklet/>.

Solar simulators as a tool for assessing the impact of UV radiation on organisms and ecosystems

A. Albert, H.K. Seidlitz, and J.B. Winkler

GSF National Research Center for Environment and Health, Neuherberg, Germany

Abstract

Several researchers have pointed out that a realistic risk assessment of damages induced by UV-B radiation in organisms, especially in plants, can only be obtained if the experiments are performed under natural light and radiation conditions. This applies particularly to the balance between the UV-B, UV-A, and the visible or photosynthetic active component of solar radiation. The natural global radiation varies during the day and year both by intensity and spectral composition, which has to be taken into account for a realistic simulation of the solar radiation.

This contribution describes solar simulators at the GSF Research Center using state-of-the-art techniques for lighting and spectral shaping methods to obtain realistic and reproducible UV scenarios. The integrated irradiances reach values close to outdoor levels measured at our field station in Neuherberg near Munich, Germany. The spectral measurements demonstrate that our artificial sunlight provides a very close approximation of natural solar radiation in the range from 280 to 850 nm especially at the steep UV-B cut-off at the shortwave edge. The use of UV filters allows us to simulate the impact of increased UV radiation on various organisms and their acclimatisation to these conditions.

Introduction

Man-made influences are changing the environmental conditions on earth globally. Due to the increased emission of chlorofluorocarbons (CFC) the stratospheric ozone layer has been decreasing in the last years followed by an increase of UV-B radiation (280 – 315 nm) (WMO, 2003). The depletion is variable over the course of the year. Although the UV-B dose is much less in late winter and early spring than in summer, the proportional increase of UV-B radiation is greatest during spring. Therefore, the growth of crops and other plants is affected nevertheless. Furthermore, the emission of CO₂ is causing an additional greenhouse effect as a result of the use of fossil fuels. Presently, the dominating environmental impact during the summer months is the tropospheric ozone owing to photochemical reactions of nitrogen oxide and hydrocarbon coming from natural and man-made sources. Organisms, especially plants, respond to these environmental impacts with changes in production, growth, pigments, and various metabolic pathways. Finally, the stability and competitive position of plants can be modified (e.g. Körner, 2000; Caldwell et al., 2003; Ashmore, 2005).

The mechanisms of plant responses to stress caused by UV radiation and their co-action with other stress factors are not yet understood completely. In order to validate the plants' responses in their natural habitat, it is necessary to perform the respective experiments under realistic and

reproducible conditions. Especially the lighting requires careful design. Not only the quantity, but also the spectral quality, has to match seasonal and diurnal variations of the global radiation as close to nature as possible. This includes the steep absorption characteristics of UV radiation resulting from the filtering of solar irradiance by stratospheric ozone as well as the balance between the UV-B (280 – 315 nm), UV-A (315 – 400 nm), and the photosynthetic active radiation (PAR, 400 – 700 nm). A typical spectrum of global radiation at the GSF field station (11.6 E, 48.2 N, 489 m above sea level) and ranges of UV-B, UV-A, and PAR is shown in Fig. 1. Therefore, a phytotron facility was developed at the GSF Research Center, which meets these requirements. Sun simulators and exposure chambers are operated, where a multitude of environmental conditions typically for the mid latitudes can be simulated (Thiel et al., 1996).

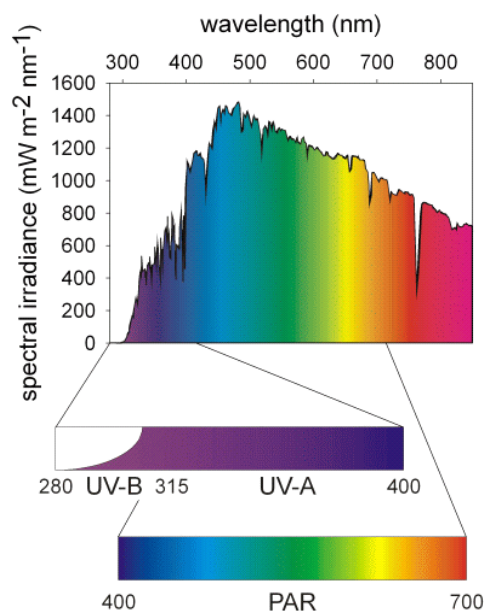


Figure 1. Typical spectrum of global irradiance and ranges of UV-B, UV-A, and PAR measured at our field station on a sunny spring day.

Technology

The phytotron facility consists of a set of seven closed chambers (length x width x height):

- four walk-in-size chambers (3.4 x 2.8 x 2.5 m³),
- two medium-size sun simulators (1.4 x 1.4 x 1.0 m³),
- one small sun simulator (1.2 x 1.2 x 0.3 m³).

As no single artificial light source can simulate both, spectral quality and spectral quantity of global irradiance, a combination of metal halide lamps, quartz halogen lamps, and blue fluorescent tubes are used in order to simulate the spectrum from the UV-A to the infrared wavelengths. Excess infrared radiation is removed by a

Thematic Network for Ultraviolet Measurements

layer of water. The missing UV-B irradiance is supplemented by UV-B fluorescent tubes. The radiation output of these fluorescent tubes, however, extends to well below 280 nm. This portion must be blocked very efficiently. Selected borosilicate and lime glass filters provide a sufficiently steep cut-off at the desired wavelength. Different combinations of these glasses allow a variation of the cut-off wavelength, thus enabling us to simulate various UV-B scenarios (Döhring et al., 1996). The diurnal variations of the irradiance are realised by switching appropriate groups of lamps on and off. Fig. 2 shows a schematic outline of our sun simulators and exposure chambers.

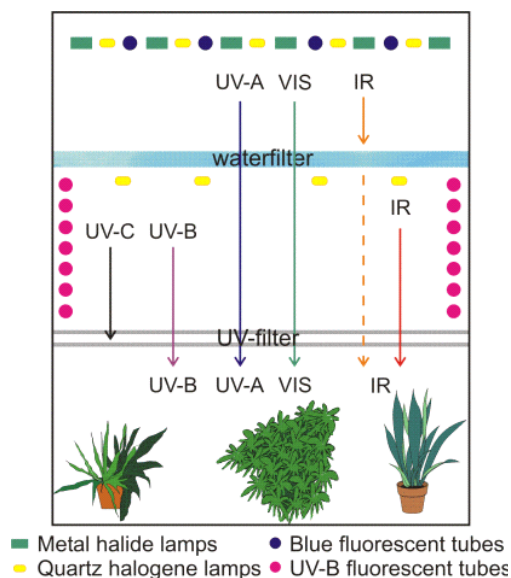


Figure 2. Schematic outline of the lamp and filter configuration of the GSF solar simulators.

The lighting data of the phytotron facility demonstrate that the lighting technology has reached a high quality level. There are two steps of quality assurance during all experiments:

- spectroradiometry from 250 to 850 nm with double monochromator (Bentham TDM300, Reading, UK) to adjust UV-B cut-off before start of experiments,
- light and radiation monitoring during experiments using integrated sensors for the UV-B, UV-A, and PAR ranges for controlling of e.g. lamp failure, filter degradation or contamination by dust or steam.

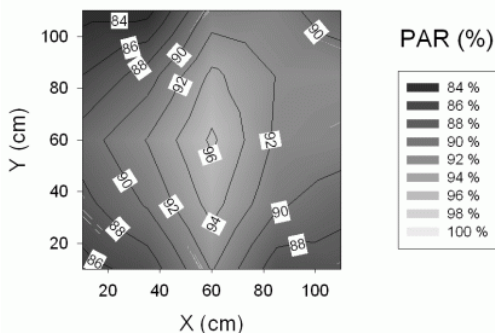


Figure 3. Horizontal distribution of PAR in the experimental space of the small sun simulator.

The data of integrated sensors are calibrated using numerical integrated spectral data of the double monochromator. The horizontal distribution of PAR in the experimental space of the small sun simulator is presented in Fig. 3. The decrease of the intensity is only about 10 – 15 % at the edges. The horizontal distribution of UV-B and UV-A radiation is similar and not shown here.

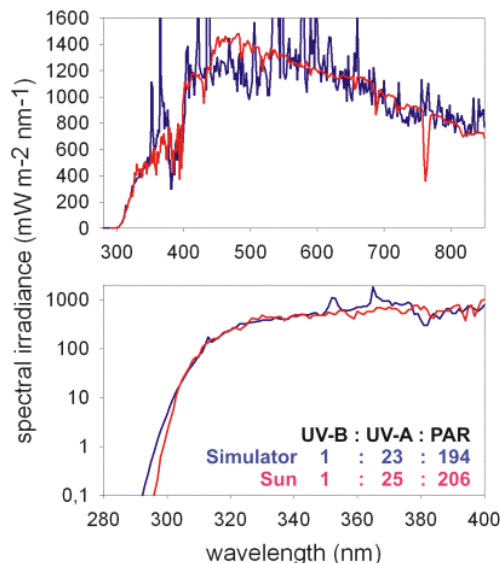


Figure 4. Spectral irradiance and UV-B:UV-A:PAR ratio in the small sun simulator (blue) compared to a typical outdoor spectrum measured at our field station (red).

Measurements in our sun simulators and exposure chambers show that the steep, realistic shape of the UV-B edge and the UV-B:UV-A:PAR ratio can be simulated very close to nature. Fig. 4 shows a comparison of the spectral irradiance of the small sun simulator and a typical outdoor spectrum measured at our field station. The UV-B:UV-A:PAR ratio of the sun simulator matches the natural conditions very well. Typical lighting data of the solar simulators compared to a field measurement (on 17/04/1996 at the GSF Research Center, solar zenith angle $\theta_s = 38^\circ$) are listed in Table 1.

Table 1. Typical lighting data of the small sun simulator (S) and the walk-in-size chambers (L) compared to a typical outdoor measurement (O).

	S	L	O	Unit
UV-B	1.53	1.20	1.10	W m ⁻²
UV-A	54.9	22.7	47.2	W m ⁻²
PAR	430	250	390	W m ⁻²
Illum.	117	71	98	klx

Besides the lighting, temperature, and humidity, the chamber atmosphere can also be controlled. Typical gaseous pollutants such as ozone, nitric oxides, and combustion residuals can be applied. The effects of carbon dioxide and hydrocarbons on plants can also be studied. Modern control technology with central monitoring allows a safe and well-defined operation.

Application

One recent project is to investigate natural compounds and gene expression of barley under the influence of UV-B radiation. Young barley is exposed one week in the sun simulator. Compared to actual conditions, reduced and enhanced UV-B scenarios are adjusted by Schott coloured glass filters (thickness 3 mm, Schott, Mainz, Germany) WG295, WG305, WG320, WG335, and WG360 in combination with a layer of soda-lime glass Sanalux (thickness 4mm, DESAG, Grünenplan, Germany). The six different spectra are shown in Fig. 5 together with a field measurement (on 27/05/2005 at GSF Research Center, solar zenith angle $\theta_s = 30^\circ$).

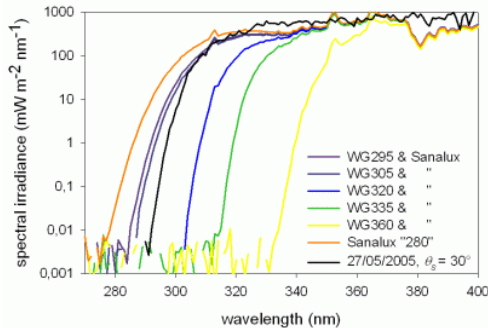


Figure 5. Different UV scenarios for investigations on barley (coloured lines) compared to a typical outdoor measurement at our field station (black line).

Figure 6 shows the diurnal course of natural and simulated (under the Schott filter WG305) UV-B radiation. PAR is varied accordingly from 114 to 363 $W m^{-2}$ ($537 - 1692 \mu mol m^{-2} s^{-1}$).

The leaves are analysed afterwards to estimate the amount of natural compounds, especially those with protective functions and influence on gene transcription. The UV-B scenarios also allow the determination of action spectra for the different processes using the biological dose function.

Conclusion

This presentation describes our phytotron facility consisting of seven solar simulators. This system allows ecological experiments for plants and other organisms under controlled and reproducible conditions of irradiance and climatic parameters. Spectral measurements have demonstrated that (i) the spectral irradiance very close to solar radiation (280 – 850 nm), (ii) a steep and realistic UV-B cut-off using different glasses and filters, and (iii) a UV-B:UV-A:PAR ratio very close to natural conditions could be obtained. Quality assurance is given by spectroradiometry before start of every experiment followed by a continuous monitoring of

integrated values of irradiance in the UV-B, UV-A, and PAR range.

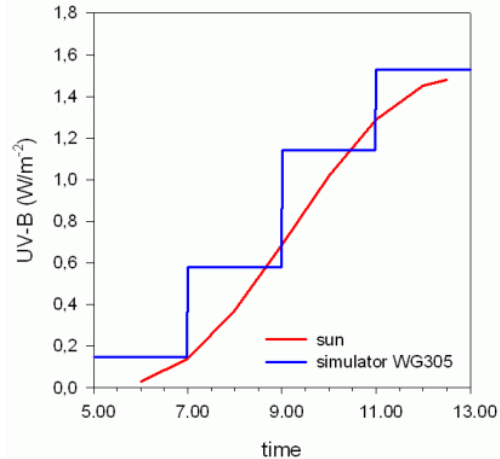


Figure 6. Diurnal variation of UV-B dose in the sun simulator (blue) for the experiment with barley compared to typical outdoor values measured at our field station (red).

Acknowledgements. Further information and pictures of the facility are available from the website <http://www.gsf.de/epoka>. We want to thank our technical staff D. Arthofer, P. Kary, J.A. Meier, A. Richter, B. Rieger, and W. Rupprecht for their efforts operating our phytotron facility.

References

- Ashmore, M.R., "Assessing the future global impacts of ozone on vegetation," *Plant, Cell and Environment* **28**, 949-964, 2005.
- Caldwell, M.M., Ballaré, C.L., Bormman, J.F., Flint, S.D., Björn, L.O., Teramura, A.H., Kulandaivelu, G., and Tevini, M., "Terrestrial ecosystems, increased solar ultraviolet radiation and interactions with other climatic change factors," *Photochem. Photobiol. Sci.* **2**, 29-38, 2003.
- Döhring, T., Köfferlein, M., Thiel, S., and Seidlitz, H.K., "Spectral shaping of artificial UV-B irradiation for vegetation stress research," *J. Plant Physiol.* **148**, 115-119, 1996.
- Körner, C., "Biosphere responses to CO2 enrichment," *Ecological Applications* **10**, 1590-1619, 2000.
- Thiel, S., Döhring, T., Köfferlein, M., Kosak, A., Martin, P., and Seidlitz, H.K., "A phytotron for plant stress research: how far can artificial lighting compare to natural sunlight?," *J. Plant Physiol.* **148**, 456-463, 1996.
- WMO (World Meteorological Organization), "Scientific Assessment of Ozone Depletion: 2002," *Global Ozone Research and Monitoring Project* **47**, 498 pp., Geneva, 2003.

Long-term measurements of UV-solar radiation in Dortmund (Germany)

*Günter Ott, Marco Janßen, Ljiljana Udovicic, and Rüdiger Pipke
Federal Institute for Occupational Safety and Health, Dortmund, Germany*

German UV-Monitoring Network

UV radiation is an important environmental parameter which has to be continuously monitored. Since 1993 the Federal Office for Radiation Protection (Bundesamt für Strahlenschutz, Salzgitter) together with the Federal Environmental Agency (Umweltbundesamt, Berlin) run a German UV-monitoring network. From the very beginning the Federal Institute for Occupational Safety and Health (Bundesanstalt für Arbeitsschutz und Arbeitsmedizin, Dortmund) has been an associated member of the network. To date, UV-monitoring is performed at ten stations (see Figure 1) by the following institutions:

- München-Neuherberg by the Federal Office for Radiation Protection
- Zingst, Langen and Schauinsland by the Federal Environmental Agency
- Lindenberg by the German Federal Meteorological Service (Deutscher Wetterdienst)
- Sylt by the University of Kiel (Christian-Albrechts-Universität zu Kiel)
- Dortmund by the Federal Institute for Occupational Safety and Health
- Kulmbach by the Bavarian Environmental Protection Agency (Bayerisches Landesamt für Umweltschutz)
- Hannover and Norderney by the Lower Saxony State Agency for Ecology (Niedersächsisches Landesamt für Ökologie)

By the choice of these locations representative regions in Germany concerning latitudes, altitudes, climatic conditions and environmental burdens in the troposphere (heavy industry, population density) are taken into account. UV data from all the stations are automatically transferred to the station in München-Neuherberg, which is a reference station with the task of quality control and assurance of all the data.

The main aim of the network is to obtain long-term series of UV data which can be used in further assessments related to the depletion of the ozone layer, to health and environmental issues of the general population as well as the outdoor workers, to report on the level of the current solar UV exposure and to provide the population with guidelines for appropriate early protection.

Information about the monitoring network, measurement data as well as UV-index values of all stations are presented online on <http://www.suvmonet.de/>. UV-index broadcast for the North, Middle and South of Germany are presented under <http://www.bfs.de/uv/uv2/uvi>.



Figure 1. German solar UV-monitoring network.

UV-Measuring Station in Dortmund

The UV-measuring station of the Federal Institute for Occupational Safety and Health in Dortmund (Figure 2) operates at 51° 32' N, 7° 27' E and 100 m above sea level. Spectrally resolved measurements of UV-solar radiation are performed with a double monochromator DTM 300 (Bentham) in the wavelength range between 290 nm and 450 nm. The total global irradiance (UV-IR) is measured by a pyranometer CM 11 (Kipp & Zonnen). The data have been measured continuously during the last nine years. The parameters of temperature, atmospheric pressure, humidity and cloudiness are delivered by the German Federal Meteorological Service.

Measuring time is every 6 minutes, starting half an hour after sunrise and finishing half an hour before sunset. One spectrum is measured in ca. 90 seconds. The system sensitivity is 1 $\mu\text{W}/\text{m}^2$ with a bandwidth of 1 nm. It is calibrated with a 1000 W halogen lamp unit (standard of the national metrology institute PTB, Physikalisch-Technische Bundesanstalt).

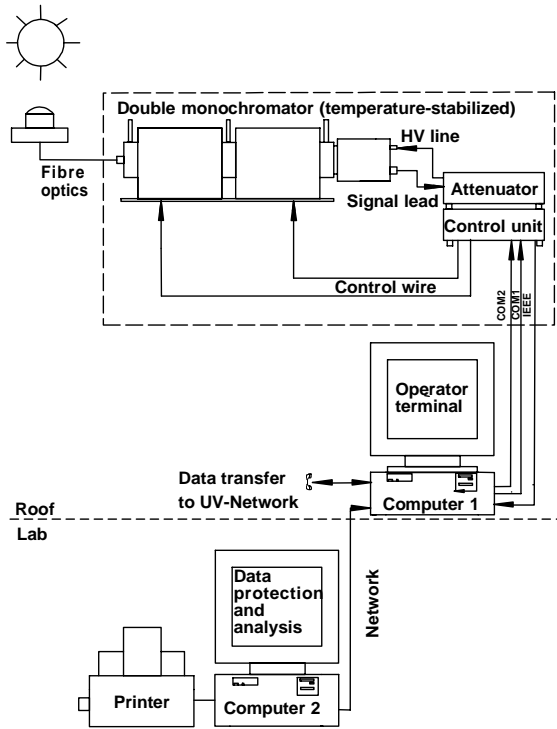


Figure 2. UV-measuring station in Dortmund: experimental setup.

The erythemal weighted irradiance is used as a measure for the biological effect of UV exposure. For this purpose, the measured spectral irradiance (as shown in Figure 3) is multiplied by the relative erythemal weighting function and the resulting function integrated from 290 nm to 400 nm. The erythemal irradiance vs time is shown in Figure 4. During summer months, the erythemal irradiance measured at our station reaches sometimes a value of 200 mW/m². This value

corresponds to a UV index of 8, i.e. the approximate time for sunburn is less than 20 minutes and, therefore, protective measures are indispensable.

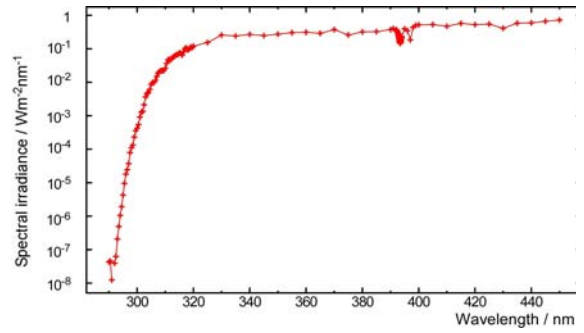


Figure 3. Non-weighted UV-solar irradiance spectrum.

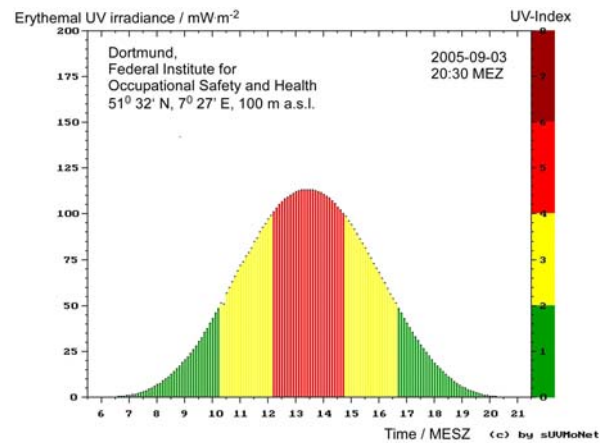


Figure 4. Erythemal UV-irradiance spectrum.

Analysis of UV-B solar radiation in C.I.B.A. laboratory, Spain

*J. Bilbao, A. Miguel, A. Pérez-Burgos and P. Salvador
Department of Applied Physics, Valladolid University, Spain*

Abstract. Experimental data concerning the integrated ultraviolet-B solar radiation (280-315nm) on a horizontal surface measured at C.I.B.A. (Low Atmosphere Research Centre), Valladolid, Spain, along the period July 2002 and June 2005 have been analyzed. A study of the most representative statistical indices: arithmetic mean, median, standard deviation, maximum, minimum, first and third quartiles, percentiles 5 (P5) and 95 (P95), inter-quartile range and coefficient of quartile variation, of the UV-B radiation for this period has been carried out. It has been found that maximum daily values are reached in June, 45 kJm⁻²day⁻¹; standard deviation values are not high but increase in the central hours of the day when UV-B irradiance is higher; June shows high stability.

Introduction

The knowledge of solar UV radiation reaching the Earth's surface has a great interest because of its significant role in atmospheric and biological processes. The UV-B solar radiation (280-315 nm) represents less than 1% of the total radiation reaching the earth surface, and it is very important for the Earth-living systems because it is a radiation of high energy. UV-B irradiance on the Earth surface depends on geographical factors such as latitude, height, earth-sun distance, solar zenith angle (SZA), etc. (Palancar and Toselli, 2004). The influence of these factors can be evaluated using different radiative models. However UV-B solar radiation depends on atmospheric parameters like ozone, clouds and aerosols. Ozone is the gas that absorbs UV-C and some UV-B solar radiation and the effect of the total ozone column is included in all radiative models. Clouds are another attenuating factor of UV-B radiation and due to their random nature they are difficult to model. Aerosol is the factor that affects radiation levels under cloudless sky conditions, (Acosta and Evans, 2000).

UVT (ultraviolet total solar irradiance) data have been studied by different authors, Martinez-Lozano et al., (1996), Miguel et al (2005), etc. The objective of this work is the study of UV-B data with the purpose of developing a standard climatology of the region that is necessary to establish its seasonal and geographical distribution and its values and oscillations. In this way, its evolution is determined with the purpose of detecting changes that can take place in short periods of time. And finally the study will be useful to evaluate processes that affect to the amount of UV radiation that reaches the terrestrial surface. It is determined by the thickness of the ozone layer, aerosols and atmospheric turbidity.

Instrumentation and Measurements

The data for this work have been registered in C.I.B.A. Laboratory, University of Valladolid, Spain, located at 35km from the city in NW direction, in a place of geographical coordinates: 42° 1' North latitude, 4° 32' West longitude and 832 m above the sea level. The sensors are located so that the obstructions of the horizon

are null. The data for this work correspond to a period between the 16th July 2002 and the 30th June 2005. The solar radiation components recorded continuously at the measurement station are the following: solar global radiation on horizontal and vertical surfaces facing south, west, north and east, using Kipp-Zonen CM6B sensors; total ultraviolet solar radiation UVT(295-385nm) and UV-B(280-315nm) using TUVB Eppley and YES UVB-1 sensors, respectively. (Miguel et al 2005). Meteorological variables like temperature, relative humidity and pressure are also registered. The average measured values are stored in a Campell data logger every 10 minutes and after a data quality control, hourly and daily values are obtained. From them the most important statistical indices, the monthly average hourly and daily values and the accumulated UV-B solar radiation have been evaluated.

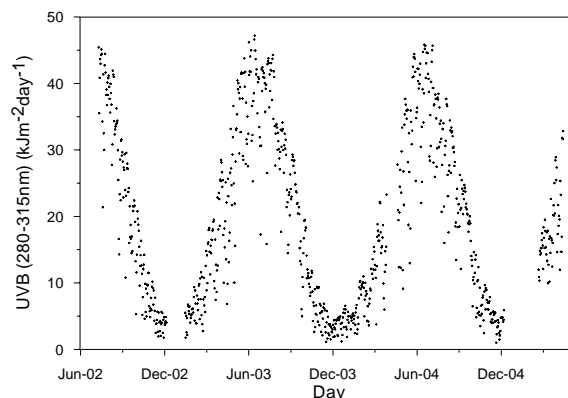


Figure 1. Evolution of daily values of UV-B on horizontal surface ($\text{kJ m}^{-2} \text{day}^{-1}$).

Results

After a quality control of the data hourly and daily values are evaluated. Figure 1 shows the evolution of daily values during the measurement period; it can be seen that maximum values are obtained in summer time and minimum ones in winter. The daily maximum value of UV-B is reached in June, 45 kJ m^{-2} and the minimum is reached in December, 2 kJ m^{-2} . Figure 2 shows the comparison between UV-B and UVT (UV total) solar radiation values, on 30th July 2003 at the measurement station. From the results, it can be said that UV-B is 4% of UVT.

1. Analysis of UV-B irradiation hourly values

A statistical study of the most representative indices of hourly values of UV-B for each month of the year has been carried out. These indices are: arithmetic mean (M), median (Md), standard deviation (SD), maximum (Mx), minimum (Mn), first and third quartiles (Q_1 and Q_3 respectively), percentiles 5 and 95 (P_5 and P_{95} respectively), inter-quartile range ($Q_3 - Q_1$) and coefficient of quartile variation (V) which is defined by the following expression: $V=100(Q_3-Q_1)/(Q_3+Q_1)$

(Martinez-Lozano et al., 1996). Data for each month were arranged in upward order and the statistical characteristics were evaluated and for June, the following results were obtained: the difference between the values of the absolute minimum and P_5 is always great. From this result it is possible to conclude that the minimum absolute is not a representative value of UV-B in Valladolid, and these values correspond with atypical days and not with a tendency. The differences between the absolute maximum and P_{95} , are very small every month. These results do not agree with (Martinez Lozano et al. 1996), perhaps due to the number of data. The median values are higher but quite similar to the arithmetic mean. The differences among them are variable and do not seem to follow any defined seasonal pattern. The coefficient of quartile variation is considered as a stability index and it reaches the minimum values in summer. That means that these months show a high stability.

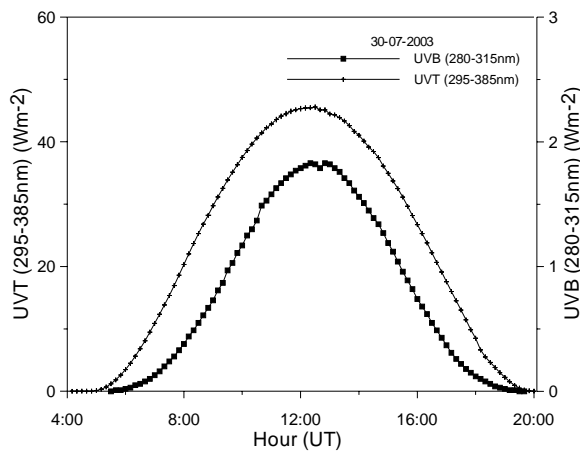


Figure 2. Comparison of UVT and UV-B horizontal solar irradiance.

Figure 3 provides the evolution of the most representative statistical indices of UV-B hourly values for July; it can be seen that median values are higher than the arithmetic mean; standard deviation values increase in the central hours of the day.

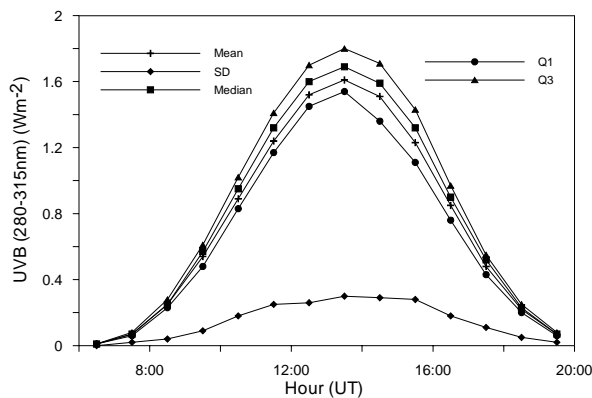


Figure 3. Statistical indices of hourly UV-B (280-315 nm) irradiance for July.

The variations of the monthly mean hourly irradiance for the period 2002-2005 are shown in Figure 4. It can be seen that the average hourly values recorded at solar noon range between 0.2 Wm^{-2} in January and 1.6 Wm^{-2} in June. These average hourly irradiance values in the central

hours of the day show a considerable symmetric evolution. In Fig. 4 we can observe the similar values of May and April in central hours of the day. This evolution shows the effects of ozone increment in April-May period.

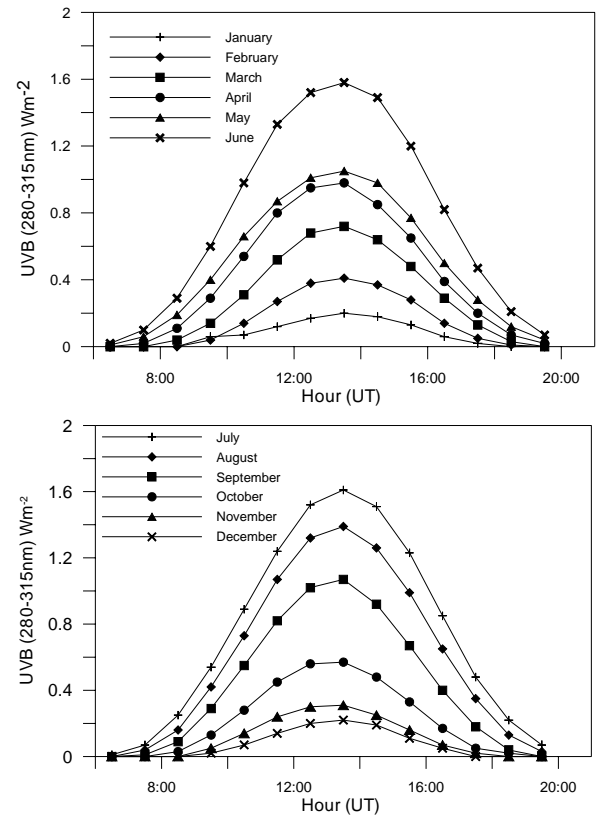


Figure 4. Monthly mean hourly UV-B horizontal solar irradiance.

2. Analysis of ultraviolet solar irradiation daily values

The evolution of daily values during the period has been evaluated in order to deduce the mean values during a year. Figure 5 shows the evolution of daily and monthly mean UV-B solar irradiation through an average year. The mean daily values show some fluctuations due to the atmospheric conditions, clouds and atmospheric transmittance. The mean monthly values show maximum in June and July and minimum in December. The figure is quite regular but not symmetrical.

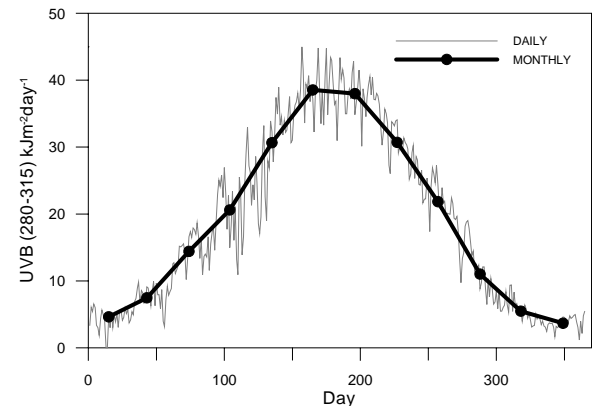


Figure 5. Monthly and daily of UV-B (280-315 nm) evolution for and average year.

Thematic Network for Ultraviolet Measurements

The statistical indices of daily UV-B solar irradiation have been evaluated and the following characteristics have been found. The difference between the absolute minimum and the percentile P_5 is not high enough; the monthly median values are higher than the arithmetic mean ones; minimum values of the variation quartile coefficient, V , are obtained in July and August, this means these months are the most stable of the period.

Conclusions

Hourly and daily values of solar UV-B irradiation (280-315nm) have been evaluated from 10-minute-measured values at the C.I.B.A. site station, in Valladolid (Spain), along the period between June 2002 and June 2005. From data series the elemental statistical characteristics have been evaluated and the hourly value analysis shows that the maximum values can be considered representative of UV-B in Valladolid, but the minimum values are not representative, especially in summer. The indices of stability (V) show that the most stable months correspond to summer time, especially July. The results of the daily value analysis show a high stability for summer and an

appreciable symmetrical evolution of UV-B. Finally the study of accumulated UV-B shows a yearly value of 7 MJm^{-2} .

Acknowledgments The authors gratefully acknowledge the financial support extended by the Spanish Science and Technology Ministry under the Project: REN2003-04522/CLI.

References

- Acosta, L.R., W.F.J. Evans, Design of the México City UV monitoring network: UV-B measurements at ground level in the urban environment. *Journal of Geophysical Research* 105, 5017-5026.
- Martinez-Lozano, J.A., F. Tena, M.P. Utrillas, Measurements and analysis of ultraviolet solar irradiation in Valencia, Spain, *International Journal of Climatology*, 14, 93-102, 1996.
- Palancar, G.G., B.M. Toselli, Effects of meteorology and troposphere aerosols on UV-B radiation: a 4-year study, *Atmospheric Environment*, 38, 2749-2757, 2004.
- Miguel, A.H., J. Bilbao, P. Salvador, A study of UV total solar irradiation at a rural area of Spain, Solaris 2005 2nd Joint Conference, Athens (Greece), 32-3, May 2005. Edit. Hellenic Illumination Committee.

UV-B and UVI measured and calculated in Valladolid, Spain.

P. Salvador, J. Bilbao, A. de Miguel, and A. Pérez-Burgos

Department of Applied Physics, Faculty of Sciences, University of Valladolid, Spain

Abstract. Broadband ultraviolet-B solar irradiance (UV-B, 280-315 nm) and ultraviolet index (UVI) were measured and modelled at C.I.B.A (Low Atmosphere Research Centre), in Valladolid, Spain, between July 2002 and May 2005. UV-B measurements were recorded with a YES (Yankee Environmental Systems) UVB-1 sensor and model evaluations were performed by radiative transfer models, CIBA 1.2 and SMARTS 2.9.2 (Simple Model for the Atmospheric Radiative Transfer of Sunshine) respectively. Total daily ozone column values were analyzed and the results show that the maximum ozone values were obtained four months before than the maximum of UVB, approximately. Maximum UVI values range from 8 to 9.17. The comparison between measured and model evaluation of UV-B hourly values for clear days shows a good agreement at solar noon, and the differences increase near the sunrise and the sunset hours.

Introduction

The spectral range of solar radiation corresponding to wavelengths $\lambda < 400$ nm, is called ultraviolet (UV). The ultraviolet is subdivided into three wavelength band regions: the UVA (315-400 nm) which is received at earth's surface, the UVB (280-315 nm) which is partially absorbed by ozone or scattered in the atmosphere and UVC (<290 nm) which is potentially the most dangerous as it has the highest energy levels, but this wavelength band region is completely absorbed by stratospheric ozone and oxygen above about 30km. The knowledge of solar UV radiation reaching the Earth's surface has a great interest because of its influence in atmospheric and biological processes.

The ozone plays a role of shield around the Earth protecting us from ultraviolet radiation. A diminution in the amount of ozone will imply an increase in the UVB that reaches the Earth's surface. The UVB radiation only represents 5 % of the UV radiation (Miguel 2005) and 0.5% of the solar radiation (Leun, 1993) but UVB is very important to human beings because it can produce different illnesses (Tevini 1993). Frequently the biologically effective irradiance is given as UV index (UVI). UVI is a dimensionless quantity and one unit is equivalent to 25 mWm⁻² of erythemal radiation.

There are different models to predict the solar radiation that reaches the surface of the Earth. These models work with different methods to solve the equation of radiative transfer. They may consider the atmosphere like only one or multiple layer and in this work we use two models, both of them are spectral; the first is a mono-layer and the SMARTS is a multiple-layer model and it uses the standard atmospheres. In this study the atmospheres chosen were the mid latitude summer and mid latitude winter.

The interest of the UVB study is due to its atmospheric and biological effects and the small quantity of available measurements stations in Castilla and León region

(Spain). The main objective of this paper is to give a description of the variation of UVB, ozone and UVI and to compare measured and predicted values using different models, in Valladolid, Spain.

Data

Measurements of UVB broadband solar irradiance, atmospheric pressure, air humidity and temperature were carried out at the C.I.B.A. Laboratory (Low Atmosphere Research Centre), University of Valladolid (Spain), www.uva.es/renova/ Solar irradiance was measured by a Yankee UVB-1 sensor mounted on a wide-open area in, located 35 km from the city in NW direction. The geographical coordinates of the place are: 42° 1' North latitude, 4° 32' West longitude and 832 m above sea level.

The UVB measures were recorded every 10-minute and some necessary quality control test were performed before the data were used. Total ozone column values were taken from the Total Ozone Mapping Spectrometer (TOMS) instrument onboard Earth Probe spacecraft and were provided by Ozone Processing Team of the National Aeronautic and Space Administration (NASA, United States).

CIBA 1.2 and SMARTS 2.9.2. models were used to calculate UVB solar irradiance. The CIBA 1.2 model has been developed by our research group and it is based on the results of (Bird et al., 1984). The SMARTS 2.9.2 model has been developed by (Gueymard 2001).

Method

UVB measurements were converted into UVE (erythemal ultraviolet irradiance) values by means of conversion factors, (Diffey factor) provided by the manufacturer (SIRSA 1998), and from them UVI (ultraviolet indices) hourly values were evaluated (WMO 1994). These UVI results have been considered as measured values and represented by (UVI)_{mea} values.

UVI values have also been obtained from spectral calculated weighted by the erythema action spectrum, they are represented by (UVI)_{model} and can be obtained by the following expression:

$$(UVI)_{model} = k_{er} \int_{290nm}^{400nm} E_{\lambda} S_{er}(\lambda) d\lambda \quad (1)$$

where k_{er} is 40 m²W⁻¹, E_{λ} is the UV spectrum wavelength dependant (Wm⁻²nm⁻¹) and S_{er} is the erythemal weighting function accepted by CIE (Commission International d'Eclairage) and given by (McKinlay and Diffey 1987).

Results

1. UVB-Ozone evolution

The evolution of daily values of ozone (DU) and UVB (kJm⁻²) solar irradiance during the measurement period

Thematic Network for Ultraviolet Measurements

are shown in Figure 1. Maximum UVB values were recorded in summer and maximum ozone column daily values were obtained at the end of the winter. The results of the analysis have been the following: The maximum of ozone daily value is reached in January 2003 (496 DU) (Figure 1) and the maximum of UVB, in June 2003 (47.2 kJm⁻²). The difference between the maximum of ozone (usually at February) and the maximum in UVB, four month later (usually in June), is due to the wind of the stratosphere. That stratospheric wind has their origin because of the difference in pressure that is guided by the differences of temperature. This winds travel from the pole hemisphere in summer to the pole hemisphere in winter where the temperatures are minimum because of the winter night. This flow is the responsible of the maximum of ozone at the end of winter (Vilaplana 2004).

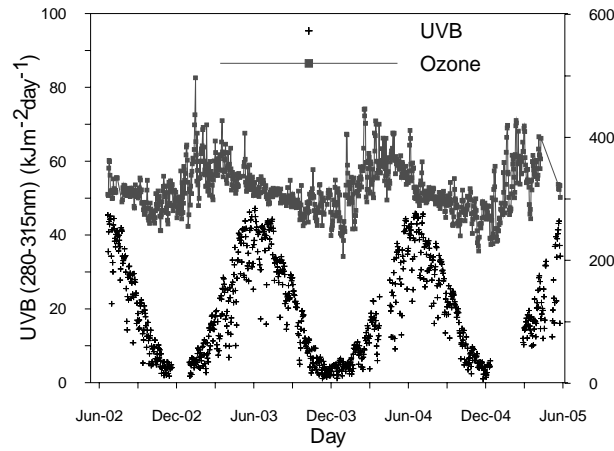


Figure 1. Evolution of the UVB (280-315nm) and ozone daily values, between 2002 and 2005.

2. Sky clearness index

In order to select the clear days, the hourly sky clearness index has been evaluated by the following expression:

$$\varepsilon = \left[\frac{D_h + I_n}{D_h} + kZ^3 \right] / \sqrt{1 + kZ^3} \quad (2)$$

where D_h is the horizontal diffuse irradiance, I_n is the normal incidence direct irradiance, Z is the solar zenith angle and k is a constant whose value is 1.041 with Z in radians, (Perez et al. 1990). By means expression (2), the dependence between the variable, ε , and the solar zenith angle has been removed. Following different authors, a clearness index higher than 6.2 is considered like a clear day (Perez et al. 1990), but in this paper, days with

clearness index higher than 12 have only been considered. After the calculations, 34 clear days were found, 91% were between June and September and 58% between June and July.

3. Model comparison

The CIBA 1.2 spectral model has been used to evaluate hourly UVB (280-315nm) values for the 33 days with a clearness index higher than twelve. The accuracy of the model was evaluated by means of widely used statistics: absolute MBE (Mean Bias Error), RMSE (Root Mean Square Error) and PE (percentage of error) at solar noon. MBE means the average deviation of the calculated values from the measured ones and it is defined by the following expression:

$$MBE = \sum_{i=1}^N (y_i - x_i) / N \quad (3)$$

RMSE is a measure of the variation of predicted values around the measured values and it is given by:

$$RMSE = \left(\sum_{i=1}^N (y_i - x_i)^2 / N \right)^{1/2} \quad (4)$$

where y_i is the i th estimated value, x_i is the i th measured value and N is the number of data.

Table 1 shows the day characteristics and the statistical estimators obtained for the 10 clearest days. The MBE, RMSE and PE average values are: 0.050 Wm⁻², 0.085 Wm⁻² and 7.12% respectively. It is remarkable that in this paper MBE values are always positive. This result means that CIBA 1.2 model overestimates UVB hourly values.

A linear regression plot was made, in order to compare UVB hourly solar noon measured values, $(UVB)_{mea}$, and evaluated ones by CIBA 1.2 model, $(UVB)_{model}$ values.. The results obtained show that $(UVB)_{model} = 1.09 (UVB)_{mea} - 0.15$. This result provides that CIBA 1.2 model overestimate UVB solar irradiance. Regression coefficient -0.15 should ideally be null and 1.09 coefficient value should be equal to one, in order to have a perfect agreement between the measured and the calculated UVB. The correlation coefficient is 0.93, which is a good result for a simple spectral model like CIBA 1.2, even at clearest days. The mean value of the $(UVB)_{model}$ is 1.648 Wm⁻² and for $(UVB)_{mea}$ is 1.651 Wm⁻².

Table 1. Sky's clearness index, Ozone (DU), Pressure (mb), Temperature (°C), Humidity (%), MBE, RMSE and PE values for the 10 clearest days.

Date	Clearness index.	Ozone (DU)	Pressure (mb)	Temperature (°C)	Relative Humidity (%)	MBE (Wm ⁻²)	RMSE (Wm ⁻²)	PE % noon
05/06/2004	15.82	323.38	920	16.82	76.7	0.08	0.11	4
04/06/2004	15.61	352.88	924	11.35	93.0	0.01	0.07	4
19/06/2003	15.48	312.50	926	18.01	73.1	0.05	0.08	4
03/06/2004	14.95	343.24	928	11.88	64.7	0.02	0.07	1
17/06/2004	14.58	329.00	922	14.39	59.5	0.09	0.12	13
14/08/2004	14.44	299.60	924	19.26	65.4	0.11	0.14	10
27/06/2004	14.37	300.46	925	16.26	96.8	0.12	0.16	19
25/07/2003	14.26	309.86	922	18.80	81.1	0.07	0.11	6
13/08/2004	13.98	294.44	923	17.26	68.7	0.11	0.14	10
18/07/2003	13.91	300.02	924	17.76	51.6	0.12	0.15	13

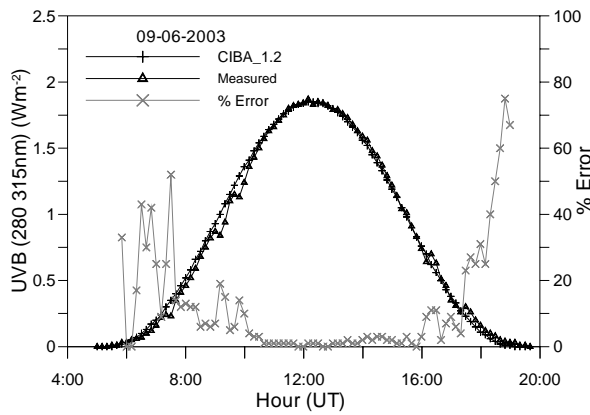


Figure 2. Comparison of measured and calculated UVB (280-315nm) hourly values, June 2003.

Figures 2 and 3 show the comparison of UVB (280-315nm) measured and calculated values by CIBA 1.2 model for the days 09-June-2003 and 29-September-2004 respectively and it can be seen that percentage of error diminishes in central hours and increases in early morning and afternoon.

Figure 4 shows the comparison of the UVB (280-315nm) hourly measured values (Wm^{-2}), the UVB evaluated values, given by the CIBA 1.2 and the SMARTS 2.9.2 models respectively, during a cloudless day in July 2002, being 9.95 the sky clearness index. That day, the ozone amount was 307.4 DU, the surface pressure 923 mb and the precipitable water vapour was 2.98 cm. The SMARTS model ran with a standard atmosphere corresponding to a mid latitude summer and a rural aerosol model. The results of modelling are closed to the measurements. At first hours of the day we can find the biggest errors around 40%, but at solar noon and in the afternoon the errors are smaller than 7% for both models, zero in some hours. We can use these models to predict the amount of solar radiation at least in cloudless days and near the solar

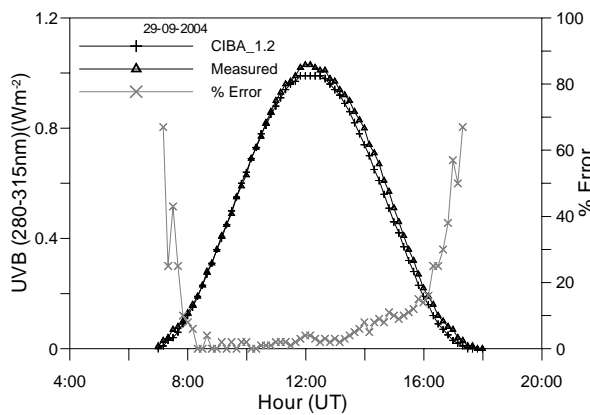


Figure 3. Comparison of measured and calculated UVB (280-315nm) hourly values, September 2004.

noon. The accuracy of these models is based on the input parameters. In this case the input parameters (except ozone) and UVB have been measured in the same place, but if we use this models in other place where input parameters are not known, standard atmospheres have to

be used and probably the results will not be so good due to the variability of these parameters.

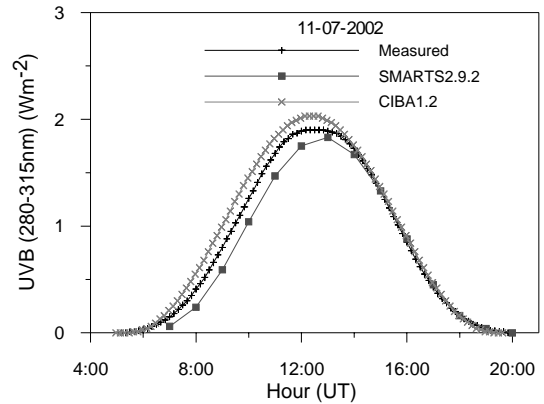


Figure 4. Comparison of measured and calculated UVB (280-315nm) hourly values, in July 2002.

4. UVI evaluations

To convert the UVB-1 instrument output voltage into UVE, Wm^{-2} units, the signal voltage has to be multiplied by a conversion factor according to the solar zenith angle when the measure was taken; this factor is provided by the manufacturer. The $(UVI)_{mea}$ has been calculated by multiplying UVE by 40 (WMO 1994) what means that a difference of a unit in the UVI correspond to a difference of $0.025 Wm^{-2}$ in the UVE. In this paper and after these evaluation, the following results have been obtained: $(UVI)_{mea}$ value is over 10, a lot of days. The highest values are 11.2, these values are too high, probably because the spectral response sensor UVB-1 differs from the spectral action proposed by CIE in the range 300-330nm and as consequence the sensor overestimate the UVE. Using the conversion factor given by (Vilaplana 2004), whose value is $0.12 Wm^{-2}volt^{-1}$, the values reached by $(UVI)_{mea}$ are lower which is in accordance with $(UVI)_{model}$ results obtained using CIBA 1.2 model. Figure 5 shows the comparison of measured, $(UVI)_{mea}$, and calculated, $(UVI)_{model}$, at solar noon, where the measured obtained maximum value is 9.17.

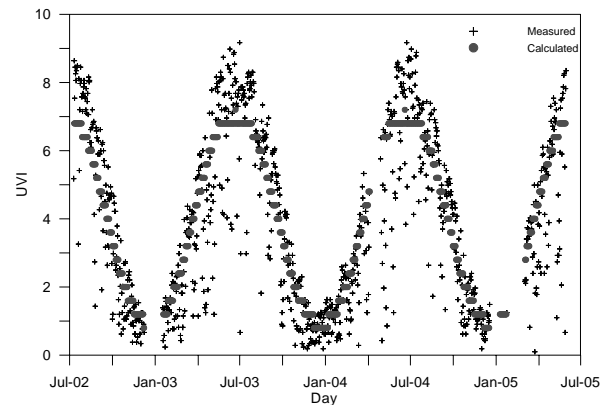


Figure 5. Comparison of measured and calculated UVI values at CIBA site at solar noon, for the period 2002-2005.

Conclusions

Hourly and daily values of UVB (280-315nm) solar irradiation have been evaluated from 10-minutes

Thematic Network for Ultraviolet Measurements

measured values at C.I.B.A. station, in Valladolid (Spain), during the period July 2002 May 2005.

Total ozone column daily values were taken from the Total Ozone Mapping Spectrometer (TOMS), from the evolution it can be seen that ozone often reaches its maximum at February with four months of difference with the respective maximum of UVB at June.

The clearness index values were evaluated and higher values than 12 usually appear in summer. Thirty four days obtained a clearness index superior to 12 between 2002 and 2005. The maximum of UVB oscillates near 2 Wm^{-2} , in these clear days.

The average MBE and RMSE values take 0.050 Wm^{-2} and 0.085 Wm^{-2} respectively, using CIBA 1.2 model. The mean PE takes 7.12 value, for CIBA 1.2 model at solar noon.

The UVI measured value registered in Valladolid is very high, reaching 11 in summer time. After the application of the factor conversion given by (Vilaplana 2004), the maximum value is 9.17, which is more realistic.

The spectral models used in this work show a very good accuracy for calculating UVB solar irradiation in the clearest days when measured input parameter values are used.

Acknowledgments The authors gratefully acknowledge the financial support extended by the Spanish Science and Technology Ministry under the Project: REN2003-04522/CLI.

References

Bird, R. E. and Riordan, C., A., (1984). Simple solar spectral modelling for direct normal and diffuse horizontal irradiance. *Solar Energy*. **32**,461-471.

Gueymard, C.A., (1983). SMARTS code, version 2.9.2, user's manual. Solar Consulting Services, Bailey, CO, USA. 2003.

Gueymard, C.A., (2001). Parameterized Transmittance Model for Direct Beam and Circumsolar Spectral Irradiance. *Solar Energy*. **71** n°5, pp. 325-346.

Iqbal, M., An introduction to solar radiation. Academic Press.

Martinez-Lozano, J.A., Tena, F. and Utrillas, M.P., (1996). Measurements and analysis of ultraviolet solar irradiation in Valencia, Spain. *International Journal of Climatology*, **14**, pp. 93-102.

Martinez-Lozano, J.A., Tena, F., Martin, M.J., Utrillas, M.P., Lorente, J., DeCabo, X., and González-Frías, C., (2002). Experimental values of the UV index during 2000 at two locations in Mediterranean Spain. *International Journal of Climatology*. **22**:501-501.

McKinlay A.F. and Diffey B.L., (1987). A reference action spectrum for ultraviolet induced erythema in human skin, *CIE Journal*, **6**, 17-22.

Miguel, A.H., J.Bilbao, P.Salvador, A study of UV total solar irradiation at a rural area of Spain, Solaris 2005 2nd Joint Conference, Athens (Greece), 32-3, May 2005. Edit. Hellenic Illumination Committee.

Palancar, G.G., (2003). Estudio de procesos cinéticos y radiativos de interes atmosférico. Tesis doctoral. Universidad Nacional de Córdoba.

Perez, R., Ineichen, P., Seals, R., (1990). Modeling daylight availability and irradiance components from direct and global irradiance. *Solar Energy*, **44**, No. 5, pp. 271-289.

S.I.R.S.A. 1998. "Manual de usuario, Sensor de radiación ultravioleta, modelo UVB-1." sirsa@sirsa.es.

Tevini, M., (1993). Molecular Biological Effects of Ultraviolet Radiation. UV-B radiation and ozone depletion: effects on humans, animals, plants, microorganism, and materials, edited by Manfred Tevini., pp. 1-17, Lewish Publishers.

Vilaplana, J.M., (2004). Medida y Análisis del Ozono y de la Radiación Solar Ultravioleta en el Arenosillo-INTA, Huelva. Tesis Doctoral. Universidad de Valladolid.

WMO, (1994). Report of the WMO meeting of experts on UV-B measurements, data quality and standardization of UV indices, Les Diablerets, Switzerland.

Realising a primary spectral irradiance scale on deuterium lamps in the ultraviolet

*Heather M. Pegrum, Emma R. Woolliams, Nigel P. Fox, Andrew R. Hanson,
David R. Gibbs, William R. Servantes, and Teresa M. Goodman
National Physical Laboratory, Teddington, UK*

Abstract. The NPL 2003 spectral irradiance scale is based on the spectral radiance from a high temperature blackbody source. This paper describes the extension of this scale down to 200 nm and the transfer of the scale to deuterium lamps. As the spectral irradiance of deuterium lamps is very different from that of a blackbody or tungsten lamp source, issues such as monochromator bandwidth and system linearity, must be considered with great care.

Introduction

The NPL spectral irradiance scale from 250 to 2500 nm [1,2] was formerly integrated into our measurement services and consequently became our disseminated scale in May 2003. This paper describes the extension of this scale down to 200 nm and the transfer of the scale to deuterium lamps. The scale is based on the use of the absolute spectral radiance emitted from a high temperature blackbody through Planck’s law. The critical input variable being thermodynamic temperature, which is determined by a filter radiometer whose spectral response has been calibrated against the NPL primary standard cryogenic radiometer.

Measurement facility

The scale was realised on the Spectral Radiance and Irradiance Primary Scale (SRIPS) facility, shown schematically in Figure 1. The primary source was a BB3500 blackbody source, operated at temperatures around 3060 K and 3170 K. The thermodynamic temperature of the blackbody was determined absolutely using a group of filter radiometers calibrated traceably to NPL’s primary cryogenic radiometer.

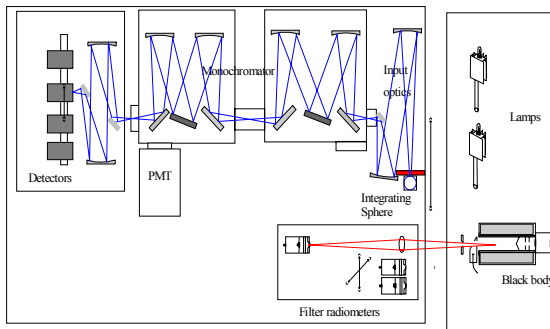


Figure 1. Schematic representation of the SRIPS facility.

A double-grating monochromator was used to select the wavelengths and measurements were made with a photomultiplier tube. The monochromator and detector were mounted on a large translation stage that could be moved in front of each source in turn. The defining aperture for the system was on the input of an integrating sphere, the

output port of which was focussed by parabolic mirrors onto the monochromator entrance slits.

Signal level

Because the blackbody and lamp have very different spectral shapes (Figure 2), issues such as detector linearity and amplifier gain must be well understood. For example, at 200 nm the signal from the lamp was 60 times higher than that from the blackbody and at 350 nm the blackbody signal was 100 times higher. The PMT detector was tested for linearity, and found to be linear to better than 0.1 % for signals below 1 μA. Care was taken to ensure that the signal did not increase above this value.

As the signal level was low for the blackbody source at 200 nm, it was not possible to use the same measurement procedures at the shortest wavelengths as elsewhere. To increase the signal, the integrating sphere was replaced by a flat PTFE diffuser. The short wavelength measurements could therefore only be considered relative, and were renormalized to the sphere results at longer wavelengths.

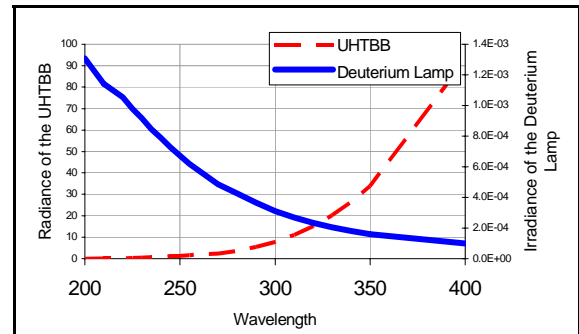


Figure 2. Irradiance of the UHTBB and deuterium lamps.

Bandwidth

Monochromator based measurements incorporate the effect of a non-zero bandwidth, so it is necessary to correct the results to a zero bandwidth situation. This problem has been investigated [3] and for a triangular slit function an approximation can be made. For a triangular slit function, of full width $2\Delta\lambda$ and a unit area, the following equation holds:

$$V(\lambda) = \bar{V}(\lambda) - \frac{1}{12}(\Delta\lambda)^2 \bar{V}''(\lambda) + \frac{1}{240}(\Delta\lambda)^4 \bar{V}^{(4)}(\lambda) + \dots \quad (1)$$

Equation (1) must be applied to each source and the ratio taken. If the two sources are very similar (as is the case for an FEL calibrated against a blackbody), the correction to the ratio is tiny, even if the correction to each individual source is significant. However as the blackbody and deuterium lamp are changing rapidly and non-linearly in opposite directions (Figure 2), a correction is required.

Thematic Network for Ultraviolet Measurements

This correction was applied to all of the lamp data before the weighted shifts were applied. In order to have sufficient wavelengths to determine an accurate second derivative, measurements were made in 2.5 nm steps.

The bandwidth was determined by scanning a mercury line with the monochromator for the two slit widths used for the comparison measurements (slits of [3-3-5] corresponded to a bandwidth of 4.06 ± 0.05 nm, and slits [1-1-3] corresponded to a bandwidth of 1.46 ± 0.05 nm).

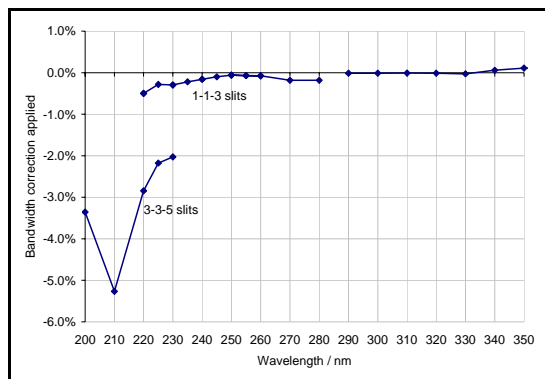


Figure 3. Bandwidth correction applied. At wavelengths with two values, the monochromator is operated at both slit sizes.

Absorption Correction

Investigations have shown [4,1] that the blackbody suffers from ultraviolet absorption due to carbon sublimation around 380 nm. To understand this absorption effect at shorter wavelengths, the blackbody was measured at different temperatures and the ratio of the measured signals between the two blackbodies was compared with the ratio expected from Planck's law. A cooler blackbody is assumed to show less absorption because there is less carbon sublimation, therefore a comparison of a blackbody at operational temperature with the blackbody at a cooler temperature, can be used to determine the absorption at the higher temperature.

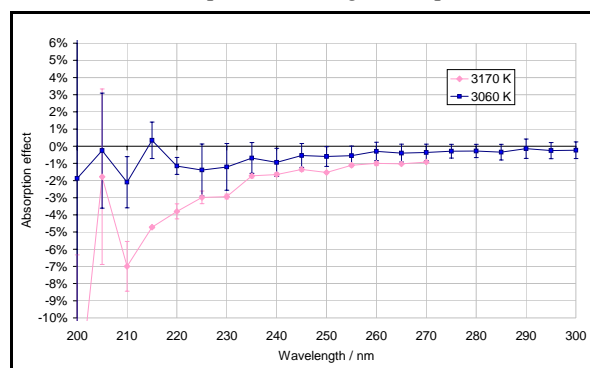


Figure 4. Absorption of blackbody – comparison of blackbody spectrum at 3170 K and 3060 K to that at 3000 K.

For the UV scale realisation, the blackbody was operated at 3050 K where possible but for the shortest wavelengths sufficient signal was only obtained with the blackbody operating at 3170 K. It was not possible to make a comparison to a blackbody cool enough to show no absorption; instead the blackbody at 3170 K and 3050 K

was compared to itself at 3000 K. Some absorption around 210 nm was discovered (Figure 4). The absorption is probably due to C_2N_2 , which has strong lines at 209.31 nm and 210.74 nm.

Transfer standard sources

As the ability to realise spectral irradiance scales at the NMIs has improved, the dominant uncertainty has become that associated with the transfer standard sources themselves. For wavelengths above 250 nm, one in three FEL lamps changes on transportation or after ~150 on-off cycles [5]. Deuterium lamps can show significant differences in absolute level between switch-ons. However, more recent lamps suffer less from this than older lamps and it is possible to monitor, and thus correct for, the changes using a photodiode [6].

Uncertainties

At the shortest wavelengths, where the signal levels are very low, the uncertainty associated with the spectral irradiance measurement is dominated by uncertainties associated with signal-to-noise. The uncertainty associated with the lamp stability can be important for older types of lamps. Lamp stability and signal-to-noise can be reduced by averaging multiple measurements of the test lamp. If this is done, then the dominant uncertainty remaining is the uncertainty associated with the blackbody radiance, which depends on the determination of temperature and the ability to correct for the absorption effect. Overall, the uncertainty associated with the primary spectral irradiance scale, as realised using the best deuterium lamps on the SRIPS facility directly against the blackbody and by averaging three measurements ($k = 2$) drops from 9 % at 200 nm, through 3 % at 230 nm to 1 % at 350 nm.

Acknowledgements. This work was supported by the National Measurement System Policy Unit of the UK Department of Trade and Industry.

References

- [1] E. R. Woolliams, N. J. Harrison, B. B. Khlevnoy, L. J. Rogers and N. P. Fox, 'Realisation and dissemination of spectral irradiance at NPL'. *UV News*, 2002. **7**, pp. 39-42.
- [2] E. R. Woolliams. 'Development and evaluation of a high temperature blackbody source for the realisation of NPL's primary spectral irradiance scale'. Thesis. 2003. *University of Manchester*.
- [3] M. G. Cox, P. M. Harris, P. D. Kenward and E. R. Woolliams. 'Spectral Characteristic Modelling'. 2003. *NPL Report CMSC 27/03*
- [4] P. Sperfeld, S. Galal-Yousef, J. Metzdorf, B. Nawo and W. Möller, 'The use of self-consistent calibrations to recover absorption bands in the black-body spectrum'. *Metrologia*, 2000. **37(5)**, pp. 373-376.
- [5] N. J. Harrison, E. R. Woolliams and N. P. Fox, 'Evaluation of spectral irradiance transfer standards'. *Metrologia*, 2000. **37(5)**, pp. 453-456.
- [6] P. Sperfeld, K. D. Stock, K.-H. Raatx, B. Nawo and J. Metzdorf, 'Characterization and use of deuterium lamps as transfer standards of spectral irradiance'. *Metrologia*, 2003. **40(1)**, pp. S111-S114.

Comparison of measurement devices for the measurement of erythemal solar ultraviolet radiation during an outdoor-worker study in Austria

Marko Weber¹, Martina Schwaiger¹, Karl Schulmeister¹, Helmut Brusl², Peter Kindl³, and Peter Knuschke⁴

1. ARC Seibersdorf research GmbH, Health Physics Division, Austria
2. Austrian Social Insurance for Occupational Risks, HUB Department, Austria
3. Institute for Material Physics, Technical University of Graz; Austria
4. Department of Dermatology, University of Technology Dresden, Germany

Abstract. To quantify erythemal ultraviolet radiation (UVR) exposure of road construction workers involved in typical outdoor work, a study was conducted using UVR-sensitive polysulphone film badges. More than 1000 man day exposures, involving 37 workers, were accumulated between July and September at 50 different construction sites in the surroundings of Vienna (latitude: 48 °N, altitude: approx. 150 m).

A conversion factor giving the ratio between the measured erythemal radiant exposure at different parts of the body and the global erythemal radiant exposure was calculated to extrapolate the erythemal radiant exposure for the workers for the following years.

To verify the measurements with the polysulphone film badges, additional UVR measurements were carried out. Intercomparison of the measured results justified using polysulphone films for quantitative UVR exposure studies.

The study found that road construction outdoor workers were exposed to high levels of UVR, in most cases without adequate sun protection. A general conversion factor for the actual exposure from global horizontally measured values could be obtained.

Methods

The workers were assigned to different groups according to their work task and posture (upright or ducked working position). They were equipped with PS film badges (thickness: 26 µm, Dr. Kockott UV-Technik, data interpretation by department of dermatology of TU Dresden) at least at the shoulder or at several parts of their body (head, arms, legs).

While conducting personal observations on site, information on environmental, personal and work practice factors that affect personal UVR exposure were collected.

We introduced a factor FAH (factor measured actual to horizontal, equation 1) giving the ratio between the measured actual erythemal radiant exposure [$J m^{-2}$] and the horizontal erythemal radiant exposure [$J m^{-2}$], such as measured by national UV-Index networks). By knowledge of the FAH and the horizontal exposure the actual exposure of the workers can be calculated for the same period on following years and with some restrictions for every day of the year for different work tasks and body parts.

$$FAH = \frac{\text{actual erythemal radiant exposure}[J m^{-2}]}{\text{horizontal erythemal radiant exposure}[J m^{-2}]} \quad (1)$$

Results

Figure 1 shows that the actual erythemal exposure at the shoulder correlates quite well with the horizontal erythemal radiant exposure. Figure 2 gives the daily UV-exposure of the shoulder for the “digging, ...”-group. The values were extrapolated by multiplying the corresponding FAH with the daily horizontal erythemal radiant exposure. The dotted red lines indicate the erythemal radiant exposures which are typical to induce an UV-erythema in skin types I – IV.

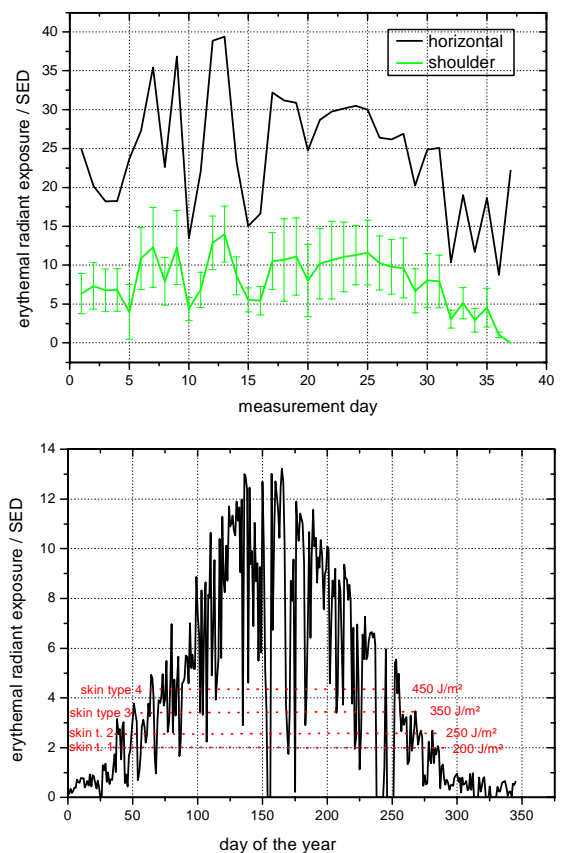


Figure 1 (top). Horizontal and actual erythemal radiant exposures at the shoulder as measured with polysulphone film badges. Figure 2 (bottom). Extrapolated daily erythemal UV-exposure of the shoulder (year 1999, “digging, ...”-group).

Table 1 shows the FAH as a function of the body part and the FAH of the shoulder as a function of the work task.

Thematic Network for Ultraviolet Measurements

Table 1. FAH as a function of the body part and as a function of the work task.

Body part	Work task	Average FAH	Standard deviation
shoulder	digging, sweeping, ...	0.32	± 35 %
shoulder	supervision and planning	0.20	± 75 %
shoulder	driving construction machines	0.15	± 50 %
head	digging, sweeping,...	0.35	± 28 %
arm	digging, sweeping,...	0.27	± 20 %

Concerning the erythral radiant exposure of the road construction workers, the results showed that the workers received an erythral radiant exposure between 1000 J m⁻² and 1400 J m⁻² per day on roughly 100 days per year. On approximately 220 days the workers exposure exceeded 2 standard erythral doses (SED) which are typical to induce UV-erythema in people of skin type I. Workers received more than 4.5 SED on 180 days, indicating that even workers of skin type IV receive significant doses of UVR. Depending on the ground reflection and the reflection of the working materials, the recommended UV-A exposure limit for the eye was exceeded by up to a factor of 4.

Intercomparison of Different UVR Measurement Devices

To verify the measurements with the PS film badges, additional UVR measurements were carried out involving the following calibrated measurement devices:

- double monochromator DM 150 (Bentham Instruments) with bialkali photomultiplier tube DH3.
- solar UV-biometer model 501 (Solar Light Inc.)
- VioSpor dosimeters which consist of an UV-sensitive photo film (immobilized spores) and a special filter-optic system.

In order to measure the horizontal erythral radiant exposure the VioSpor and polysulphone film dosimeters were exposed to the sun from 9 a.m. to 5 p.m. on several days, being placed on a plane horizontal surface in a shadeless area. At the same location, measurements with the double monochromator (bandwidth: 2 nm, input optics: teflon diffuser) were carried out hourly and the erythral radiant exposure was calculated afterwards.

Measurements with the solar light model 501 UV-biometer were made by the University of Veterinary Medicine in Vienna, which participates in the Austrian UV-index network, some 20 km from the location of the other measurement devices.

A comparison of the results of the various measurement devices is given in figure 3, figure 4 shows the variation of the effective radiant exposure between the devices in percent (the reference results herein are the results from the Solar Light Model 501).

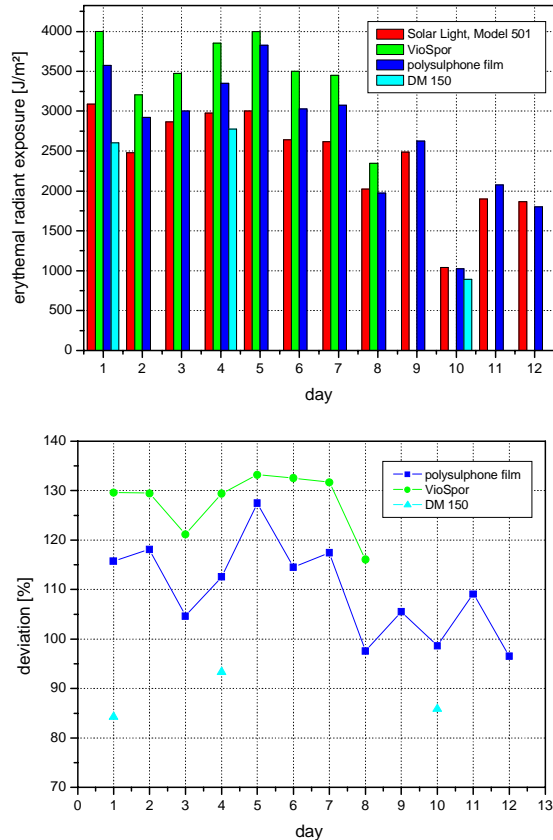


Figure 3 (top). Erythral radiant exposure as measured by the different devices, Figure 4 (bottom). Deviation of the results in percent compared to the Solar Light model 501.

Figure 4 shows that the variation of the results between the polysulphone film dosimeters and the other devices is less than 30 %, which justifies using polysulphone films for quantitative exposure studies.

Realization of a new commercial radiometer for measurement of the total UV effective irradiance of sunbeds

M.G. Pelizzo^{1,2}, P. Ceccherini³, D. Garoli^{1,2}, P. Nicolosi^{1,2}, P. Masut³, and D. Grove⁴

1. Istituto Nazionale per la Fisica della Materia (INFN), LUXOR Laboratory
2. University of Padova, Department of Information Engineering
3. DELTA OHM s.r.l., Caselle di Selvazzano (Padova), Italy
4. LUXEL Corp., WA 98250 USA

Long exposition to sun radiation causes burns, skin aging, erythema and even melanoma cancer [1]. In the European regulation EN60335-2-27 [2] the toxicity of UV radiation emitting machines for domestic use is discussed and upper-limit exposition effective dose are established. As well as other artificial sources, sun tanning units should be monitored and certified according with the law. There is the necessity to develop a clear measurement procedure to verify sunbed irradiance in metrological laboratories, and to develop portable instrumentation for the irradiance verification in situ. In order to measure the total effective irradiance of sunbeds and sun lamps a new radiometer with a spectral response curve equivalent to the CIE Erythral Action Curve (EAC) [3] (Fig.1) has been designed and realized. An action spectrum describes the relative effectiveness of UV radiation at a particular wavelength in producing a particular biological response; the EAC was defined by McKinlay and Diffey (1987) and has been accepted by the Commission Internationale de l'Eclairage (CIE) as the standard representation of the average skin response to UVB and UVA. The radiometer developed measures the total effective irradiance (W_{eff}/m^2) by integrating the irradiance weighted by the EAC over the whole UVA-UVB range. The sensor is hand portable, user friendly and competitive on the market. A request for an Italian patent has been deposited by Istituto Nazionale per la Fisica della Materia (INFN), Italy [4].

The system consists of a transmission diffuser, an interferential filter and a photodiode detector (Fig.2).

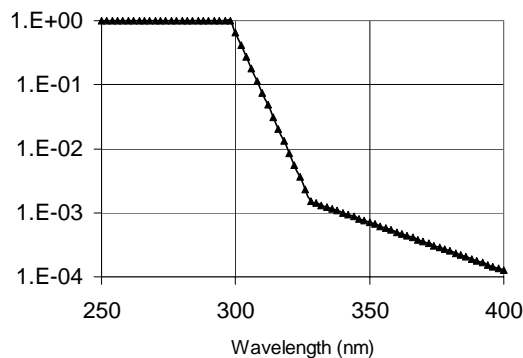


Figure 1. The CIE Erythral Action Curve (EAC).

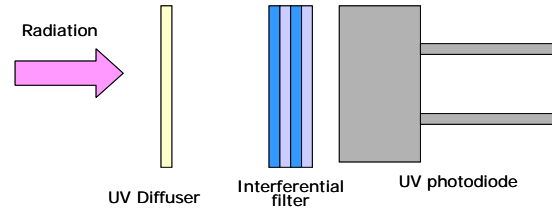


Figure 2. Radiometer optical scheme.

The diffuser can be either a teflon film or a quartz glass, being the first more indicated for its diffusion properties. In order to select the most appropriate detector, many different commercial photodiodes have been considered [1]. They are all blind in the visible and IR. The one that have been purchased are:

- SiC photodiodes, nominal area 0.22 mm² (6)
- p-i-n GaN photodiodes, nominal area 0.5 mm² (2)
- Different AlGaIn Schottky photodiodes, nominal area 0.5 mm²:
- Peak response at 250 nm (2)
- Peak response at 300 nm (2)
- Peak response at 300 nm + Visible filter (2)

Both relative and absolute response (Fig.3) have been measured.

The following are some outcomes of the measurements:

- AlGaIn and GaN seems to have a low sensibility with respect to SiC, therefore to measure the same irradiance value larger active areas are necessary, fact that implies an increase of the costs.
- GaN seems to be not so sensitive above 360 nm, so they are suitable to cover the whole 250-400 nm range.
- AlGaIn with 300 nm cutoff are usually sold for the matching between their spectral response and the erythral action curve. From our measurements it appears that there is still a difference between EAC and AlGaIn spectral response.
- All 6 SiC photodiode have a very similar absolute spectral responses over the whole spectral range of interest

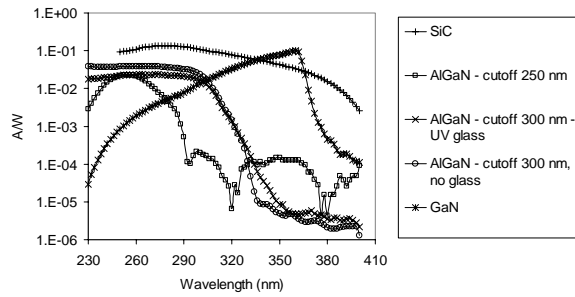


Figure 3. Absolute spectral response curve of different photodiodes.

SiC have been selected also for the higher efficiency, high shunt resistance and stability over time. In order to match the CIE EAC curve an innovative interferential filter has been designed. The filter transmission curve is optimized in such a way that its product with the photodiode spectral response curve and the diffuser transmission curve matches the EAC according with the following:

$$\frac{\text{CIE Curve}(\lambda)}{R_{\text{ph}}(\lambda) * R_{\text{diff}}(\lambda)} = R_{\text{filter}}(\lambda) \quad (1)$$

where the CIE Curve (λ) is the Erythemal Action Curve of Fig.1, $R_{\text{ph}}(\lambda)$ is the photodiode spectral response as recovered by our measurements, $R_{\text{diff}}(\lambda)$ is the diffuser transmission, $R_{\text{filter}}(\lambda)$ is the filter transmission. The theoretical response of the whole system has been evaluated and compared to EAC (Fig.4), showing a almost perfect match.

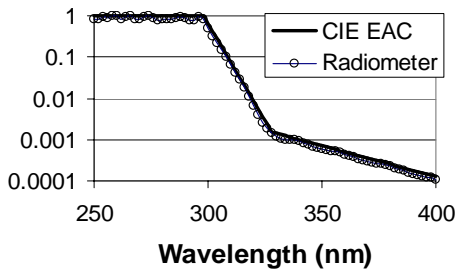


Figure 4. Radiometer theoretical spectral response (normalized) compared to the CIE Erythemal Action Curve.

Filter has been deposited by LUXEL Corp. and its optical properties have been verified as stable after thermal cycling. A first prototype of the radiometer has then been

assembled (Fig.5). Spectral response of the prototype has been measured (Fig.6) showing very interesting results. Further improvement is expected after optimization of the filter deposition process. The new instrument concept can be used to develop an outdoor radiometer for ambient UV monitoring.



Figure 5. Radiometer prototype.

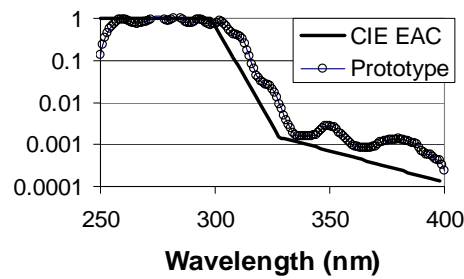


Figure 6. Radiometer measured spectral response (normalized) compared to the CIE Erythemal Action Curve.

References

- [1] P. Autier, "Perspective in melanoma prevention: the case of sunbeds", European Journal of cancer 40, pp.2367-2376, (2004)
- [2] EN 60335-2-27, 1997-03; IEC 60335-2-27, 1995-05.2
- [3] CIE (International Commission on Illumination) Research Note 1987, "A reference action spectrum for the ultraviolet induced erythema in human skin, CIE J.6, 17-22.
- [4] Italian Patent, TO 2005 A 000249
- [5] M.G. Pelizzo, P. Ceccherini, D. Garoli, P. Masut, P. Nicolosi, "Absolute spectral response measurements of different photodiodes useful for applications in the UV spectral region", Proc. SPIE Vol. 5529, p. 285-293, Nonimaging Optics and Efficient Illumination Systems, Roland Winston, R. John Koshel, Eds., 2004

Investigation of comparison methods for UVA irradiance responsivity calibration facilities

J. Envall¹, L. Ylianttila², H. Moseley³, A. Coleman⁴, M. Durak⁵, P. Kärhä¹, and E. Ikonen^{1,6}

1. Metrology Research Institute, Helsinki University of Technology, TKK, Espoo, Finland.
2. STUK, Radiation and Nuclear Safety Authority, Helsinki, Finland.
3. The Photobiology Unit, University of Dundee, UK.
4. Medical Physics Department, Guy's & St Thomas' NHS Foundation Trust, London, UK.
5. National Metrology Institute of Turkey, TUBITAK-UME, Gebze-Kocaeli, Turkey.
6. Centre for Metrology and Accreditation (MIKES), Helsinki, Finland.

Abstract. A new method is described for comparing calibration facilities for broadband UV meters. The method is validated in a successful pilot comparison between five European laboratories performing UVA irradiance responsivity calibrations. Participating laboratories calibrated a broadband UVA detector using their ordinary procedures that differed both by calibration methodology and radiation sources used. Pilot laboratory calculated different reference values for each laboratory based on the specified calibration methods and prior knowledge on the calibrated artifact. The results were in agreement within $\pm 5\%$ which demonstrates a factor of two improvement in agreement as compared to earlier intercomparisons.

Introduction

Broadband UV detectors find use in several fields of science and technology. Calibration of such detectors is a complicated task which requires fundamental understanding of the properties of the detector and the methodology used. The calibration of a broadband detector is source dependent; it applies only to the type of the source that was used in the calibration.^{1,2}

There are several methods to calibrate broadband detectors.^{1,2} If properly done, all methods should give the same result, but practice has shown that severe discrepancies may occur if the measurements and the analysis of the results are not done with care, or if the principle of the calibration is not fully understood.³ Even in the most successful intercomparisons⁴, deviations of the order of $\pm 10\%$ have been reported for UVA meters.

In this pilot comparison, five European laboratories calibrated a commercial UVA meter. Each laboratory was to perform the measurements with the exact procedure that they utilize in their regular work. The laboratories would also specify to the TKK, the pilot laboratory in this comparison, the spectrum of their radiation source used and the exact geometry in the measurements. Using these data, together with earlier measured spectral irradiance responsivity and cosine response of the detector, TKK calculated different reference values for the individual laboratories. These numbers could then be compared with those measured by the participant laboratories.

Calibration methods and results

TKK as the pilot laboratory measured the spectral irradiance responsivity of the UVA meter (Gigahertz-Optik GmbH, model UV-3701) for collimated light in

overfilled mode⁵. Furthermore, the cosine response of the UVA meter was measured.

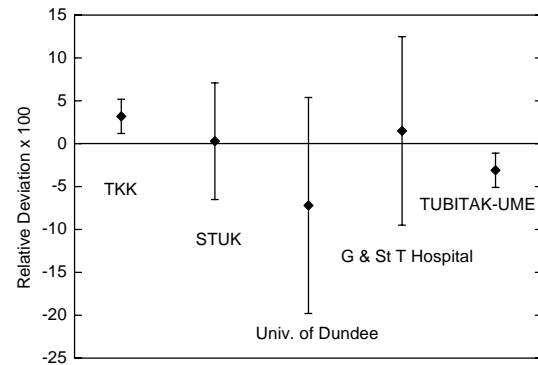


Figure 1. Results of the comparison, given as the relative deviation from the reference value. The error bars indicate the measurement uncertainties ($k=2$) specified by each laboratory. It should be noted that the uncertainty of the reference value has not been taken into account. This is potentially a significant component of uncertainty, since the reference value is obtained from a set of bilateral comparisons with largely varying measurement uncertainties.

STUK performed a spectroradiometric calibration using a single 180-cm long solarium tube of type Philips TL 100W/WW as the radiation source at a distance of 7 cm. University of Dundee performed a similar calibration at a distance of 30 cm using a bank of six 180-cm long tubes of type Philips 100W R as the radiation source. Guy's & St Thomas's Hospital measured the spectral irradiance responsivity of the meter and used the data to calculate responsivity for a measurement in a patient treatment chamber utilising tubes of type Waldmann PUVA. UME also measured the spectral irradiance responsivity. This data was used to calculate responsivity for a tube of type Waldmann PUVA.

The results of the pilot comparison⁶ are given in Figure 1. In the analysis of the results, TKK calculated reference values for each laboratory, against which the values of the participants were compared. From this set of numbers (TKK being unity, others being compared to TKK) a weighted average was calculated to be used as the reference value for the final comparison. The weight of each laboratory was the inverse of the stated measurement uncertainty squared.

Conclusions

The results of the comparison are within $\pm 5\%$ and indicate excellent agreement between the participants, especially when compared to many earlier attempts in the field. The participating calibration laboratories seem to have a good understanding of their measurement capabilities. Participating national standards laboratories are perhaps somewhat optimistic with their uncertainties. Based on the experience gained we may propose that the presented method of comparison could be used as a basis for a larger international comparison.

References

1. G. Xu and X. Huang, "Characterization and calibration of broadband ultraviolet radiometers," *Metrologia* **37**, 235-242 (2000).
2. P. Kärhä, "Calibration and intercomparison issues with broadband UV meters," *UVNews* **7** 29-34 (2002).
3. A.J. Coleman, M. Collins, and J.E. Saunders, "Traceable calibration of ultraviolet meters used with broadband, extended sources," *Phys. Med. Biol.* **45**, 185-196 (2000).
4. J.J. Lloyd, "Initial survey of UV meter calibration centres," *UVNews* **5**, 38-41 (2000).
5. J. Envall, P. Kärhä, and E. Ikonen, "Calibration of broadband ultraviolet detectors by measurement of spectral irradiance responsivity," *Rev. Sci. Instrum.* **77**, 063110 (8 pages) (2006).
6. J. Envall, L. Ylianttila, H. Moseley, A. Coleman, M. Durak, P. Kärhä, and E. Ikonen, "Investigation of comparison methods for UVA irradiance responsivity calibration facilities," *Metrologia* **43**, S27-S30 (2006).

The use of a single-monochromator diode array spectroradiometer for UV-radiation measurements

Lasse Ylianttila

STUK, Radiation and Nuclear Safety Authority, Helsinki, Finland

Abstract. The suitability of single-monochromator diode array spectroradiometer for UV-radiation measurements, especially sunbed measurements, was evaluated. The spectroradiometer was characterized and correction methods for major error sources were developed. The uncertainty of the corrected UV measurements is estimated to be 14% (2σ).

Introduction

The suitability of an Ocean Optics S2000 spectroradiometer for sunbed UV-radiation measurements was evaluated [Ylianttila et. al. 2005]. The spectroradiometer was characterized and correction methods for major error sources were developed. The corrected spectra measured with the Ocean Optics S2000 spectroradiometer were compared to the spectra measured with Optronic 742 and Bentham 150 double-monochromator spectroradiometers. The measurement uncertainty of Ocean optics S2000 spectroradiometer in sunbed measurements was estimated.

Material and Methods

The Ocean Optics S2000 is a single-monochromator CCD-array spectroradiometer. The wavelength range is 200 nm - 800 nm and the FWHM bandwidth is 1.6 nm. The input optics consists of a PTFE (Teflon[®]) diffuser and a 4 m long optical fiber. An Oriel 51122 visible-light absorbing filter is used to reduce stray-light.

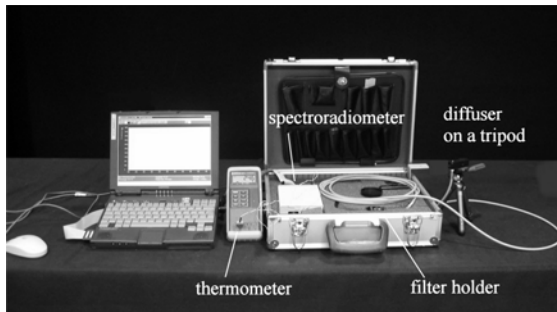


Figure 1. The Ocean Optics S2000 spectroradiometer in the measuring setup. The spectroradiometer is not removed from the transport case in normal use.

The linearity, dark signal, stray-light and slit function, angular response, and temperature response of the spectroradiometer were measured. A stray-light correction method based on the measured slit function was developed. The cosine correction factors for sunbed use were calculated. The standard wavelength scale determination method was improved.

The spectroradiometer was calibrated with a quartz-halogen 1000 W FEL lamp. A 40 W deuterium lamp was used to improve the signal-noise ratio in the UV-B range.

To verify the accuracy of the corrected spectra measured with the Ocean Optics S2000 spectroradiometer, various

sunbed and medical UV therapy lamps, a sunbed and solar spectra were measured. The spectra were compared to the spectra measured with Optronic 742 and Bentham 150 double-monochromator spectroradiometers. The measurement uncertainty of Ocean Optics S2000 spectroradiometer in sunbed measurements was estimated.

Results

The main error sources are cosine response and stray-light. The cosine response was not good, the cosine correction factor in sunbed measurements is 1.25 and the correction for uniform diffuse radiation is 1.20.

The correction of stray-light is essential, when the UV-B part of UV-radiation source should be measured accurately. The developed stray-light correction method works satisfactorily, but without any stray-light correction the measured UV-B irradiance could have over 50% error.

The temperature of the instrument and the integration time influence the instrument's dark signal. Therefore the dark signal should be measured jointly with each spectral measurement.

The wavelength shift due the temperature change is around 0.03 nm/°C. The sensitivity change caused by temperature is small between 20°C - 30°C. Outside this temperature range the sensitivity fell of by 5-30%, thus making the temperatures between 20°C and 30°C practical limits for instrument's temperature.

The instrument has small 5% non-linearity, for which a correction is applied. By using a quasi-Gaussian fit of the slit function for wavelength scale determination, wavelength accuracy of 0.05 nm can be achieved between 250 nm and 400 nm.

In the single lamp comparison measurements the integrated UV, UV-A, UV-B, and CIE-erythema weighted irradiances were within 10% from the values measured with the double-monochromator spectroradiometers. In the sunbed and solar irradiance measurements the differences were below 13%.

An example of spectral comparison is presented in figure 2, where a spectrum of a Philips Cleo Natural sunbed lamp measured with Ocean Optics S2000 spectroradiometer and Optronic 742 double-monochromator spectroradiometer are drawn. In the figure 2 b the ratio between Ocean Optics S2000 spectrum and Optronic 742 spectrum is drawn. The Ocean Optics S2000 spectrum has been interpolated for the comparison. (The wavelength of data points is defined by the pixel position in Ocean Optics S2000 spectrum, whereas the spectrum of Optronic 742 was measured with 1 nm steps.) In the UV-A the agreement is excellent, whereas in the UV-B the irradiance measured by Ocean

Optics S2000 is slightly smaller and the detection limit is higher.

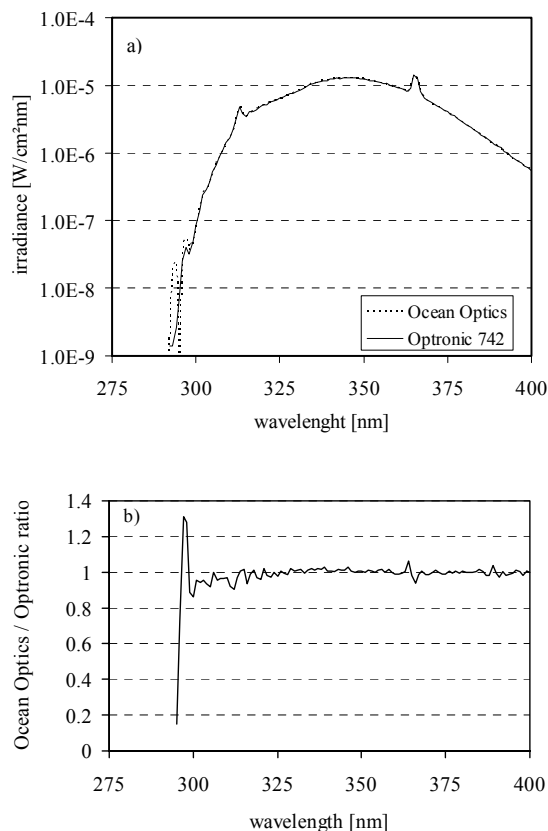


Figure 2. A comparison between sunbed-lamp spectra measured with single-monochromator Ocean Optics S2000 and double-monochromator Optronic 742 spectroradiometers. The measured spectra are drawn in a) and the ratio of the spectra is drawn in b). Note that the Ocean Optics spectrum has been interpolated for the comparison.

An uncertainty estimation for sunbed measurement that takes into account the major error sources is presented in table 1. The combined standard uncertainty of the UV measurement is 6.9% (confidence level 63%). With

coverage factor 2 (95% confidence level), the expanded uncertainty is 14%. For typical sunbed measurements this uncertainty is sufficient. By improving the cosine response, stabilizing the temperature, and refining the stray-light correction, the expanded uncertainty could be decreased slightly below 10%. Without any corrections the measurement error could exceed 50%.

Table 1. Uncertainty budget for UV-dose measurements.

uncertainty component	relative standard uncertainty [%]
calibration	3
stray-light	4
cosine response	3
temperature	3
wavelength	1
other sources	2
combined uncertainty	6.9
expanded uncertainty ($k = 2$)	13.9

Conclusions

The achieved measurement accuracy is sufficient for sunbed UV-radiation measurements. The easy portability of the Ocean Optics S2000 spectroradiometer makes the market surveillance measurements easier than with the conventional double-monochromator spectroradiometers. However, an extensive and laborious instrument characterization and complicated corrections are needed to make the measurements accurate. For the proper use of the instrument, the user should have knowledge of the instruments operating principles and potential error sources.

Acknowledgment. This work has been supported by the Finnish National Agency for Medicines.

Reference

Ylianttila, L., R. Visuri, L. Huurto, and K. Jokela, Evaluation of a Single-monochromator Diode Array Spectroradiometer for Sunbed UV-radiation Measurements, *Photochem. Photobiol.* **81**, 333-341, 2005.

GaAsP trap detector for UV measurement

*J-M. Coutin, F. Chandoul, and J Bastie
LNE-INM / CNAM, Paris, France*

Abstract. Several GaAsP detectors have been studied mainly in linearity and local responsivity. The stability under UV irradiation has also been studied. After these studies a trap detector has been realized and calibrated several time over a four year period of time in order to check if this type of detector could be used as transfer standard for radiometric measurements in the UV spectral range.

Introduction

In order to develop transfer standard detectors and a scale of spectral irradiance based on filter radiometers in the UV spectral range, studies have been undertaken on GaAsP detectors which could be an interesting candidate for realizing trap detectors. These detectors have a good responsivity in the UV spectral range. The maximum of responsivity at 610 nm and a spectral range from 190 to 680 nm could provide a good rejection of the stray light coming from long wavelengths. The studied photodiodes were the G 2119 type from Hamamatsu with an active area of 10x10 mm². The following characteristics have been checked : linearity, local responsivity, stability under strong UV irradiation, short term and long term stability.

Characterization of GaAsP photodiodes

Linearity measurement : The linearity of the photodiodes was measured using a flux addition method. The radiation impinging on the detectors was provided by quartz halogen lamps running at a color temperature of about 3000 K and filtered by a Schott KG 1 filter in order to remove the IR radiation. Metal on quartz filters were used for extending the dynamic range. The results of this study are shown in figure 1 for two photodiodes referenced 98 E and 98 F respectively. The linearity is better than 10⁻⁴ from approximately 10 nA to 100 μA.

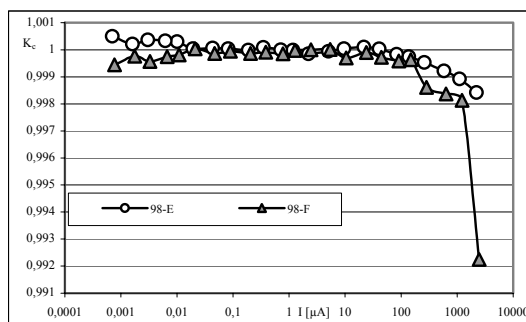


Figure 1. Linearity correction factor, for two GaAsP photodiodes versus the photocurrent of the photodiodes.

The shunt resistance and the noise in the using conditions have also been measured. For all the checked photodiodes the shunt resistance was greater than 1 GΩ and the noise was in the range of 0.5 to 2 pA.(standard deviation of dark current measurement).

Local responsivity measurement : The local responsivity of more than 10 photodiodes was measured at, at least, 3 wavelengths, 260, 300 and 380 nm with a spectral bandwidth of 3 nm. The spot on the detector had a diameter of little less than 1 mm and the scanning step was 1 mm. In general the local responsivity of these photodiodes was not very good ranging from some percent for the best (figure 2) to some tenth of percent for the worst.

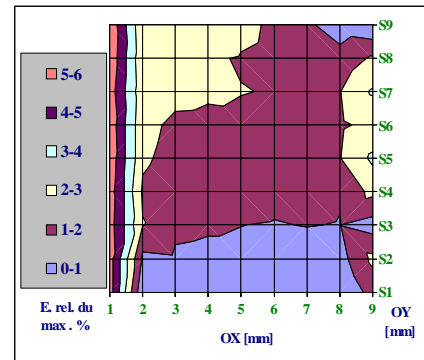


Figure 2. Local responsivity of a GaAsP photodiode of a reasonably good quality.

The local responsivity of some of the detectors was also checked at 488nm using an argon laser. The results were of the same type as the results in the UV range and generally worse. The reflectance factor of the photodiodes have also been measured in the spectral range 250 to 400 nm for two incidence angles, 10° and 45°. It was found in the range of 45% to 50% varying slightly with wavelength.

Stability under UV irradiance : The stability of the detectors under UV irradiance was checked using a deuterium lamp at an irradiance level of 130 mW.cm⁻² (total irradiance) during about 20 hours. The variation of the responsivity was measured at 220, 260, 300, 340 and 380 nm every hour. During about the 5 first hours of irradiation the detectors have exhibited a variation of 1% to 5% depending on the wavelength. After that, they seemed to become stable with variations lower than the uncertainty of measurements.

Realization of a trap detector

Starting from the results obtained on GaAsP photodiodes it was decided to realize a three elements reflection trap detector to be used as reference detector in the UV spectral range. For that 12 photodiodes of G 2119 type from Hamamatsu with an active area of 10x10 mm² have been bought and three of them having the best local responsivity have been used for realizing the trap detector. But before mounting them in the trap they have been aged under UV radiation coming from a deuterium lamp at a level of irradiance of 130 mW. After that, the trap detector called P-UV-1 have been calibrated in spectral responsivity. The calibration have been carried

Thematic Network for Ultraviolet Measurements

out in a 2 step method. In a first step the relative spectral responsivity is measured by comparison with a non selective cavity shape pyroelectric detector. In a second step the absolute spectral responsivity is measured by direct or indirect comparison to the cryogenic radiometer at some laser wavelengths in the visible range.

A typical absolute spectral responsivity curve of the GaAsP trap detector P-UV-1 is shown in figure 3.

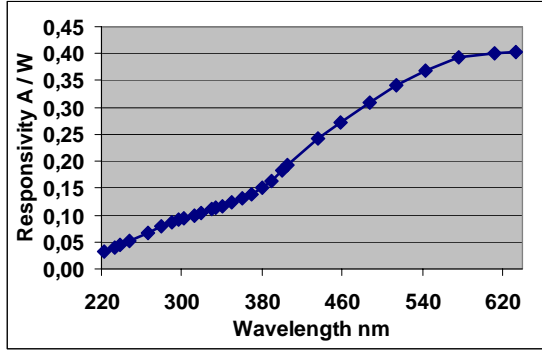


Figure 3. Spectral responsivity curve of the GaAsP trap detector P-UV-1.

Absolute calibrations : The first absolute calibration of this detector was carried out in April 2001 at the laser wavelengths of 487, 514, 543, 612 and 633 nm. Then it was again calibrated at the same wavelengths in February 2002, April 2004 and May 2005. The relative variation of the spectral responsivity of the detector between the various calibrations are shown in figure 4 taking as reference the first calibration.

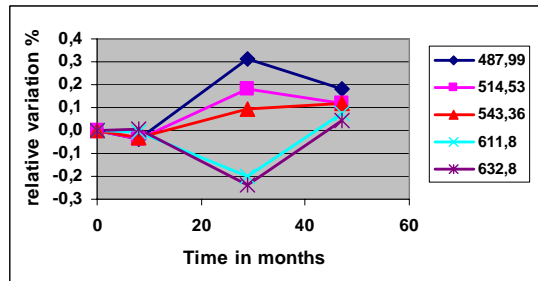


Figure 4. Stability of the absolute spectral responsivity of the trap detector P-UV-1 over a four year period.

The first, the second and the fourth calibration have been carried out by comparison behind a monochromator with a rather large beam, to a silicon trap detector calibrated against the cryogenic radiometer with laser beams. The third calibration has been carried out directly against the cryogenic radiometer with laser beams. In order to explain the different behavior of the third calibration compared to the others the local responsivity of the detector was checked at the wavelength of 543 nm over a diameter of 3 mm with a diameter of the laser beam less than 1 mm. The maximum deviation was $5.2 \cdot 10^{-4}$. The

calibration have been also carried out at the wavelength of 488 nm, at two power levels of 100 and 50 μ W in order to check potential linearity problems. The two results were well within the uncertainties.

Relative calibrations : The relative spectral responsivity calibration were carried out three times in June 2001, in February 2002 and in May 2005 by direct or indirect comparison to a non selective cavity pyroelectric detector over the spectral range 280 to 633 nm.

The results of these measurements are shown in figure 5. The reference value used for determining the relative spectral responsivity was the mean value of the spectral responsivity at the wavelengths of 487, 514, 543, 612 and 633 nm. This reference value has been chosen because the absolute calibrations for linking the relative and the absolute values are done using all these wavelengths.

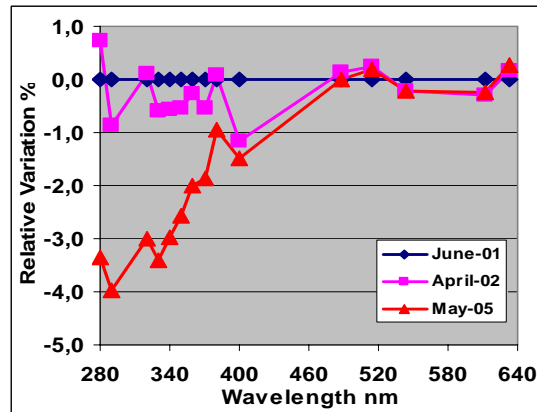


Figure 5. Stability of the relative spectral responsivity of the trap detector P-UV-1 over a four year period.

Conclusion

Several GaAsP detectors have been studied in order to realize a trap detector to be used as transfer detector. The linearity of this type of detector is good over a dynamic range of more than 5 decades but the local responsivity is rather poor. Mounting in a trap configuration this type of detector improves the local responsivity.

The spectral responsivity of the detector exhibit a small drift during the first hours of UV irradiation and after that become stable (short term stability). The long term stability checked over a four year period has shown a very small drift in the visible range. This drift increases for decreasing wavelengths. The annual drift is about 1% a year at 280 nm. This drift is too large for using this detector as transfer standard for very accurate measurements. Nevertheless it could be useful for usual calibrations du to its rather high spectral responsivity in the UV range and its limited spectral range in the visible.

Characterization of integrating spheres for ultraviolet radiometry

*Zhigang Li, Ping-Shine Shaw, Uwe Arp, Howard W. Yoon, Robert D. Saunders, and Keith R. Lykke
National Institute of Standards and Technology (NIST), Gaithersburg, MD, USA*

In UV radiometry, concerns over the stability and contamination of diffusing materials, such as polytetrafluoroethylene (PTFE), have been raised for a long time. To date, there are only a few studies mostly on the material reflectance under UV irradiation from sources such as Hg or Xe lamps [1,2,3]. Significant degradation in reflectance was observed and it was attributed to contaminants [1]. For integrating spheres, whose throughput is highly sensitive to material reflectance, it was suggested that fluorescence under UV irradiation could be an additional issue for accurate radiometric measurements [4]. To the best knowledge of the authors, the cause for fluorescence and the stability of integrating spheres exposed to UV radiation are unknown.

The excellent radiation diffusivity and depolarization properties of an integrating sphere makes it a good choice in preparing radiation from sources, such as deuterium lamps and synchrotron radiation, for high accuracy detection and transfer of radiation scales. The combination of deuterium lamp and integrating sphere could pose serious measurement challenges if UV radiation from the deuterium lamp either spoils the throughput over time or induces fluorescence. Here, we report the investigation of the performance of integrating spheres under UV irradiation from deuterium lamps. The integrating spheres studied are made with PTFE both in pressed and sintered forms. The pressed PTFE spheres are made at NIST and the sintered PTFE spheres are obtained from commercial products.

The study of integrating spheres under UV irradiation consists of two parts. In the first study, the integrating sphere under investigation is exposed to a deuterium lamp. The radiation exited from the integrating sphere is directed through a monochromator and detected by a photomultiplier tube. We measured and compared the spectral throughput for a variety of integrating spheres and observed different UV absorption spectra between integrating sphere. We also studied the change in the spectral throughput of integrating spheres after prolonged irradiation by the deuterium lamp. Furthermore, we used a second setup to identify fluorescence in the measured UV spectra. In this setup, the integrating sphere is exposed to a monochromatic UV laser beam as short as 210 nm from a tunable laser at NIST's SIRCUS facility. The output beam from the integrating sphere is analyzed by a spectrograph to identify any fluorescence excited by the incident laser. An example of measured results is shown in Fig. 1.

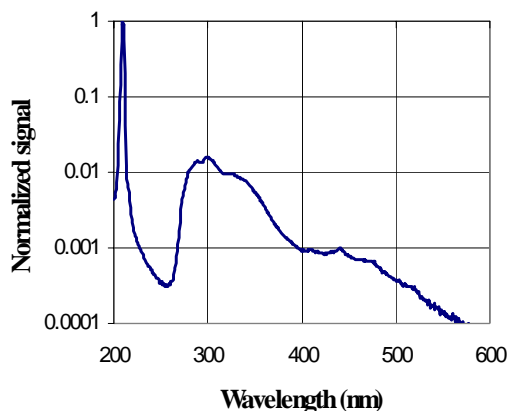


Figure 1. Spectral output from a sintered PTFE integrating sphere irradiated by a 210 nm laser beam. The structure around 300 nm is caused by fluorescence.

Our measurement results clearly show distinct UV absorption and fluorescence features by PTFE integrating spheres. In accordance with previous studies, we found contaminants are mostly responsible for the observed absorption and fluorescence as well as the degradation of integrating spheres. However, baking in vacuum can remove some but not all contaminants. In addition, fluorescence from the UV laser provided important clues for identifying the chemical nature of contaminants. We have identified several contaminants from the environment that have serious effects on the performance of PTFE integrating spheres. Detailed results and analysis as well as recommendation for the choice of integrating spheres for UV work will be given.

References

1. A.E. Stiegman, C.J. Bruegge, and A.W. Springsteen, Ultraviolet stability and contamination analysis of Spectralon diffuse reflectance material, *Opt. Eng.* 32, 799 (1993).
2. D.R. Gibbs, F.J. Duncan, R.P. Lambe, and T.M. Goodman, Ageing of materials under intense UV radiation, *Metrologia* 32, 607 1995/1996.
3. W. Möller, K-P. Nikolaus, and A. Höpe, Degradation of the diffuse reflectance of Spectralon under low-level irradiation, *Metrologia* 40, S212 (2003).
4. R.D. Saunders and W.R. Ott, Spectral irradiance measurements: effect of uv-produced fluorescence in integrating spheres, *Appl. Opt.* 15, 827 (1976).

Surveillance of UV-sensors in UV-disinfection plants in water works

A.Cabaj¹, R. Sommer², M.Klenner³, and H. Wright⁴

1. Institut für Medizinische Physik und Biostatistik, Veterinärmedizinische Universität Wien, Department für Naturwissenschaften, Austria
2. Klinisches Institut für Hygiene und Medizinische Mikrobiologie, Medizinische Universität Wien, Austria
3. Niederösterreichische Landesregierung, St. Pölten, Austria
4. Carollo Engineers, Boise, Idaho, USA

Keywords: Sensors, drinking water, UV-radiation, disinfection

Introduction

In the frame of two projects [one by American Water Works Association Research Foundation (AWWARF RFP 2977), the other by Niederösterreichische Landesregierung] water works with UV-disinfection plants for drinking water were visited and the reference irradiances measured by the plant sensors were compared with measurements done with reference sensors. Except of these sensor measurements the UV-transmittance of the water and other parameters were checked. The measurements mainly were based on the Austrian standard for disinfection plants for drinking water using low pressure mercury lamps (ÖNORM M5873-1, 2001) and a pre-standard for plants with medium pressure lamps (VORNORM ÖNORM M5873-2, 2003). Measurements were performed in several countries: Austria, Germany, Finland and Sweden. The measurement in Paderborn/Germany was based on the work-sheet W294(1997) from DVGW (Deutsche Vereinigung für das Gas- und Wasserfach). An examples of UV-disinfection plants can be seen in figs. 1a,b. The efficiency of UV-plants is tested by biosimetry in using calibrated spores of *Bacillus subtilis* as “measuring instrument”. Biosimetry gives as result the Reduction Equivalent Fluence (REF) and in measuring the reference irradiance during the biosimetric test, a parameter is defined which can be used for monitoring the UV-plant in the water work. The above mentioned standards define, among others, requirements for the monitoring sensors. The standards distinguish between reference sensors and plant sensors. For the reference sensor the parameters which have to be tested are: calibration of irradiance, spectral response, measuring range and linearity, measurement uncertainty, temperature response, stability over time and the geometrical dimensions of the sensor. The measurements in the water works often showed high discrepancies between the values measured with a reference sensor compared with the plant sensor.



Figure 1a (top) UV-disinfection plants in water work Pitkääkoski/Helsinki, Finland. Figure 1b (bottom) several plant sensors can be seen at the side of the UV-plant.

Measurements were performed in water works with low-pressure mercury lamps which emit predominantly UV-radiation at 253,7 nm and in one water work with medium pressure lamps. The measurement of the reference irradiance for low pressure plants is much easier because of the quasi-monochromatic nature of the radiation. When medium pressure lamps are used the sensor must weight the radiation according to the microbicidal action spectrum of *Bacillus subtilis*, the biosimulator. In figure 2 this action spectrum is given (ÖNORM M5873-2).

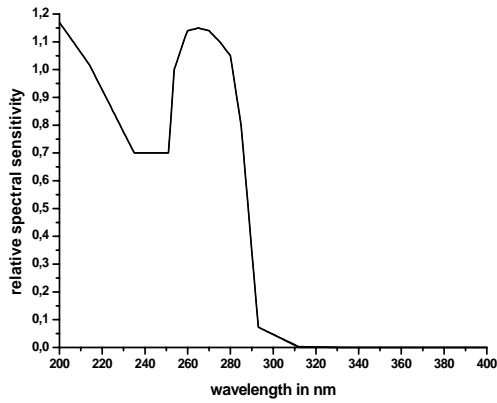


Figure 2. spectral response of spores of Bacillus subtilis according to ÖNORM M5873-2.

Results

Some results from the measurements in Helsinki are given in table 1.

Table 1. Reference irradiances measured with plant sensors and reference sensors. Measurements were also done with an older version of the ÖNORM-sensor which gives slightly higher irradiances. The German DVGW-sensor cannot be directly compared with the ÖNORM-sensor because of different entrance optics.

Sensor Nr.	Plant sensor ÖNORM M5873-1 (W/m²)	Reference -sensor ÖNORM M5873-1 (W/m²)	Reference -sensor ÖNORM M5873 (1996) (W/m²)	Reference -sensor DVGW W294 (W/m²)	Remarks
Reactor 1					Flow: 2800 m³/h
1	126	158	170	53	
2	135	165	175	55	
3	128	172	187	58	
4	126	171	181	58	
Reactor 2					Flow: very low
1	146	190	199	62	
2	150	193,3	211	67	
3	132	218	233	71	
4	156	204	219	68	
Reactor 3					Flow: 2800 m³/h
1	98	134	141,6	48	
2	99	137,7	146,3	47,5	
3	114	147	168,4	53,9	
4	127	162,8	173,5	56	

References

- ÖNORM M5873-1 E (2001). Plants for disinfection of water using ultraviolet radiation: requirements and testing, Part 1: Low pressure mercury lamp plants. ON Österreichisches Normungsinstitut, Vienna, Austria.
- PRESTANDARD ÖNORM M5873-2 E (2003). Plants for disinfection of water using ultraviolet radiation: requirements and testing, Part 2: Medium pressure mercury lamp plants. ON Österreichisches Normungsinstitut, Vienna, Austria.
- DVGW W294(1997), Bonn, Germany.

Calibration and characterization of UV sensors for water disinfection

T. Larason and Y. Ohno

National Institute of Standards and Technology (NIST), Gaithersburg, MD, USA

Introduction

Ultraviolet radiation (UV) effectively inactivates common pathogens found in ground and surface waters such as *Cryptosporidium*, *Giardia*, and most bacterial pathogens (e.g., *E. coli*). Water treatment facilities recently started using ultraviolet radiation for disinfection of drinking water, replacing standard chemical treatment. Typically, low-pressure and medium-pressure mercury lamps (LPM and MPM, respectively) are used in the UV reactors at the facilities. In these reactors, water flowing at a given rate should receive an appropriate UV dose. UV sensors mounted on the wall of the UV reactor or inserted into the water flow monitor the dose level by measuring the irradiance from the lamps. The UV sensors currently in use have a variety of designs and performance characteristics. Austria and Germany have developed or are developing standards for the sensor design and performance. These two standards differ in their requirements and do not address many of the problems associated with the UV monitors. Furthermore, there are already many water plants employing UV sensor systems consistent with one or the other standard. To resolve this confusion, American Water Works Association Research Foundation (AwwaRF) decided to develop new guidelines for UV monitors. The National Institute of Standards and Technology, USA (NIST) is participating in this project in collaboration with Carollo Engineers (Boise, ID), CDM (Denver, CO), and the University of Veterinary Medicine (Vienna, Austria). NIST studied the current UV water disinfection standards, ÖNORM M5873-1 and M5873-2 [1] (Austria), and DVGW W294 3 [2] (Germany), on the requirements for UV sensors for LPM and MPM lamp systems. Pertinent to the study, NIST is measuring and analyzing the characteristics of various types of UV sensors. This information will aid in the development of new guidelines which will address issues such as sensor requirements, calibration methods, uncertainty, and traceability.

Problems with irradiance calibration of sensors

The physical quantity to be measured is the microbicidal irradiance, defined as the total irradiance (W/m^2) weighted by the microbicidal action spectrum $s_{\text{mik,rel}}(\lambda)$ as shown in Fig. 1. According to ÖNORM M5873-1, M5873-2, and DVGW W294-3, UV sensors for both LPM and MPM systems are calibrated for irradiance responsivity against an LPM lamp. Since the value of $s_{\text{mik,rel}}(\lambda)$ is unity at 254 nm, and LPM lamps only have significant flux at 254 nm, the measured irradiance from an LPM lamp is equal to the microbicidal irradiance. Instruments can be calibrated for microbicidal irradiance responsivity using an LPM lamp, regardless of the sensor's spectral responsivity. This method works very well for LPM lamp systems. However, there is a problem for MPM lamp systems. The spectral output from MPM lamps differs significantly from LPM lamps. In addition,

real UV sensors never have spectral responsivities perfectly matched to $s_{\text{mik,rel}}(\lambda)$. In fact, many of the sensors used for MPM lamp systems have fairly large deviations from $s_{\text{mik,rel}}(\lambda)$. As a consequence of the differences between LPM and MPM spectral distributions and differences between the sensor spectral responsivities and $s_{\text{mik,rel}}(\lambda)$, measurement errors of the microbicidal irradiance occur. This source of measurement error, called a spectral mismatch error, is well known in other applications, e.g., photometry, where a detector's responsivity is tuned to match the action spectrum, $V(\lambda)$. Note that if a UV sensor had a spectral responsivity perfectly matched to $s_{\text{mik,rel}}(\lambda)$, there would be no problem, that is, the measured irradiance value would be equal to the microbicidal irradiance.

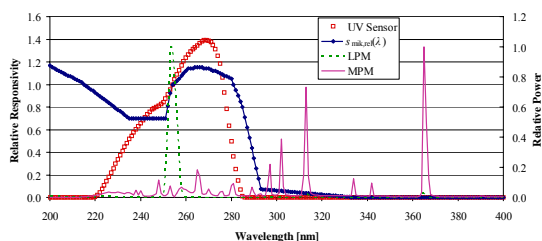


Figure 1. The microbicidal action spectrum, $s_{\text{mik,rel}}(\lambda)$; the spectrum of an LPM lamp and a MPM lamp; and the spectral responsivity of a UV sensor.

To ensure that such errors will not be significant, the ÖNORM and DVGW standards specify requirements for the relative spectral responsivity of sensors used for MPM lamp systems. DVGW W294-3 requires that a term $f_{1,z}$ be calculated from the relative spectral responsivity of the sensor, and the sensors must meet $f_{1,z} \leq 0.25$ (reference sensors) or $f_{1,z} \leq 0.40$ (duty sensors). ÖNORM M5873-2 does not require the relative spectral responsivity of the sensors. However, it requires measurement with two specified cutoff filters and a MPM lamp that is to be calibrated with a spectroradiometer. The D value (relative difference between the microbicidal irradiance measured by the sensor and spectroradiometer) is calculated from these results. The sensors must meet $D < 0.2$ for both filters. The evaluation of relative spectral responsivity is critical but not easy in either standard. In addition, NIST found that many of the currently used commercial sensors do not meet these requirements. Reference sensors that meet the requirements can still have errors as much as 20 %.

Proposed calibration scheme

To solve the practical problems found in the calibration methods and evaluation of spectral responsivity requirements for sensors designed for MPM lamp systems NIST is proposing an alternate sensor calibration method for MPM lamp systems. The root of the problem is that the MPM lamp has a very different (multi-line) spectrum than the LPM calibration lamp (a single emission line at

254 nm). The proposed method is to use a MPM lamp as a calibration source for the sensors used to measure MPM lamp systems. This approach is based on the well-established principle that errors are minimized in any measurement system when the standard and test sample are of the same type (strict substitution). In strict substitution, many of the measurement error components are cancelled out. If the UV sensor is calibrated using an MPM lamp, and subsequently measures MPM lamps having the same spectral distributions, the error will be zero, theoretically, regardless of the spectral responsivity of the sensor. In real cases, there are variations in the spectra of MPM lamps, so the errors will not be zero, but errors will be significantly reduced even with sensors having a large deviation from $s_{\text{mik,rel}}(\lambda)$.

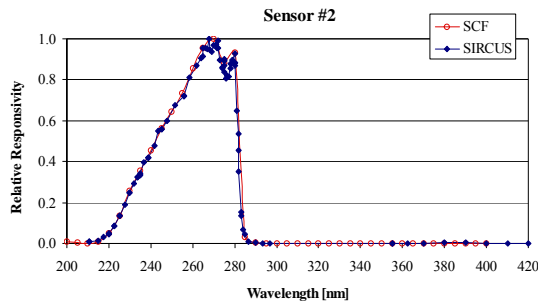


Figure 2. Relative spectral irradiance responsivity data of one of the sensors measured by SCF and SIRCUS.

The actual calibration of sensors with this method can be done simply. It only requires a MPM lamp and a reference standard sensor calibrated for MPM microbicidal irradiance responsivity. Then, the UV sensor under test can be calibrated simply by comparison to the reference standard sensor under illumination by a MPM lamp. This method is analogous the situation in photometry where the $V(\lambda)$ function defines the spectral response of a photometer. To ensure consistency in the calibration approach, a reference MPM lamp spectrum may need to be defined; ÖNORM M5873 2 already lists a nominal MPM lamp spectrum. A similar example exists in photometry with the CIE standard source, Illuminant A. The source has a standardized, defined spectral distribution, an incandescent source (lamp) approximating a blackbody at a temperature of 2856 K. All photometers are calibrated using a standard incandescent lamp having a spectrum close to the CIE standard Illuminant A. With this approach, photometric calibration results are universal.

Characterization of the UV sensors

10 different UV sensors from 6 different manufacturers designed for water disinfection monitoring have been characterized at NIST for several parameters. The relative spectral responsivity measurements were taken at two NIST facilities. The first is a monochromator-based

spectral responsivity measurement facility referred to as the Spectral Comparator Facility (SCF). This system was designed for spectral power responsivity measurements. The facility also has the capability to measure a detector's irradiance responsivity. The absolute irradiance responsivity in $V/(W/m^2)$ or $A/(W/m^2)$ is measured by spatially scanning the beam across the detector entrance aperture in very small distance intervals using an X-Y stage. In this manner, NIST was able to measure the relative spectral irradiance responsivity of 10 sensors though measurements of some of the sensors had very large uncertainties due to extremely low signal. The incident flux in this facility is fairly low, on the order of $1 \mu W$, while these sensors are designed for very high irradiance levels (up to $2000 W/m^2$).

The relative spectral responsivity for eight of the sensors was also measured in another NIST facility capable of generating higher monochromatic UV flux. This facility, the Spectral Irradiance and Radiance Responsivity Calibrations using Uniform Sources facility (SIRCUS), can generate monochromatic beams with up to ~ 100 mW of power in the 200 nm to 400 nm region using the frequency doubled, tripled and quadrupled output from pulsed Ti-Sapphire laser, which has a quasi-CW emission (pulses at very high frequency, 76 MHz). To measure the irradiance responsivity of the sensors, a frosted quartz diffuser plate was placed in front of the detectors to generate a quasi-uniform irradiance field at the detector reference plane. The irradiance levels ranged from approximately $2 W/m^2$ to $20 W/m^2$ at 254 nm.

An example of relative spectral responsivity data is shown in Fig. 2. The responsivity measurement results indicate a large variation in the spectral responsivities of the commercial sensors. The spectral mismatch of these sensors (deviation of the relative spectral responsivity curve from the microbicidal action spectrum $s_{\text{mik,rel}}(\lambda)$) causes significant errors in the measured microbicidal irradiance as large as 160 %. Many of the sensors did not meet ÖNORM M5873-2 and DVGW W294-3 requirements for relative spectral sensitivities of the sensors.

The linearity (limited range), temperature dependence ($10^\circ C$ to $35^\circ C$), and angular responsivity of these sensors at 254 nm have also been measured and evaluated. Some significant nonlinearity at low levels for some of the sensors was observed.

References

1. ÖNORM M5873-1 "Plants for the Disinfection of Water using Ultraviolet Radiation: Requirements and Testing Low Pressure Mercury Lamp Plants" (2001) and ÖNORM M5873-2 "Plants for the Disinfection of Water using Ultraviolet Radiation: Requirements and Testing Medium Pressure Mercury Lamp Plants" (2003).
2. DVGW W294-3 "UV Disinfection Devices for Drinking Water Supply - Requirements and Testing" (2003).

Monitoring of low- and medium pressure mercury lamps in UV-disinfection plants for drinking water

A. Cabaj¹, A.W. Schmalwieser¹, and R. Sommer²

1. Institut für Medizinische Physik und Biostatistik, Veterinärmedizinische Universität Wien, Department für Naturwissenschaften, Austria
2. Klinisches Institut für Hygiene und Medizinische Mikrobiologie, Medizinische Universität Wien, Austria

Keywords: Sensors, spectral response, angular response, linearity, disinfection, temperature response, UV-radiation

Introduction

An Austrian standard for disinfection plants for drinking water using low pressure mercury lamps was established in 2001 (ÖNORM M5873-1, 2001) and a pre-standard for plants with medium pressure lamps has been finished in 2003 (VORNORM ÖNORM M5873-2, 2003). An example of a UV-disinfection plant can be seen in figs. 1a,b. The efficiency of UV-plants is tested by biosimetry in using calibrated spores of *Bacillus subtilis* as “measuring instrument”. Biosimetry gives as result the Reduction Equivalent Fluence (REF) and in measuring the reference irradiance during the biosimetric test, a parameter is defined which can be used for monitoring the UV-plant in the water work. The two above mentioned standards define, among others, requirements for the monitoring sensors. The standards distinguish between reference sensors and plant sensors. For the reference sensor the parameters which have to be tested are: calibration of irradiance, spectral response, measuring range and linearity, measurement uncertainty, temperature response, stability over time and the geometrical dimensions of the sensor. The plant sensor has to be tested with respect to the maximum measurement uncertainty, measuring range and resolution, temperature response, temporal stability, geometrical dimensions and marking. Both sensor types have to fulfill requirements for angular response.

Results

Angular response

The requirements for the angular response of the sensor are given by the Austrian standard as a function of inclination. The measurements were done in tilting the sensor against the beam whereas the UV-source and a sensor for control of the lamp were left in a constant position. The angular response is calculated as the ratio between the measured irradiance and the irradiance which would be expected by assuming an ideal cosine response.



Figure 1a (Top) UV-disinfection plant for 1 800 m³/h in Vienna. Figure 1b (Bottom) sensor and sensor port.

Linearity

Linearity was tested either by the method of beam addition or by a comparison of the sensor which was tested with a linearity corrected instrument. Our laboratory standard radiometer (International Light IL 1700 with sensor SED240) deviates 2% over a range of 5 magnitudes of irradiance. Figure 2 shows the relative deviations from linearity for another hand held device. The second monitoring system in this plot consists of the same type of sensor but an electronic control unit from another manufacturer. This example demonstrates clearly the influence of the electronic control unit.

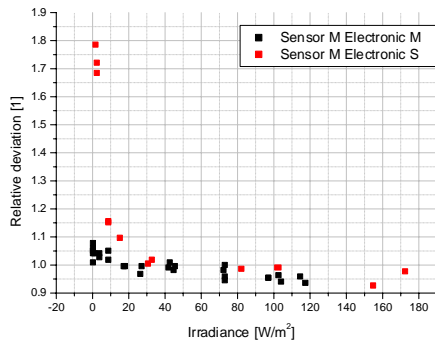


Figure 2. Relative deviation from linearity for two different radiometers. While both use the same type of sensor electronics, the control units are different.

Temperature response

The temperature response is another critical point of sensors and electronic control units. For reference sensors the Austrian Standard purports an upper limit for the temperature drift of 0.1%/K in the range from 0°C to 40°C, that is 4% for the whole range. Figure 3 shows the temperature behaviour of two UV-radiometers.

Spectral response

For medium pressure plants the spectral response of the sensor has to correspond to the spectral action spectrum of microorganisms. To proof the accordance first of all a spectral measurement of the Hg-medium pressure lamp used for the test is necessary. In weighting its spectrum with the microbicidal action spectrum the effective irradiance is gained. A measurement of this irradiance then has to be done with the sensor to be tested. The difference between values of weighted irradiance measured with the sensor and calculated weighted irradiances (weighting of spectral irradiance, measured by spectroradiometer) delivers a measure of quality. For our test the polychromatic radiation came from a medium pressure mercury lamp Heraeus DFH DQ 1023. While for wavelengths shorter than 240 nm relatively good agreements could be found, high deviations occur due to radiation with wavelengths longer than 280 nm. The sensors show high overestimation of longwave UV radiation and therefore overestimation of disinfection efficiency.

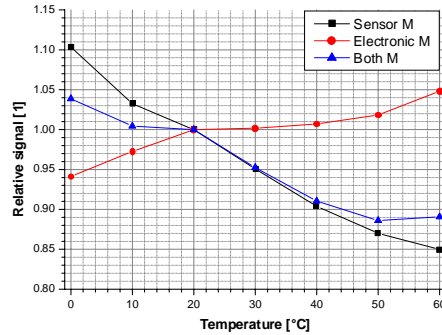
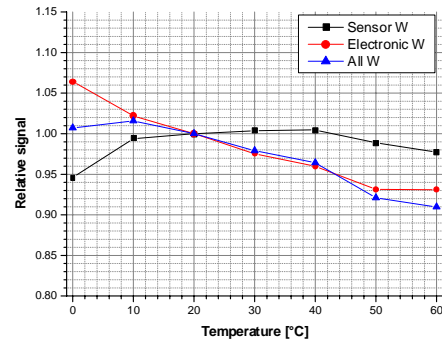


Figure 3. Relative signal depending on temperature for two UV-control systems. Shown are the results for the pure sensor (black), the electronic unit (red) and the whole system (blue).

References

ÖNORM M5873-1 E (2001). Plants for disinfection of water using ultraviolet radiation: requirements and testing, Part 1: Low pressure mercury lamp plants. ON Österreichisches Normungsinstitut, Vienna, Austria.

PRESTANDARD ÖNORM M5873-2 E (2003). Plants for disinfection of water using ultraviolet radiation: requirements and testing, Part 2: Medium pressure mercury lamp plants. ON Österreichisches Normungsinstitut, Vienna, Austria.

Sanders R. (1972). Accurate Measurements of and Corrections for Nonlinearities in Radiometers. *Journal of Research of the National Bureau of Standards-A. Physics and Chemistry A.* **75A**, No.5, 437-453.

Improved entrance optic for global irradiance measurements with a Brewer spectrophotometer

Josef Schreder

Calibration Measurement Softwaresolutions - Ing. Dr. Schreder, Kirchbichl, Austria

This presentation outlines a new input optic for measuring spectral UV irradiance with a Brewer spectrophotometer. The first system was installed in 2002 (Fig. 1) in the Brewer MKIII #163 [1].



Figure 1. Brewer MKIII #163 with the global input optic for measuring spectral UV irradiance. The first optic was installed in 2002. It was replaced in 2004 by the new and further improved global input optic. Courtesy J. Gröbner, JRC, Ispra.

The system provides considerably improved measurement accuracy in comparison to the traditional flat input optic (Fig. 2). The direct cosine error of this system is less than 5% for incidence angles between 0° and 80° [2]. The integral cosine error for isotropic radiation is less than 2.4% with an uncertainty of +1%.

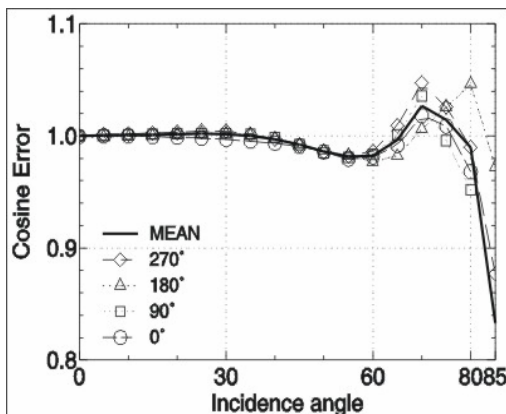


Figure 2. Ratio of the angular response function of the new entrance optic relative to the desired cosine relation in four planes. The angular responses of all four planes are within 5% of the ideal response for incidence angles. Figure taken from [1].

The system was replaced in 2004 by the further improved and now commercially available system UV-J1015 (Fig. 4).

Traditionally, the Brewer spectrophotometer uses a flat global input optic which underestimates the true global solar irradiance by a factor of up to and exceeding 10%. This factor is not constant but depends on the time of day and the atmospheric conditions [3].

So far, special shaped global input optics with nearly perfect characteristics have become available only for instruments using optical light guides that link the entrance optic to the detector [4].

The new global optic is flexible enough to be easily installed on every brewer spectrophotometer. An initial optimization of the angular response function for each individual Brewer spectrophotometer is required.

The uncertainties in global irradiance measurements due to the angular response of the new global input optic have been shown to be around +1% [1]. This is a substantial improvement to the traditional Brewer spectrophotometers.

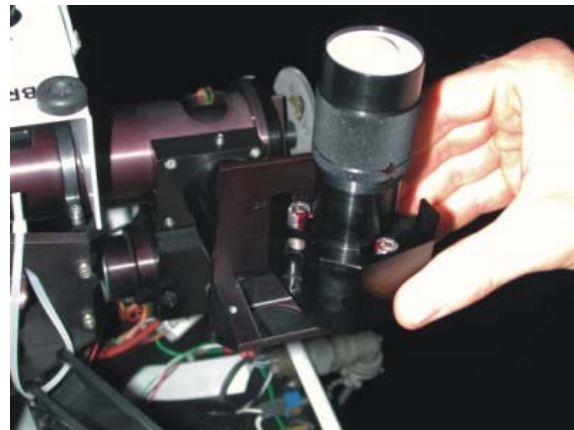


Figure 3. Installation of the improved entrance optic for global irradiance measurements.

References

1. J. Gröbner: Improved entrance optic for global irradiance measurements with a Brewer spectrophotometer, Appl. Opt. 42, 3516-3521, 2003.
2. German Institute of Standardization DIN 5032, part 6, Beuth Verlag, Berlin, 1994.
3. A.F.Bais, S. Kayadzis, D. Balis, C.S.Cerefos, M. Blumthaler, Correcting global solar ultraviolet spectra recorded by a Brewer spectrophotometer for its angular response error. Appl. Opt. 37, 6339-6344, 1998.
4. J.G.Schreder, M. Blumthaler, M. Huber, Design of an input optic for solar UV measurements. Internet Photochem. Photobiol. <http://www.photobiology.com/UVR98/schreder/index.htm>, 1998.

Time resolved measurements of spectral radiant flux from VUV to NIR ($160 \text{ nm} < \lambda < \approx 1000 \text{ nm}$) on Xe excimer lamps

*K. E. Trampert, M. Paravia, and W. Heering
Lighting Technology Institute, University Karlsruhe, Germany*

Abstract A radiometric set-up is presented to measure the radiant efficacy of pulsed Xe excimer lamps. It allows time and spectral resolved radiant flux measurements from the VUV to NIR region. The results will provide a better understanding of the plasma processes in Xe excimer lamps. We measure the Xe excimer emission $\lambda_{\text{Xe}_2^*} = 172 \text{ nm}$ in the VUV and spectral lines at $\lambda_{\text{Xe}^*} \approx 828 \text{ nm}$.

We use two different monochromators with fast photomultipliers because the duration of Xe excimer micro discharges is only several 10 ns. To determine the total flux of the lamp, we choose a goniometric set-up.

Xe excimer lamp

Recent papers show that its possible to increase the radiant efficacy of dielectric barrier discharges (DBD) by using very fast pulse excitation. Improvements by a factor of 3.2 in comparison with the AC excitation were reported (Mildren et al. 2000).

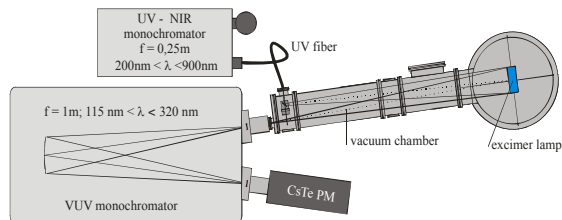


Figure 1. Set-Up with vacuum chamber, one Monochromator for VUV and one for UV to NIR and the turnable lamp at the right.

The authors measured the VUV output indirectly by means of phosphor conversion from VUV into the VIS. Furthermore up to now, the radiant flux of excimer lamps has been determined by interpolation from a single determined radiant value. So the reported flux values have big experimental uncertainties and are difficult to be compared. (Falkenstein et al. 1997). The large differences between reported efficacies of Xe excimer lamps would be better understood if the VUV measurements were less uncertain. The absence of reliable standard lamps in this spectral region might be the reason why commercially available Xe excimer lamps are used to calibrate UV sensors. (Carman et al. 2004)

The Xe_2^* excimer molecule emits the main part of its radiation by spontaneous decay of Xe_2^* into an emission band in the VUV around a wavelength of $\lambda = 172 \text{ nm}$ (10 nm FWHM). For a better understanding of the plasma processes, it is also very interesting to measure lines from higher energy levels. Here lines in the NIR are of special interest, e.g. $\lambda = 823 \text{ nm}$ and $\lambda = 828 \text{ nm}$. They fill the excimer levels. This is why the ratio between the VUV emission and these lines is an indicator for the radiant efficacy of a Xe_2^* plasma. Time-, wavelength- and angle-resolved measurements on cylindrical lamps from the

VUV $\lambda = 120 \text{ nm}$ up to the NIR $\lambda = 1000 \text{ nm}$ have been performed.

VUV - NIR goniophotometer

In air, radiation with wavelength below $\lambda < 200 \text{ nm}$ is nearly totally absorbed by oxygen. To measure such wavelengths it is necessary to eliminate the oxygen out of the optical path. Either you use a non-absorbing atmosphere like N_2 or Ar, or you evacuate the whole path. We use a vacuum chamber to make long term measurements affordable. Figure 1 shows the set-up with two monochromators, one for the VUV-UV region ($120 \text{ nm} < \lambda < 320 \text{ nm}$) and another for the UV to NIR region ($200 < \lambda < 1000 \text{ nm}$) and a turning arm which supports the lamp in the vacuum chamber.

To determine the radiant intensity, a diffuser made of MgF_2 is placed in front of the VUV monochromator entrance. As the distance between lamp and diffuser was chosen ten times of the largest radiation field dimension the photometric distance law can be applied. So it was possible to calibrate the irradiance on the diffuser with a deuterium lamp, though this lamp is only a standard of radiant intensity.

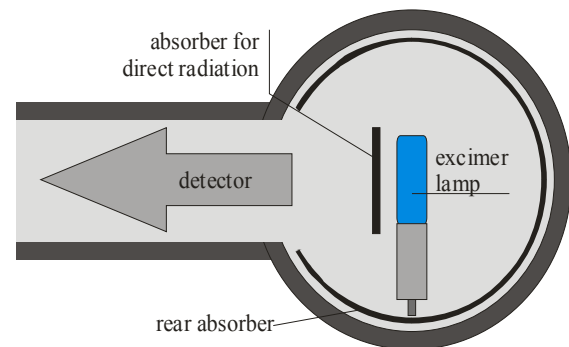


Figure 2. Set-up for stray light measurement.

The timescale of the DBD is in the range of several 10 ns. To dissolve the time dependent behavior of the plasma fast photomultipliers are used. In the lower spectral range ($120 \text{ nm} < \lambda < 320 \text{ nm}$) a solar blind CsTe PM is used. This PM is mounted at the exit port of a 1 m monochromator with normal incident grating. The longer wavelengths are detected with an $f = 0.25 \text{ m}$ Czerny-Turner monochromator with multi alkali PM. The radiation is guided through a special UV fiber to the entrance slit. At the entrance of the fiber a quartz diffuser is used.

Stray light reduction

The vacuum chamber is made of stainless steel and reflects down to the VUV. For absolutely calibrated measurements it is necessary to have a special focus on stray light reduction. For this reason we put in both optical paths three apertures. We experienced out that

Thematic Network for Ultraviolet Measurements

carbon black gives a good and cheap absorbing coating for the wall behind the lamp. The disadvantage of this coating is that carbon black should not be touched anytime. Carbon black hardly adsorbs oxygen so that the vacuum will not be reduced.

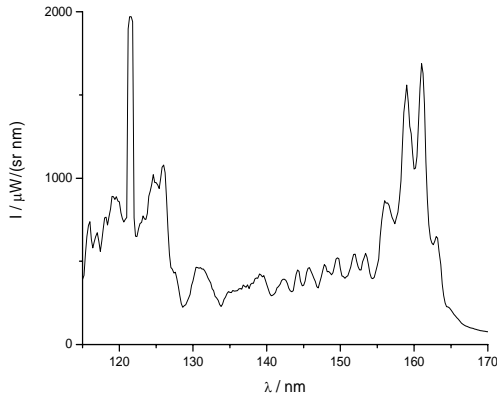


Figure 3. Spectrum of an deuterium lamp in the VUV region.

To measure the stray light ratio we put a shutter in front of the lamp so that only the rear reflected part of the lamp output is detected. (Figure 2) To reduce the stray light fraction we also coated the rear absorber with carbon black. At the moment we analyze how the carbon in the

vacuum influences the transmission of the MgF_2 in the VUV.

Calibration

We calibrate our set-up with an deuterium lamp of known radiant intensity. For wavelengths below 160 nm this is the only available calibrated lamp. Unfortunately the spectrum of the Deuterium lamp is as shown in Figure 3. The spectrum exists of many lines. So it is indispensable to measure with the same resolution as it was done during calibration.

To specify the spectral resolution of our monochromator we measured the lines of Hg low pressure lamp (PenRay®) in dependence of the slit width.

References

- Carman, R. J., R. P. Mildren, et al. (2004). "High-pressure (> 1 bar) dielectric barrier discharge lamps generating short pulses of high-peak power vacuum ultraviolet radiation." *Journal of Physics D: Applied Physics* **37**(17): 2399.
- Falkenstein, Z. and J. J. Coogan (1997). "The development of a silent discharge-driven XeBr⁺ excimer UV light source." *J. Phys D: Appl. Phys.* **30**: 2704-2710.
- Mildren, R. P., R. Morrow, et al. (2000). *Enhanced efficiency from a Xe excimer barrier discharge lamp employing short-pulsed excitation*. SPIE-Int. Soc. Opt. Eng. Proceedings of Spie - the International Society for Optical Engineering, vol.4071, 2000, pp.283-90. USA.

Improvements of a fast scanning double monochromator for UV-B monitoring

G. Mathe
Instrument Systems GmbH, Munich, Germany

The SPECTRO 320 D scanning double monochromator was first introduced in 1995 as a fast measurement system for the monitoring of UV-B radiation. The measurement of the complete UV-B range up to 450 nm is accomplished within 1 minute. Later the extension of the scan range to visible and infrared radiation was available. The paper describes new developments and improvements regarding the optomechanical layout and the control electronics.

The SPECTRO 320 D is based on a modified Czerny-Turner monochromator with a focal length of 320 mm. In figure 1 the optical layout of the double monochromator is shown. To record the spectra quickly at high wavelength accuracy, the diffraction grating is driven directly by a steadily rotating DC motor. A complex, mechanical drive is no longer essential as a precision angle encoder synchronizes the data acquisition during rotation. This guarantees a high absolute wavelength accuracy and linearity. Since all available diffraction gratings are located on the same axis, irregular rotational movements between the two individual monochromator parts during the scan are thus eliminated. A wide spectral range from UV to IR within one single instrument is offered. Moreover, up to three detectors can be located at the exit slit of the monochromator. A movable mirror guides the light beam to one of the detectors as required. The change-over of the gratings and detectors in use takes place automatically. The overlapping area of the respective spectral ranges is used by the software in order to join the individual spectra to each other correctly.

In the new release 5 of the SPECTRO 320 D several new features were implemented:

- An improved mechanical design of the mirror mounts leads to a significantly smaller temperature drift of the measurement signal.
- The measurement parameters are no longer fixed for the whole wavelength range. An unlimited number of sub-ranges can be defined, each of it with individual measurement parameters due to specific requirements of the test source. This enables the user to define ranges with faster or slower scan speeds which is essential to achieve short measurement times.
- The new control electronics is equipped with electronic switches instead of mechanical relays. This makes the switching between different amplifier gains much faster.
- Due to a new mechanical layout a cooled UV optimized photomultiplier can be used together with two other detectors, like InGaAs, PbS, etc. This offers the possibility for a measurement over a broad wavelength range using up to three different gratings in a single scan.

The new release of the SPECTRO 320 D provides a variety of features in a unique combination. Short measurement times can be realized whereas the unsurpassed flexibility of the measurement system regarding wavelength range, launching optics etc. remains untouched.

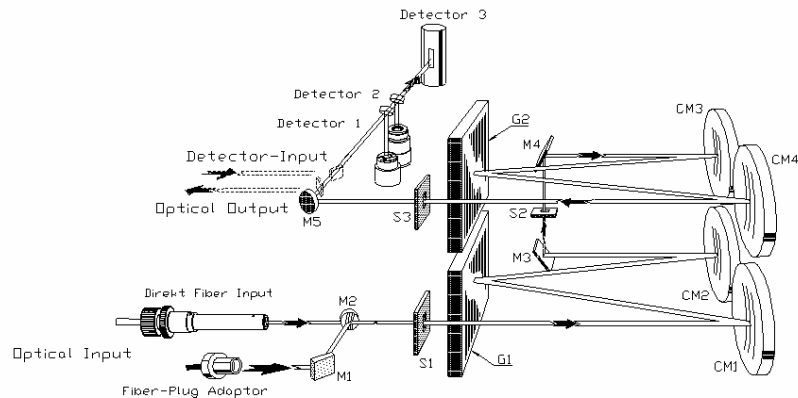


Figure 1. Optomechanical layout of the SPECTRO 320 D. Up to three different pairs of gratings are mounted on a common turret.

Reference

Espinar, B., Blanke, J., Ramirez, L., Bolós, M., Rodríguez, J.A., Blanco, M., Measurement of the spectral distribution of global solar radiation and its components by the SPECTRO 320D Scanning Spectrometer, *Measurement and modeling of Solar Radiation & Day-light Conference*, Edinburgh, Sept. 2003.

Long-term experience in using deuterium lamp systems as secondary standards of UV spectral irradiance

P. Sperfeld, J. Metzdorf, and S. Pape
Physikalisch-Technische Bundesanstalt, Braunschweig, Germany

Abstract. During the CCPR-K1.b key comparison “Spectral irradiance in the wavelength range 200 nm to 350 nm,” a set of 6 newly developed deuterium lamp systems (DLS) have been used as transfer standards. The long-term experiences during this intercomparison demonstrated the quality of the system and confirmed the intention to provide the DLS for the use as a transfer standard of spectral irradiance in the UV spectral range.

The deuterium Lamp system DLS

The DLS consisting of up to four lamps each, a power supply and a monitor-detector have been developed by the Physikalisch-Technische-Bundesanstalt (PTB). They are the result of a thorough investigation of a variety of deuterium lamps and operating conditions in order to test and optimize their capability (stability, reproducibility, sensitivity to misalignment) for the use as traveling standard [1].



Figure 1. Deuterium lamp system (DLS). Lamp housing with lamp exchangeably and reproducibly mounted inside and monitor detector that can reproducibly be aligned on the optical axis in front of the housing.

A Cathodeon J64 30W deuterium lamp is the central part of the DLS. The lamp is mounted within a housing in order to protect the lamp and to achieve sufficiently stable and reproducible operating conditions. It is pre-aligned so that the mechanical axis of the housing is in coincidence to the optical axis of the lamp defined by the direction of the maximum output. The exit port of the housing is designed to either hold an alignment target (jig) or a monitor detector as shown in Fig. 1. The reflecting jig with a reticle in its centre defines both the optical and mechanical axis and the reference plane of the lamp system.

A built-in resistor as well as several electronic circuits are used to permanently monitor electrical voltage, current and heating voltage of the lamp during operation.

A group of these housed lamps are reproducibly operated within one DLS which also comprises an external power supply assigned to the DLS. A typical spectrum of a DLS lamp is shown in Fig. 2.

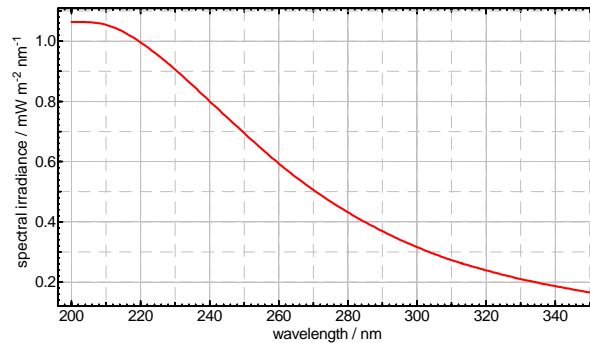


Figure 2. Typical irradiance spectrum of a DLS lamp.

Lamp stability during the intercomparison

During the CCPR key comparison K1.b the lamp systems have been treated in different ways: Two systems remained at the PTB, two systems have been hand-carried to and from the participants and two systems were shipped by courier. In combination with the ageing of the lamps during their operation time of up to 45 hrs and the associated realignment and re-ignition processes, the stability and reproducibility of the DLS could be investigated. Earlier investigations of the lamp system showed that under laboratory conditions the long-term drift is less than $-3 \cdot 10^{-4} \text{ h}^{-1}$ and the re-ignition reproducibility is better than $\pm 0.1 \%$ [1].

The analysis of the intercomparison which is still in progress showed that during the intercomparison the majority of the lamps changed by less than 2 % in the whole spectral region from 200 nm to 350 nm during up to 45 hrs of burning time. At the PTB which acted as a pilot laboratory for the intercomparison, the mean drift of all 20 lamps was below -2 %. Compared to precedent experiences with UV working standards [2] and compared to the results of the lamp characterizations, this drift is acceptable low.

Implementation of monitor detectors

In conjunction with these promising results, the ability of external SiC photodiodes to monitor the stability of the DLS could be demonstrated. The monitor detector is an optional part of each DLS. It consists of a hybrid SiC photodiode with built-in operational amplifier. The monitor detector can easily and reproducibly be flanged to the lamp housing and is used before and after spectral

measurements of the lamp to monitor the drift of the lamp irradiance at about 280 nm during and between miscellaneous measurements.

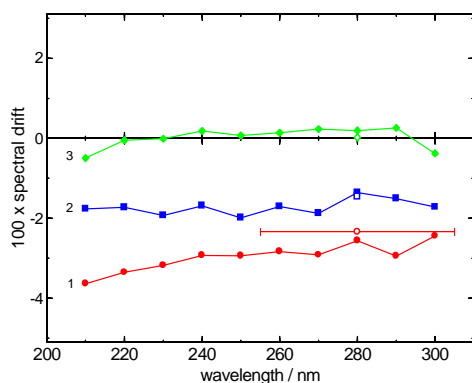


Figure 3. Spectral changes of three different lamps between the first and second calibration sequence at the PTB (the lamp with the highest drift (1), typical example of lamp with medium (2) and low drift (3), respectively). The open symbols at 280 nm refer to the corresponding changes of the monitor detector signals, where the FWHM of the SiC photodiode is indicated.

Using this technique, sudden changes of the lamps as well as the long-term drift can be identified and documented. Thus, it is then possible to at least correct the calibration data by a constant factor which represents the drift. If the spectral drift of a lamp has been measured during the

lamp characterization, it is also possible to carry out a spectral correction.

In Fig. 3 three typical examples of lamp changes (low, medium and high drift) and the corresponding variation of the monitor detector signals are shown. This demonstrates the applicability of monitor detectors.

Conclusion and outlook

It could be verified that the new deuterium lamp system (DLS) can be used as transfer standard of spectral irradiance in the spectral region from 200 nm to 350 nm. The use of monitor detectors allows documenting the long-term changes of the lamps and gives the possibility to correct calibration data for lamp changes.

This gives the possibility to extend the recalibration periods of such transfer standards. The DLS which has been developed by the PTB will be the recommended working standard for the UV spectral range. It is commercially available by the Austrian company Schreder CMS [3].

References

- [1] Sperfeld P., Stock K. D., Raatz K.-H., Nawo B., Metzdorf J., Metrologia, 2003, 40, S111 S114.
- [2] Hollandt J., Becker U., Paustian W., Richter M., Ulm G., Metrologia, 2000, 37, 563-566.
- [3] Schreder J., <http://www.schreder-cms.com/>, Austria, 2005.

Expanded Measurement Uncertainty of Spectral Measurements Outside of the Laboratory

A. Gugg-Helminger¹ and C. Henjes²

1. Gigahertz-Optik GmbH, Puchheim/Munich, Germany
2. IABG, Ottobrunn, Germany

Introduction

In an accredited optical radiation calibration laboratory all variables that can affect measurement results are well regulated and documented. On site, variables such as temperature, electromagnetic and magnetic fields very often cannot be controlled and can influence detection devices. Also lack of mechanical positioning equipment like an optical bench can add to the overall measurement uncertainty. In order to produce accurate measurements in the field the uncertainties introduced through the entire calibration chain starting from the primary standard obtained from the national or international standards laboratory to the internal transfer standards used by the secondary calibration organization must be known as well as the uncertainty added due to the performance of the measurement outside the laboratory. This paper discusses sources of error in the field and how to calculate the expanded uncertainty.

Preliminary Work

For accurate calibration the test detectors measurement uncertainty must be known. To illustrate this a photo multiplier tube (pmt) and silicon detector (Si) output signal was compared using a double monochromator based spectroradiometer. On a linear scale the real difference in signal level would not be discernable. The ratio of the two curves shows that PMT produces about 10000 times higher signal in UV as the photodiode. To discover the crossover point of the detectors the standard deviation ($k=2$) of 3 measurements are calculated. The crossover point is in the ultraviolet spectral region where the pmt signal is more than 8000 times higher. Inspection of only the detectors signal levels does not reveal this crossover point which greatly affects measurement accuracy

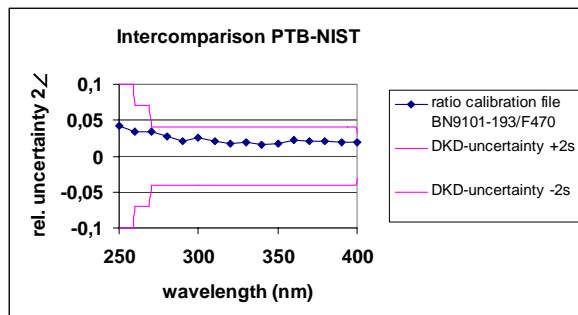


Figure 1. Ratio of two calibration files (PTB/NIST) with standard deviation ($k=2$) and DKD uncertainty budget.

Now with this information in hand, the next step of comparing national and international standards can be

performed. In this study an irradiance standard from PTB (Germany) and NIST (USA) was compared. (Figure 1).

As shown the intercomparison data falls within the stated DKD uncertainty budget. This allows a statement of traceability to international standard laboratories to be provided on the calibration certificate. Also the normal lab uncertainty budget can be calculated for the secondary lamp transfer standard for use in field calibrations.

Uncertainties for field calibration

There are two methods to specify the level of uncertainty. It can be stated for each wavelength or for wavelength regions. The lowest uncertainty level for field calibrations has been designated as "WORKS-uncertainty".



Figure 2. Solar Simulator WSA/TVA at IABG.

Twelve measurements were performed over the past seven years on the same irradiance source (Figure 2). The source was well maintained by the technical staff at IABG in Ottobrunn Germany.

The measurements were done nearly in the centre of the 6m diameter solar simulator. All measurement equipment has to be placed in a suitable high. This extraterrestrial solar simulator is placed in a clean room and the erythemal dose of 250J/m² effective dose will be reached within 13s. Therefore clean room clothes and eye and skin protection is a must. The protection is done with a fully shielded face screen and sun screen with a protection factor of 30 on face, hands and neck. To compare all of the spectra all were normalized to 1370kW/m² and then the mean calculated.

With acceptance of an absolute stable source we can calculate an overall uncertainty within the 7 years. If we calculate the stated uncertainty to the real uncertainty calculated from 12 independent measurements over the last 7 years, the results are shown in figure 3. This is very confident to the measurements and the given uncertainty.

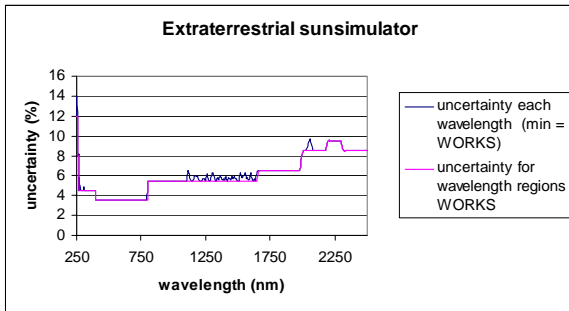


Figure 3. Uncertainty given at each wavelength either for wavelength regions or for one measurement.

The combined relative standard uncertainty $\sigma_C(E)$ is based on the combination in quadrature of the standard uncertainty in irradiance given by the PTB (Physikalisch Technische Bundesanstalt Braunschweig und Berlin), $\sigma_{CP}(E)$ of the traceable irradiance standard used, $\sigma_{CPT}(E)$ for the measurement of the irradiance standard at calibration of the transfer standard with uncertainty of $\sigma_{CT}(E)$, the uncertainty during the initial calibration of the double monochromator system at customer site $\sigma_{CCB}(E)$, the uncertainty while calibrating the double monochromator system at the end of testing at customer site $\sigma_{CCE}(E)$, and $\sigma_{CL}(E)$, given by the standard deviation of the independent sample measurements and additional system specific terms $\sigma_{CS}(E)$, given by the accuracy of the instrument.

The system specific terms $\sigma_{CS}(E)$, is the absolute deviation of the ratio at the end of the calibration to the transfer standard irradiance values at the customer site.

The expanded uncertainties

$$U_{GO}(E) = 2 \sigma_C(E) = k [\sigma_{CP}^2(E) + \sigma_{CPT}^2(E) + \sigma_{CT}^2(E) + \sigma_{CC}^2(E) + \sigma_{CL}^2(E) + \sigma_{CS}^2(E)]^{1/2} \quad (1)$$

in %, represent a confidence level of 95%. They were obtained by assuming a normal distribution and multiplying the combined standard uncertainties by a coverage factor $k=2$.

$U_{GO}(E)$ is the uncertainty stated in the certificates from Gigahertz-Optik GmbH Calibration laboratory

System check for calibration

Depending on the measurement there are some tests that are necessary before measurement of the customer source. For an accurate measurement of a terrestrial sun simulator for example, the wavelength precision, wavelength in the measurement range, slit function, stray light reduction of the measurement device and the detection threshold have to be tested.

Other factors to consider in field calibration work

The environmental conditions at the field site of the calibration should be checked beforehand if possible. The unit under test maybe very large or located at some height requiring special mounting of the measurement instrument perhaps on a steep slope (Figure 4). Sometimes a need of hard work to get entrance to the object is needed. In figure 4 a snow sweeper was needed to come into the cabin.

Or space for your measurement equipment may be limited requiring the components to be situated close together. This can influence results, for example the photomultiplier tube will be affected by the electromagnetic field from the power supply of your electronics or personal computer and monitor. Measurements may have to be performed in a clean room where special clothing is required making the task personally uncomfortable and tedious. The operating temperature must be above 21°C and below 27°C.



Figure 4. Snow-sweeping before enter the location.

The measurement must be performed very carefully and immediately verified while on site. This is because commonly access to the light source or facility itself is limited due to scheduling by other test groups or only available at specified times.

As shown as an example the movement of the measurement system can influence accuracy. The system specific terms $\sigma_{CS}(E)$, of absolute deviation of the ratio of the calibration to the transfer standard irradiance values at the start and at the end of testing at the customer site must be known as it will have a lot of influence on the uncertainty that can be stated on the calibration certificate. In figure 5 the system was moved about 70m. It was disconnected to the mains and after new installation recalibrated. Without recalibration a huge additional uncertainty will be given.

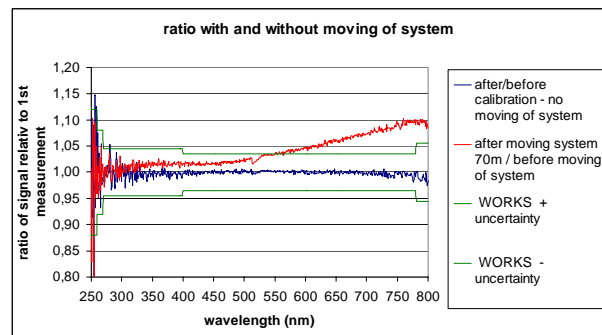


Figure 5. Signal ratio of calibrations with and without moving the system in linear scale.

Conclusions:

On site field calibration is much more complicated than simply moving the measurement device to the customer facility and performing a measurement. A good amount of technical knowledge and experience is required to produce accurate measurements with a low uncertainty

budget. Also, many independent tests on the measurement equipment are necessary before actually calibrating the device under test.

References

Technical note TN-TR30-1729 Investigation on the stability and measurement precision of the spectral distribution of the solar simulator WSA/TVA at IABG, Ottobrunn – Germany, 23. August 2001

European Thematic Network for Ultraviolet Measurements UVNEWS issue 6 Nov. 2000; “Characterizing the Performance of Integral Measuring UV-Meters“. Helsinki University of Technology, Metrology Institute, P.O. Box 3000, FIN-02015 HUT, Finland

Application & Product guide 2004/2005, Gigahertz-Optik GmbH

UV-Monitoring at Outdoor Workplaces - A Base for Well-Balanced Health Prevention Regulations

I. Unverricht¹, M. Janßen², G. Ott², and P. Knuschke¹

1. Dept. of Dermatology, Technische Universität Dresden, Germany

2. Federal Institute of Occupational Safety and Health, Dortmund, Germany

Introduction

The annual skin cancer incidence per 100.000 inhabitants in Germany is: 80 for basal cell carcinomas, 25 for squamous cell carcinomas and 12 for malignant melanomas [1]. Epidemiological studies corroborate: the solar UV radiation is an important co-factor in skin tumour genesis. One hand, increasing life expectancy causes higher cumulative life time doses of UV radiation. On the other hand, the changed outdoor life style in the last decades leads to higher cumulative UV life time doses too. The experience of our dermatological department underline, most of the basal cell and squamous cell carcinoma patients are person who have an increased of solar exposure round the year in its anamnesis.

In consequence, it is necessary to apply adequate protection measures against harmful UV overexposure - as well at workplace as in recreational time.

In Germany there are about 3 million outdoor workplaces. The ICNIRP “Guidelines on UV radiation exposure limits” [2] were established for indoor workplaces and artificial UV sources. The natural self protection ability of the skin was excluded in this threshold values. In this way, an application of the ICNIRP values to solar UV exposed outdoor workplaces would permit a working time of 10...15 minutes at noon time on a sunny summer day.

A precondition to establish well balanced health protection regulations to outdoor workplaces was to measure the real individual solar UV exposure levels of employees whose workplaces were solar exposed permanently or intermitted respectively. For a careful evaluation of the individual UV exposure level at the workplace it is necessary to compare this level with the UV exposure levels in leisure time and holidays.

Method - Personal UV monitoring at solar exposed workplaces

The aim of the FIOSH(Federal Institute for Occupational Safety and Health)-research project F1777 (2002-2006) „Personal UV Monitoring in Outdoor Workers “ was to investigate the individual UV exposure levels in

representative occupational groups with solar exposed workplaces by a routine personal UV monitoring. Beyond the personal UV dosimetry of workday exposures, leisure time exposures and holiday exposures in the course of a year, global and subjective factors influencing the individual UV-exposure were stored in the database of the personal UV monitoring (global factors: global UV radiation, meteorological data; subjective factors: e.g. protocol on times staying outdoors/clothing status/sunscreen use, leisure time behaviour in the measurement periods, skin type). Furthermore, measurements of the seasonal changing body distribution of the solar UV exposure under everyday life conditions were included in the personal UV monitoring.

Investigated occupational groups:

- Outdoor workers: 3 groups ($n = 15$ per group)
 - building construction workers / agricultural workers (plant cultivation) / dustmen
- Occupational groups working outdoors and indoors: 3 groups ($n = 15$ per group)
 - nursery school teachers / physical education (PE) teachers / window cleaners
- Indoor workers
 - Control group ($n = 3$)
 - indoor worker data from previous personal UV monitoring studies ($n = 150$)
(BMBF-projects: 07UVB54B 1996-1998 [3], 07UVB54C3 2000-2002 [4])

To measure the individual UV radiant exposure we used polysulphone film (PSF) dosimeter (Dermatology / Technische Universität Dresden, Germany) as complete physically described UV sensor [3, 5]. For time-resolved UV measurements during the course of the day and the year two person per group and the three indoor workers wore an X2000 data logger personal UV dosimeter (Fa. Gigahertz Optik GmbH, Puchheim / Germany) simultaneously to the PSF dosimeter. The biological effective UV exposures (Erythema [6], ICNIRP, NMSC [7]) were measured for workdays, for weekend days and in holiday time separately. The reference measurement position was the chest region.

The comprehensive description of the personal UV monitoring and the study design were explained in previous publications [3, 4, 8].

Results and Discussion

The cumulative annual UV exposures of the outdoor workers were dominated by the exposure during summertime. Figure 1 presents the weekly UV exposure (erythema effective radiant exposure H_{ery} in SED per week) of 5 workdays and 2 weekend days measured in May/June 2003 (solar noon elevation $\gamma_s = 60^\circ$, Dresden: 51.0° N) and September 2003 ($\gamma_s = 42^\circ$) respectively. The results of the outdoor workers were compared to indoor worker data measured previously (like above mentioned).

Remark: Data of mean individual UV exposure investigated in analogues measurement periods (solar noon elevation) but in different years are only comparable within or between behaviour groups, if the global radiation and meteorological conditions were very similar. In case of mismatching of such data sets large errors could be possible [8].

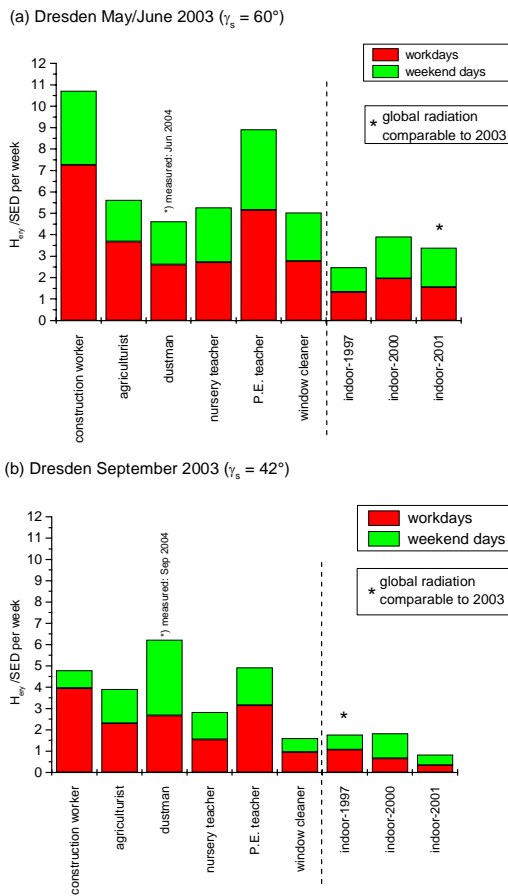


Figure 1. Mean weekly UV exposure H_{ery} (a) May/June 2003 (b) September 2003 [1 SED = 100 J/m² erythema-effective].

As expected, the group of building construction workers achieved the highest mean amount of UV exposure on workdays as well in May/June as in September. A similar workday exposure level was found for the PE-teachers. But the special behaviour of this profession group has to take into account: These teachers execute their lessons outdoors in case of good weather conditions. Furthermore

- as documented in the diary protocol on times being outdoors and leisure time behaviour - most of the PE-teachers coach sport groups in the afternoon and they are active in outdoor sport like jogging or tennis.

The measured UV exposure levels of the agricultural workers were unexpected low on workdays (May/June 2003: 5,5 SED/week; September 2003: 3,5 SED/week) - even if the diary protocols documented: In the vegetation period the agriculturists worked outdoors up to seven days per week. In an additional questionnaire they should specify the occupational outdoor activities. Typically, most of the time was spent in cabins of agricultural cars or machines. In this way, these agricultural workers were protected to solar UV exposure in a certain degree.

The typical course of a nursery school teacher's workday comprises times spent outdoors with the children between 9 and 11 a.m. and between 15 and 17 p.m. Staying indoors at lunch and rest time of the children causes the lower of UV exposure levels compared to building construction workers or PE teachers.

The working routine of dustmen is characterized by a work task rotation weekly: one week dustcart driving, one week dust loading. These work tasks are permanent over the year - independent on weather conditions. In contrast, the planning of outdoor activities of nursery school teachers is meanly influenced by weather conditions. While on workdays in May/June the mean UV exposure level of dustmen is comparable to the result of the nursery school teachers, the ratio shifted in September by about a factor 2 (dustmen: 0,53 SED/d, nursery school teachers: 0,3 SED/d). It was noticed that this tendency was rising in winter time (results not shown).

On workdays the measured UV exposures (chest position) of the window cleaners were lower than expected. The workplace analysis on one hand and the measurement of the UV body distribution on the other solved the discrepancy. In summer the working time started at 4 p.m. and ended at 12 p.m. (as protection against high temperature and reflected solar radiation at noon). The exposure ratio between the neck or back position and the chest position was about 4...5 to 1.

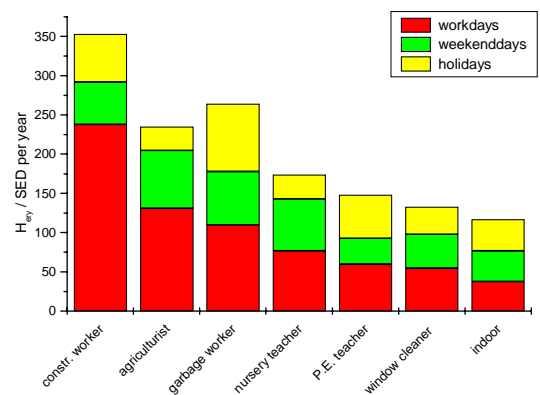


Figure 2. Annual UV exposure (chest position) of different groups of outdoor workers in comparison to indoor workers in 2003/2004.

Thematic Network for Ultraviolet Measurements

The results the annual UV exposure (chest position) of the different groups of outdoor professions in comparison to indoor workers (control group) is presented in figure 2.

Summary and Conclusion

In result of this project a database was established on the solar UV exposure levels of the investigated representative groups of employees working outdoors permanently or intermitted. A model realized biometrical calculations on the annual UV exposures including the exposure distribution to 19 different body sites for the investigated outdoor profession groups.

To assess the heighten of seasonal or annual UV exposure in the outdoor worker and the possible risks a reference baseline UV exposure level was required. The authors

recommend as a reference baseline UV exposure: the UV exposure level of indoor workers with less outdoor activities in leisure time (representative for about 80 % of the indoor workers). The required data pool for (German) indoor worker is available [3, 4].

Compared to the indoor workers the UV exposure levels of outdoor workers present a season-depending increase of the workday UV exposure. Furthermore an increase of the annual UV exposure was stated. We found that the mean annual UV exposure levels in profession groups with intermitted solar UV exposure at the workplaces were increased to 170...270 %. In occupational groups working outdoor permanently, the mean annual UV exposures ranged between 260 % and 470 % compared to indoor workers (Tab. 1).

Table 1. Increased UV exposure of outdoor workers related to indoor workers.

Occupational group	Increase in UV exposure on workdays compared to indoor workers		Workday percentage of annual UV exposure	Annual UV exposure in relation to indoor workers
	Summer / %	Winter / %		
indoor workers	100	100	33	100
Construction workers	500 - 1000	400 - 600	66	470
Agricultural workers	250 - 500		55	260
garbage workers	200	300	40	310
nursery teachers	150 - 300	200	41	270
P.E. teachers	350 - 700	100	43	200
Window cleaners	250	100	39	170

In conclusion, the data of the FIOSH-research project F1777 can serve as a scientific base to provide the discussions on well-balanced health prevention regulations of outdoor workplaces.

References

[1] Stellungnahme der Strahlenschutzkommission: Environmental UV-Radiation, Risk of Skin Cancer and Primary Prevention. SSK Band 34, Stuttgart: Gustav Fischer 1996

[2] International Commission for Nonionizing Radiation Protection: Guidelines on UV radiation exposure limits. Health physics Vol. 71, No 6 (December), p. 978, 1996

[3] Knuschke P, Krins A. (2000) UV-Personendosimetrie Teil B: Mit Verwendung des Polysulfonfilms als UV-Sensor. Schlußbericht BMBF-Vorhaben 07UVB54B, Standort: Univeritätsbibliothek Hannover und Technische Informationsbibliothek F 00 B 1544

[4] Knuschke P, Kurpiers M, Koch R, Kuhlisch W, Witte K (2004) Mittlere UV-Expositionen der Bevölkerung. Schlussbericht BMBF-Vorhaben 07UVB54B, Standort: TIB Hannover F 05 B 898

[5] Krins A. Untersuchungen der physikalischen Eigenschaften von Polysulfonfilm zur Anwendung in der UV-Dosimetrie, Promotionsarbeit ausgefertigt an der TU Dresden/Institut für Strahlenschutzphysik (1999)

[6] ISO 17166 /CIE S007. Erythema Reference Action Spectrum and Standard Erythema Dose

[7] Draft standard CIE DS 019.2 Photocarcinogenesis Action Spectrum (Non-Melanoma Skin Cancer)

[8] Unverricht I, Janßen M, Ott G, Knuschke P (2004) UV-Monitoring an Arbeitsplätzen im Freien - eine Basis für ausgewogene Richtlinien zum Gesundheitsschutz. In: Reidenbach H-D, Dollinger K, Hofmann J (Hrsg.): Nichtionisierende Strahlung - Sicherheit und Gesundheit. TÜV-Verlag, Köln, 2004, 599-609 Publikationsreihe Fortschritte im Strahlenschutz FS-04-128-T

Extreme Ultra-Violet Phototherapy

Harry Moseley

University of Dundee, The Photobiology Unit, Ninewells Hospital & Medical School, Dundee, U. K.

Introduction

There are three standard methods of applying UV phototherapy. One involves the combination of psoralen and UVA (known as PUVA); the other two relate to the use of UVB, namely broad-band and narrow-band (or TL01). All of these techniques have been shown to be useful in the management of certain skin conditions, particularly psoriasis.

In 1981, a group working in Munich developed a new lamp that emitted very high levels of UVA1 (340-400nm) radiation (Mutzhas et al 1981). It was claimed that this emitted 140 mW cm⁻² of UVA1 (340-400nm), 10 times more UV than a conventional phototherapy cabinet. Although technically interesting, this lamp aroused little curiosity within the dermatological community. At the mechanistic level, it was shown that UVA1 induced T-lymphocyte apoptosis, reduced the number of Langerhans cells and mast cells, increased production of collagenase, and induced photoprotection by tanning (Dawe 2003). Recently, interest has been kindled in clinical application in conditions that do not respond well to current treatments and where, based on the possible mechanisms of action, this therapy could have a role. These conditions include atopic dermatitis, systemic lupus erythematosus, and scleroderma (Dittmar et al 2001; Polderman et al 2001; Stege et al 1997).



Figure 1. UV mapping of the irradiance over the area normally occupied by the patient. The sheet was used to avoid reflections.

Materials and Methods

Accordingly, we took delivery of a High Dose UVA1 Dermalight system manufactured by Dr Honle, Medizintechnik GmbH, Munchen, Germany. This comprised twenty four filtered 2 kW metal halide lamps. It has a power rating of 26.5 kW; air exchange of 1600 cbm/h; 2 intake and 2 extraction ducts each of 25 cm diameter.

We have developed a reliable and reproducible method of dosimetry. We calibrated an International Light UVA

detector (IL 1400 UVA TD) using a portable UVA1 Dermalight that incorporated a single filtered 2 kW metal halide lamp. Calibration was carried out in our optical laboratory, using a Bentham double grating spectroradiometer (Bentham Instruments, Berks, England) which was calibrated using deuterium arc and tungsten filament lamps calibrated at the National Physical Laboratory (NPL, Teddington, England). We used the IL detector to map out the UV irradiance at 15 positions, corresponding to the surface of the patient (Figure 1).

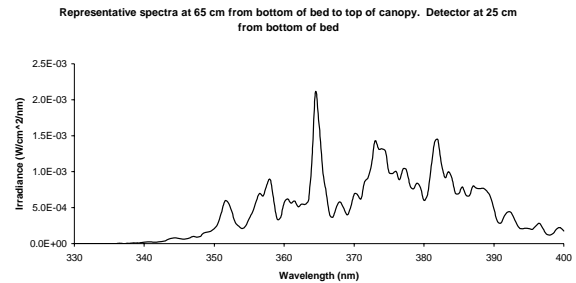


Figure 2. Spectral emission from Dermalight Ultra1.

Results

The mean of the 15 measurements was the mean patient irradiance and this was 67.1 mW cm⁻². The spectral emission is shown in Figure 2. Clinical results are presented in Figure 3.

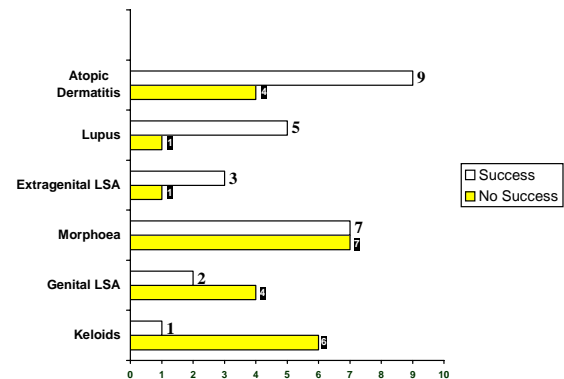


Figure 3. Analysis of our first 50 patients treated with high dose UVA1 therapy. These are all patients with difficult to treat conditions.

Discussion

According to our measurements, UV levels are considerably higher than in conventional phototherapy cabins but only about half as much as stated by other investigators. This allows an objective scientifically-based evaluation of the treatment, since much of the literature to date has been anecdotal in nature with no evidence to support any stated light dose. We have now treated over 50 patients, with conditions that were

Thematic Network for Ultraviolet Measurements

difficult to control and severely debilitating, and our initial impression is that many have derived considerable benefit from this new extreme form of ultra-violet phototherapy. Our treatments are all supported by dosimetry that is traceable to national measurement standards.

Further study is required before it will be known where high dose UVA1 fits within dermatological practice but early results are encouraging.

References

Dawe RS. Ultraviolet A1 phototherapy. *British Journal of Dermatology* 148: 626-637, 2003.

Dittmar HC, Pflieger D, Schopf E, Simon JC. UVA1 therapy dose-finding study in patients with acute exacerbated atopic

dermatitis. *International Archives of Allergy and Immunology* 124: 386-388, 2001.

Mutzhans MF, Holzle E, Hofmann C, Plewig G. A new apparatus with high radiation energy between 320-460 nm: Physical description and dermatological applications. *The journal of Investigative Dermatology* 76: 42-47, 1981.

Polderman MC, Huizinga TW, Le Cessie S, Pavel S. UVA-1 cold light treatment of SLE: a double blind, placebo controlled, crossover trial. *Annals of Rheumatic Disease* 60: 112-115, 2001.

Stege H, Berneburg M, Humke S et al. High dose UVA1 radiation therapy for localized scleroderma. *Journal of American Academy of Dermatology* 36: 938-944, 1997.

Photobiological quality control in UV phototherapy

P. Knuschke¹, A. Gugg-Helminger², Ch. Pfeiffer¹, and M. Meurer¹

1. Dept. of Dermatology, Technische Universität Dresden, Germany

2. Gigahertz-Optik GmbH, Puchheim, Germany

Up to now in Germany there are no preconditions in UV phototherapy to measure, evaluate and document patient exposure data comparable in general. Often, there is no compatibility between the data set of the photodermatological departments in each case. Therefore no assessments of the life-long received treatment exposures of the patients are possible.

To overcome this distinct shortcoming we proposed the following procedure which facilitates the documentation of comparable, possible to add and in future retrospective assessable exposure data of patients undergoing UV phototherapies:

1. Before starting the UV-phototherapy cycle: determination of the present minimal erythema dose (MED) of the patient on-site in therapeutic irradiation position. (Fig. 1)
2. Documentation of the MED of the patient measured erythema-effective in units of the standard-erythema dose (SED [1]). (Fig. 2)
3. Documentation of UV treatment doses and increments of dose increasing in multiples of the determined MED and documentation of the MED-related exposure data together with its expression in SED-units (UV single dose, fraction of UV dose increase, cumulative UV dose of the treatment cycle).



Figure 1. MED-test-set to determine patient's MED on-site in therapeutic irradiation position before starting the UV phototherapy.

Background of the proposed procedure is: On one hand the UV phototherapy is orientated to the UV-erythema with the MED as an upper limit of treatment exposure. On the other hand, the relative action spectrum the UV erythema and of the risk to produce a nonmelanoma skin cancer are similar in the wavelength range therapeutic UV

sources. So, basing on the proposed procedure a retrospective risk assessment of patients life-long accumulated UV treatment exposures will be possible (Remark: In case of change to photochemical treatments the procedure will be the same basing on the minimal phototoxic dose MPD. Because of its quiet different action spectrum to the phototherapy the exposure data had to be documented separately).



Figure 2. Determination of the MED in units of the standard-erythema dose SED by a well-adapted Broadband-radiometer.

We realized this procedure in practice. To determine patients MED in the later treatment position (Fig. 1) we can present an own developed MED-test set using in routine since 1995.

Using a broadband radiometer well adapted to the standard erythema actionspectrum and the cosine function (Fa. Gigahertz-Optik GmbH Puchheim/Germany) we determined the MED of 30 volunteers (Fig. 2). Each volunteer was exposed to four different types of UVB-lamps or UVAB-lamps. The intraindividual variation in MED expressed in SED units and the mean the SED values was less than 20%. Technically, the measurement was easy to perform for our trained personnel.

In summary we conclude that our described guidelines for therapy documentation and long-term documentation are technically feasible and allow documenting the cumulative UV exposure of patients in a comparable, biologically meaningful and reproducible way.

Reference

- [1] ISO/CIE 17166, Erythema Reference Action Spectrum and Standard Erythema Dose.

Personal UV-monitoring in health prevention and risk analysis

Peter Knuschke

Dept. of Dermatology, Technische Universität Dresden, Germany

It is well known, ultraviolet radiation (UVR) produces as well beneficial as acute or chronic hazard effects in man. UV radiation of the same waveband range is effective in the essential vitamin D production but could be a risk factor concerning several skin cancers or can have an effect as a skin or eye disease-causing agent too. It depends on the UV dose - the biological effective radiant exposure. In everyday live the most important UV source is the natural solar UV radiation.

In the past two decades caused by the decreasing stratosphere ozone layer there is the risk of persisting increase of the biological effective UV radiation on earth surface. And in this way, the hazard risks of UVR could increase, while the indispensable UV dose to guarantee the vitamin D production is low (30 % of the individual MED twice a week on the skin area of face, hand and arm exposed by [1]). Efficient protection measures against the hazard risks due to UV radiation require the knowledge of individual solar exposures levels in the different sections of the population.



Figure 1. Personal UV dosimeters to measure biological-effective UV radiation (A) Polysulphone film dosimeter (Dermatology/Technische Universität Dresden, Germany) (B) VioSpor dosimeter (Fa. Biosense, Bornheim, Germany) (C) X2000 data logger dosimeter (Fa. Gigahertz-Optik, Puchheim, Germany) (D) UVDAN data logger dosimeter (Fa. ESYS, Berlin / AWI Bremerhaven, Germany).

To watch the development in global solar UV radiation a world wide measurement network exists. In Germany a UV-monitoring network of 10 measurement stations spread throughout the country was established in 1994. It provides scientific data of the total global solar UV-radiation reaching the earth surface.

In contrast, the individual personal UV exposure by the sun depends as well on global factors such as geographical position, season, time of day, altitude, cloudiness as on individual behaviour factors such as times spent outdoors, individual activities, clothing or use of sunscreens. This data set of additional information we unified with the measurements by personal UV dosimetry to the complex method of the personal UV monitoring. This method enables to register the individual cumulated fraction of the total solar UV exposure getting biological effective to skin and eyes.

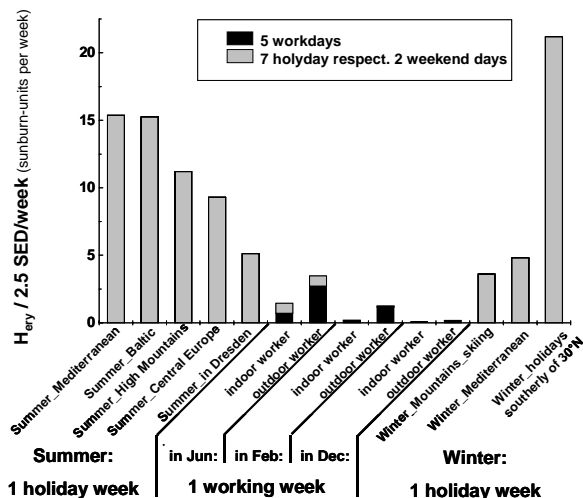


Figure 2. Weekly UV exposure of one holiday week in comparison to one working week (5 workdays + 2 weekend days) in June, end of February and December.

Embedded in the former UVB-programme of the German Ministry of Education and Research (BMBF) we established a routine method of a personal UV-monitoring in the BMBF-research project 07UVB54B. To measure the individual UV exposure, primarily we used polysulphone film (PSF) dosimeters (Dermatologie/Technische Universität Dresden, Germany) but several types of data logger personal dosimeters or film UV dosimeters too. The further aim of the project was a first cross section study of the distribution of individual UV exposures in the German population [2]. The investigated 13 population groups ($n = 150$, Dresden/Germany) ranged from a group of kindergarten children up to inhabitants of an old people's home with pupils, students, housewives, retired persons, indoor worker, outdoor workers in the between. From 1996 to 1998 the personal UV monitoring was carried out in seasonal measurement campaigns for two years (to minimize meteorological influences). In each season the individual UV doses (chest position) were measured on 10 workdays and in leisure time (6 weekend days) separately. In result it was possible to cluster the different sections of the population in only a few groups. In a further BMBF-research project 07UVB54C/3 three representative behaviour groups of the population (each divided into two subgroups) were investigated by a comparable study design of the personal UV monitoring. The groups of indoor worker ($n = 120$) and outdoor worker ($n = 120$) were divided into two subgroups characterized by lower outdoor activities in leisure times (typical for about 70 % to 80 % of the population) and deliberate outdoor activities. Furthermore a children group ($n = 80$) was investigated (first year: kindergarten; second year: first class of a primary school) [3]. To assess the extent of increased exposure levels in typical groups

of employees who are solar UV exposed at workplace either permanently or intermitted, the method was used in the FIOSH research project F1777 (Federal Institute of Occupational Safety and Health) too [4].

Beside the workday and the leisure time exposure, the holiday time exposure is an important fraction of the annual personal UV dose (up to 50 %). In seven typical holiday regions and holiday periods of the Germans the individual UV exposures of holiday makers ($n = 25..40$ per region) were measured with remarkable results. Figure 2 presents the relations between the weekly UV exposure extent under everyday life condition in comparison to UV exposure level of one holiday week with remarkable results [3]. The results are useful to support health education programs against excessive solar exposures with facts like: in summer the holiday exposure peak is 20 times higher compared to the weekly exposure of an indoor worker. But in winter (in a period of low natural self protection of the skin!) and in case of holidays in a region south of 30°N, the holiday exposure peak compared to the indoor worker level in this season in Germany rises up to 200 fold in February or 500 fold in December respectively.

Furthermore, to complete the personal UV monitoring data set, the investigation result on the behaviour depending, seasonal changing body distribution of 19 different body sites to the solar UV exposure (Fig. 3) was included in its database system.

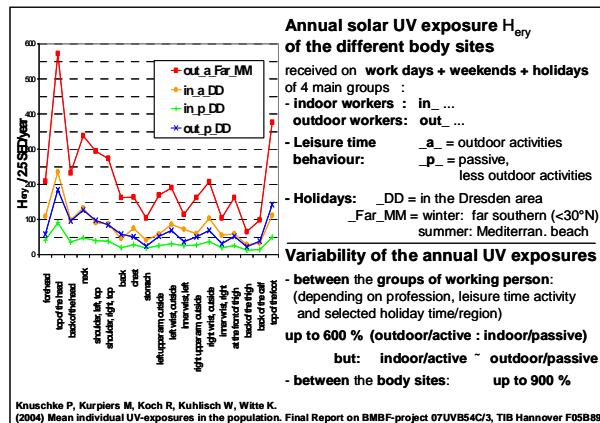


Figure 3. Variability of the annual UV exposure - intraindividual and between different behaviour groups of the population.

Now, these data base system enables the biometric calculations of mean annual UV-exposures to the different body sides of selectable sections of the population taken into account the different workday activities, leisure time behaviour and furthermore the holidays in different seasons and locations. An overview on the variability of the annual UV exposure presents Figure 3.

In health prevention and care on workplaces to be at risk on increased exposure level due to artificial or solar UV-radiation the measurement and assessment shall be stated. In an European Standard EN 14255-1 (artificial UV-sources [5]) and in a draft of the prEN 14255-3 (solar UV-radiation [6]) the different methods of measurement and assessment are to be defined. Depending on the actual

situation the personal UV-monitoring can be the preferable method.

In the discussion on well-balanced recommendations to solar exposed workplaces the personal UV-monitoring investigations serves data on real UV exposure levels.

In basic research of occupational health to investigate the natural photoprotection of the skin against UV-radiation by melanin pigmentation and skin thickening in outdoor workers a personal UV-monitoring provides the data on individual UV-exposure leading to the alteration in the skin in the course of one year (FIOSH-project F 1986).

In medicine the personal UV-monitoring is a usable method in photodiagnostics of patients with photodermatosis. The measured patient data can be related to healthy groups of comparable person to estimate the necessary protection level or/and to correct the behaviour of the patient.

Long-term decreased solar UV-exposure levels (especially in elderly) leads to diseases caused by a vitamin D-deficiency. By personal UV monitoring the correlation in the course of the year between the decreased UV-exposure levels and the vitamin D-deficiency was able to proof [1]. Normal ranges can be found in relation to investigations in younger person groups.

In conclusion, the data pool of the personal UV-monitoring presents a quantitative base to support public UV-education and UV-prevention programs. It is a valid measurement method in scientific research, in occupational healthy control and in medicine.

References

- [1] Knuschke P, Darrelmann M, Gerlach B, Lehmann B, Liepe K, Neumann U, Wozel G. Restoration of normal vitamin D-serum levels in elderly people by a long-term low dosage UV-phototherapy. 6th Annual Meeting of the Photomedicine Society, San Francisco / USA, 20.03.1997 Photodermatol Photoimmunol Photomed 12 (1996) 251
- [2] Knuschke P, Krins A. (2000) Personal UV dosimetry using Polysulphonfilms as a UV sensor. Final Report on BMBF-Project 07UVB54B, Location: Univeritätsbibliothek Hannover and Technische Informationsbibliothek F 00 B 1544
- [3] Knuschke P, Kurpiers M, Koch R, Kuhlisch W, Witte K (2004) Mean individual UV-exposures in the population. Final report BMBF-research project 07UVB54C/3, TIB Hannover F05B898
- [4] Unverricht I, Janßen M, Ott G, Knuschke P (2004) UV-Monitoring an Arbeitsplätzen im Freien - eine Basis für ausgewogene Richtlinien zum Gesundheitsschutz. In: Reidenbach H-D, Dollinger K, Hofmann J (Hrsg.): Nichtionisierende Strahlung - Sicherheit und Gesundheit. TÜV-Verlag, Köln, 2004, 599-609 Publikationsreihe Fortschritte im Strahlenschutz FS-04-128-T
- [5] EN 14255-1 Measurement and assessment of personal exposures to incoherent optical radiation - Part 1: Ultraviolet radiation emitted by artificial sources in the workplace
- [6] prEN 14255-3 Measurement and assessment of personal exposures to incoherent optical radiation - Part 3: UV-Radiation emitted by the sun.

Service Card

Receiver: Helsinki University of Technology

Petri Kärhä

Telefax: +358 - 9 - 451 2222

**You may also E-mail the corresponding information to
petri.karha@tkk.fi**

- Remove me from your mailing lists and do not send me material related to the Thematic Network for Ultraviolet Measurements anymore.
- Add me to your mailing lists and send me material related to the Thematic Network for Ultraviolet Measurements in the future.
- Update my contact information
- _____

Sender:

Company: _____

Departement / Lab.: _____

Name: _____

Title (circle): Prof. Dr. Mr. Mrs. Ms. Other: _____

Address: _____

Country: _____

Telephone: _____

Telefax: _____

E-mail: _____



HELSINKI UNIVERSITY OF TECHNOLOGY

